12-2014

Investigating the Effects of Biochemical and Biophysical Signals on Vascular Smooth Muscle Cell Differentiation

Ruikai Chen
Clemson University, ruikaic@g.clemson.edu

Follow this and additional works at: https://tigerprints.clemson.edu/all_dissertations

Part of the Biomechanics Commons

INVESTIGATING THE EFFECTS OF BIOCHEMICAL AND BIOPHYSICAL

SIGNALS ON VASCULAR SMOOTH MUSCLE CELL DIFFERENTIATION

A Dissertation
Presented to
the Graduate school of
Clemson University

In Partial Fulfillment
of the Requirements for the Degree
Doctor of Philosophy
Bioengineering

by
Ruikai Chen
December 2014

Accepted by:
Dr. Delphine Dean, Committee Chair
Dr. Bruce Gao
Dr. Dan Simionescu
Dr. Frank Alexis

ABSTRACT

In blood vessel engineering, an optimal bioartifical scaffold can be characterized as a 3D tubular structure with high porosity for nutrient diffusion and enough mechanical strength to sustain in vivo dynamic environment. The luminal surface of the scaffold is supposed to have a continuous layer of endothelial cell that is ideally non-immunogenic and non-thrombogenic while the media layer of the construct is assigned for the ingrowth of vascular smooth muscle cell which can provide structural integrity and contractility. While reconstructing endothelial cell layer has been at the center of interest in most polymeric vascular replacements related research, growing VSMCs has had less attention due to the high risk of their excessive proliferation and unexpected phenotype shifts that can result in vessel restenosis. In addition, finding a reliable source of VSMC can be a formidable task. As such, we believe that if VSMCs can be modulated to remain quiescent and functional over time after they are obtained from an alternative source, they might eventually be considered to incorporate into artificial vascular substitute.

To achieve this goal, first we investigated the potential of using stem cell to differentiate into functional VSMCs. Next, we designed a 3D culture construct to mimic blood vessel with distinct layers and analyzed the effect of combining different biochemical and biomechanical signals on modulating VSMCs behavior. Finally, we developed a biomechanical model that can incorporate the mechanical property of differentiated cell and distinct layers with geometrical information acquired from confocal images to predict cellular behavior under different conditions.

The results of these studies provide insights from a basic science prospective about the potential of using stem cell to obtain functional VSMCs and the impact of environmental factors on VSMCs behavior. Researchers may use these results to optimize the culture condition of VSMCs in order to modulate its proliferation, phenotype and mechanical property. The model developed in this study might be used to predict cellular behavior under different culture environments without repetitive experiments.

DEDICATION

This work is dedicated to my family and friends who have supported and encouraged me throughout my graduate education. I would like to specially thank my parents, Chi Chen and Jun Yi for teaching me to believe in hard work and so much could be done with little. I would also like to thank Yunjing Ouyang who made me believe in myself and strengthened my resolve in the pursuit of doctorate degree. I undoubtedly could not have done this without your love and support.

ACKNOWLEDGEMENT

First, I would like to thank my advisor, Dr. Delphine Dean for giving me the opportunity to study abroad and pursue my Ph.D. degree under her guidance. She has always been helpful and encouraging to me no matter how small or insignificant goals I achieved in my research. She has set an example of excellence as a researcher, mentor, instructor, and role model. I would also like to acknowledge my committee Dr. Bruce Gao, Dr. Dan Simionescu and Dr. Frank Alexis whose instruction and guidance helped guide my research. I would especially like to thank Dr. Bruce Gao for providing me the instruments and resources I used for my PDMS fabrication.

In addition, I would like to thank all the members of my lab and other student especially Sandy Deitch, Scott Wood, Gary Thompson, Yang Wei who have assisted me in various aspects of my research.

TABLE OF CONTENTS

Table of Contents (Continued)

Table of Contents (Continued)

LIST OF TABLES

LIST OF FIGURES

List of Figures (Continued)

List of Figures (Continued)

List of Figures (Continued)

Figure   Page

List of Figures (Continued)

Figure   Page

CHAPTER ONE

INTRODUCTION

1.1 Motivation

Tissue engineering of small-diameter blood vessels holds great promise in treating

peripheral arterial disease. However, several major obstacles have severely limited the

use of combining biomaterials and vascular cells. Among all of them, finding a reliable

source of VSMCs that can be made functional over the time has proven to be a

formidable task. Terminally differentiated SMCs, which have been used previously, lack

the ability to proliferate extensively. In addition, they are limited in supply due to the fact

that there are no obvious arteries that can be removed from the body to isolate arterial

SMCs. These disadvantages make it necessary to explore alternative cell source to

provide large number of functional VSMCs that can be used in blood vessel engineering.

We hypothesized that stem cell can be used as an alternative cell source to differentiate

into functional smooth muscle cell if modulated with proper environmental signals.

The purpose of this research was to investigate the potential of using stem cells to

differentiate towards VSMC lineages for vascular engineering. Specifically, we

compared the mechanical property of VSMC differentiated from bone marrow derived

stem cell and adipose derived stem cell. We also studied the effect of the combination of

different biochemical and biophysical signals on cellular proliferation, alignment and

viscoelastic property during differentiation. Based on the design of our culture conditions,

1

we developed a computational model to characterize cellular behavior using COMSOL software. Our specific aims are described below

1.2 Research Aims

1.2.1 Aim 1: Investigate the potential of using stem cells to differentiate into functional VSMCs

Tissue engineering holds great promise in treating many diseases including arteriosclerosis. However, several major obstacles have severely limited the use of engineered tissues for clinical applications. These include issues with proper vascularization of engineered tissues, limited choices of matrices that can provide sufficient mechanical support, and the ability of cells to remain functional and proliferative over time[1-3]. Vascular smooth muscle cells (VSMCs) exist in a quiescent, differentiated state in the adult arterial media and plays an important role in regulating blood flow and pressure by contracting and relaxing in response to a variety of stimuli. Thus, VSMCs should logically be incorporated in the development of tissue-engineered blood vessels and treated as one of the crucial constituents in human vascular regeneration [4].

Among all the challenges faced in vascular tissue engineering, finding a reliable source of VSMCs that can be made functional over the time has proven to be a formidable task. Terminally differentiated SMCs, which have been used previously, lack the ability to proliferate extensively. In addition, they are limited in supply due to the fact that there are no obvious arteries that can be removed from the body to isolate arterial SMCs. The

purpose of my proposed research is to investigate the potential of using an alternative source of cells for VSMCs in vascular tissue engineering. Specifically, we will study the differentiation of stem cells to VSMCs and the effects of different microenvironments on the cellular mechanical properties. The results will lead to a better understanding of cellular behavior under different conditions and can be used to verify the suitability of different types of multipotential progenitor cells as the supply of VSMCs in vascular engineering. The specific research aims are as follows:

1.2.2 Aim 2: Determine the effects of biophysical and biochemical signals on VSMC behavior

The proliferation and differentiation of VSMCs are known to be regulated by biochemical signals including platelet-derived growth factor (PDGF) and transforming growth factor- β (TGF-β) [5]. However, the effect of biophysical cues such as topography, stiffness, and mechanical loading on VSMC differentiation has not been fully studied. We hypothesize that by combining a variety of different physical stimuli, the differentiation of VSMC can be controlled and optimized. To test this hypothesis, soft lithography will be used to fabricate patterned PDMS substrates for cell culture and type I collagen will be layered on top of cells to mimic physiological conditions. A Flex-Cell system will be used to apply cyclic stress and strain on PDMS substrates and a custom bioreactor will provide fluid flow around the cultured cells. The shape and cellular mechanical properties will be compared under different physical conditions and the expression of SMC specific markers will be used to verify the cell phenotype.

1.2.3 Aim 3: Use biomechanical models to predict cellular and tissue-level behavior under specific condition

Biomechanical models have been adopted as a useful tool in predicting both cellular and tissue-level behavior under specific conditions. Vascular smooth muscle cells play an important role in native vessel function and might impart functional characteristics to tissue engineered blood vessels as well. Thus, the ultimate goal of this proposed work is to develop a biomechanical model composed of the environmental factors important to VSMC differentiation that can predict the result of seeding VSMCs on pseudo-vessels. In this aim, COMSOL will be used to model the behavior of VSMCs cultured in a collagen sandwich. The mechanical loading provided in the previous experiments (Aim2) and the results of the AFM indentation during VSMC differentiation (Aim1) will be incorporated into the model. Imaging tools will be used to record the shape change in cell and substrate for model reconstruction.

1.3 Significance

This research was the first study to compare the potential of differentiating different stem cells into functional vascular smooth muscle cell in terms of achieving sufficient mechanical strength. Previous studies have suggested that VSMC phenotype and differentiation can be regulated by a variety of different environmental factors including soluble factors, substrate and mechanical loading. However few studies investigated the effect of combining multiple stimuli on cellular behavior. In this work, we designed a 3D culture construct to simulate the distinct layers of blood vessel for VSMC growth and investigated the effect of multiple environmental factors on cell behavior. The results of

these studies provide insight on how VSMC differentiation and phenotype is controlled by the combination of biochemical and biomechanical signals and can be used to optimize the culture condition for VSMC differentiation in order to achieve large quantity of functional VSMCs without excessive proliferation and phenotype shift after enough cells have populated target construct. We also developed a multiphysics model to predict cellular behavior under certain mechanical condition based on our experimental data using flexcell system. The modeling study provided data that may be used as a first step to estimate VSMC behavior before cells are transplanted into tissue engineered vessel or graft.

1.4 References

[1] Dahl, S. L. M., Koh J., Prabhakar V., and Niklason L. E. *Decellularized native and engineered arterial scaffolds for transplantation*. Cell Transplantation, 2003. 12: 659-666.

[2] Tschoeke, B., Sriharwoko M., Ella V., Koch S., Glitz A., Schmitz-Rode T., Gries T., Kellomaki M., and Jockenhoevel S. *Tissue engineering of small calibre vascular grafts*. Tissue Engineering, 2007. 13: 1770-1770.

[3] Wu, H. C., Wang T. W., Kang P. L., Tsuang Y. H., Sun J. S., and Lin F. H. *Coculture of endothelial and smooth muscle cells on a collagen membrane in the development of a small-diameter vascular graft*. Biomaterials, 2007. 28: 1385-1392.

[4] Parizek, M., Novotna K., and Bacakova L. *The Role of Smooth Muscle Cells in Vessel Wall Pathophysiology and Reconstruction Using Bioactive Synthetic Polymers*. Physiological Research, 2011. 60: 419-437.

[5] Lacolley, P., Regnault V., Nicoletti A., Li Z. L., and Michel J. B. *The vascular smooth muscle cell in arterial pathology: a cell that can take on multiple roles*. Cardiovascular Research, 2012. 95: 194-204.

CHAPTER TWO

LITERATURE REVIEW

2.1 Cell Mechanics

2.1.1 Cellular architecture

In our human body, millions of cells exist and serve as the fundamental structural and functional unit of tissues and organs. There are about 200 different cells performing specific function as they have different microstructure and express different genes. Since it is obvious that the internal constitution of a single cell is responsible for its mechanical property, understanding the microstructural of single cell by analyzing its distributions, orientations and interconnections is essential for single cell biomechanics.
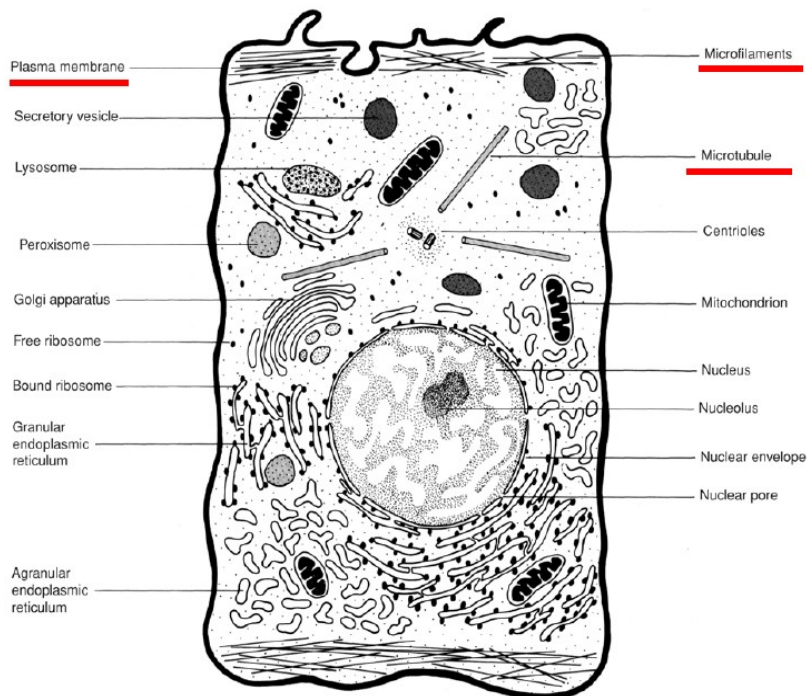
Figure 2.1 Structures and organelles found in most human cells [1].

Figure 2.1 is a schema of a typical cell indicating the major features of the cellular

organelles. It has a membrane that envelops the cell, separating its inner part from the

surrounding environment. The membrane is made up with phospholipid bilayer

containing many proteins that serve as different functions such as channels, gates and

receptors for external molecules. Inside the membrane, a salty cytoplasm takes up most

of the cell volume. However, it is the cytoskeletal that maintains the shape of the cell,

enables cell to move and plays important role during cell division [2,3]. Thus, it is one of

the most discussed topics in cell mechanics.

Cytoskeleton is contained within the cytoplasm and is an elaborate network of fibrous

proteins. The components of cytoskeleton are classified according to their diameter into

three main kinds of filaments, which are actin filaments, intermediate filaments, and

microtubules.

Actin filaments

Actin filaments are the thinnest filaments of the cytoskeleton. Specifically, they are

around 6nm in diameter and are relatively flexible and strong. They are polarized and

polymers of actin subunits. The subcellular location allows its responsiveness to

transmembrane receptor action. The elongation in the barbed end and the contraction in

the pointed-end enables filament in total moves.

Intermediate filaments

Intermediate filaments are named because the diameter of them is around 10nm lying

between actin filament and microtubules. There are six classes of intermediate filament

proteins and each class contains multiple members indicating its diversity compared to

the other two filaments. Despite their diversity, they share common structural and sequence features: a parallel dimer constituted with two α-helical chains forming a coiled coil rod. They provide a supporting net-work for the cell and are capable of cell-cell and cell matrix adhesion. Considering their biomechanical properties, they are rather stretchable and can be deformed several times longer than their initial length due to their hierarchical structural.

Microtubules

Microtubules exist as cylinders in a diameter of approximately 25nm and a length range from 200nm to 25μm. They also play an important role in the structure network. Moreover, they participate in many other processes like cell division, generating force by growing and shrinking, letting organelles to move along. Typically, it has a higher bending stiffness than the other two types of filaments but is less stiff for elongation.
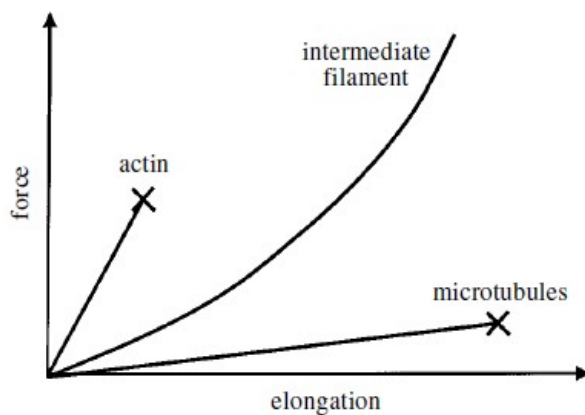
Figure 2.2 Mechanical property of the three types of filaments [4].

2.1.2 Mechanotrasduction

Mechanotrasduction is a process in which cells convert external mechanical stimuli into biochemical activity. Many studies have been focused on investigating how cells sense mechanical signals and transduce them into biological responses, however, the precise mechanism is remain unclear. Several theories for these mechanisms have been proposed [5,6]. For instance, Ingber's group suggests that cells use tensegrity structures to sense mechanical signals [5]. Based on the theory, they point out the important role that ECM and cell structural plays in the process and the regulation performed by molecular mediators such as signaling moleculars and integrins [6]. Future research requires the investigation of the interaction between mechanical force and soluble factor including growth factor, cytokines which are associated with the development and remodeling of tissue. Studies related to the response of specific cell type to external force are of interest for understanding the progression of certain disease. In addition, identifying the exact force that cause a receptor to sense the external loading and that results in altered cellular function will be crucial for further research.

2.1.3 Techniques of imaging and manipulating cells used in biomechanics

As biomechanics has participated in virtually every modern advance of medical science and technology [7], people seek to better understand the structure-property-function relationship of living cells among extracellular environment in order to find possible connection between physiological change and certain diseases. With the development of techniques to manipulate mechanical and structural property range from micro to the picoscale, we are now able to perform mechanical test for single cell in physiological

condition. Moreover, arising from the advancing imaging techniques developed in the past decade, it is possible to image intracellular structure together with the shape and geometry of the cell which is a primary concern in cell modeling.

AFM (atomic force microscope)

Atomic force microscope is a cutting-edge technique used in both cellular mechanical testing and imaging. The basic principle of AFM is the detection of cantilever deflection arising from the forces applied between a sharp tip on the end of cantilever and sample's surface.
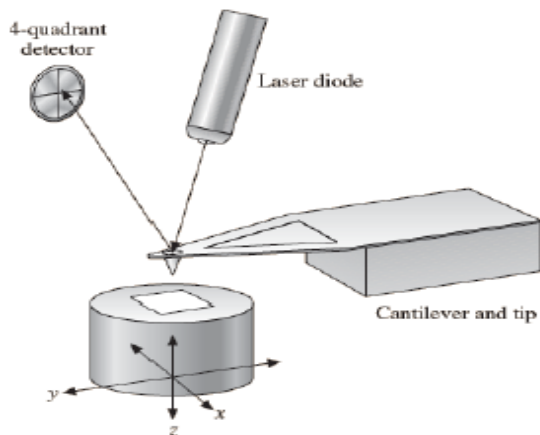
Figure 2.3 Schematic of typical AFM [8].

The most important feature for AFM in imaging is it can acquire images of cells in fluid which match their physiological environment in vivo. According to that, it makes AFM an indispensable imaging technique in studying biological samples. Moreover, AFM is capable of measuring cellular elastic property by collecting indentation depth and force while inserting tip into the cell [9]. Picture below shows a typical force curve for the

indentation of tip. The combination of fluorescent labeling and AFM makes it possible to analyze the contribution of different cytoskeleton components in cell mechanical property. Study has shown that the actin filaments contribute more to the cells stiffness than microtubules even the latter has a greater diameter [10].
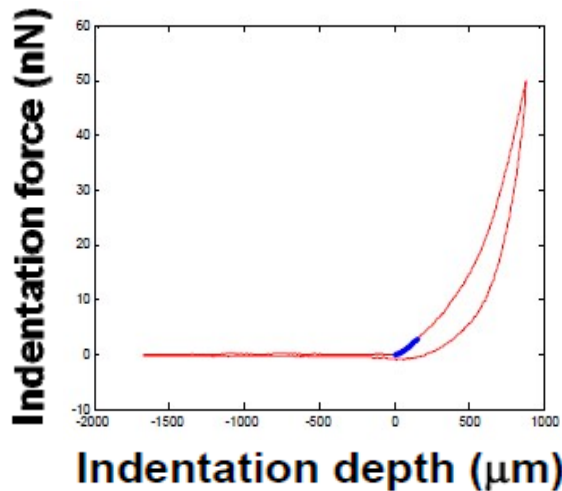
Figure 2.4 Typical Indentation depth and force curve [11].

AFM can also be utilized in cell-cell and cell-substrate adhesion by adhering living cells on the tip [12]. Similarly, it can be applied to study the ligand-receptor or antigen-antibody binding force [13].

Although AFM has become a popular tool in the study of cell mechanical property, limitation exists in certain aspects. First, since the cantilever is inclined approximately 15 degrees, the tip is not approaching normal to the surface thus generating lateral stress to the cell. In addition, the classical model used in AFM indentation analysis assumes the cell is linear elastic and the function is time-independent. These assumptions are invalid

for living cell. For the imaging part, because AFM is a rastering technique, it takes time to generate the whole picture of the sample which makes it difficult to investigate dynamic processes of living cells.

Optical traps

Optical traps is often used to deal with cell mechanics, When a laser transmits through an object with a high refractive index, the momentum change result in a force generated toward the center of focus point. Thus, the object can be moved in that direction under a certain force. The trap is stabilized by the repulsive force along the laser axis. It can be used to measure an externally applied force by considering the resulting motion from the center of focus point [14]. By considering the function caused by displacement between sample and focal point as typical spring, we can reach a simple equation Fg =-kx where k is the stiffness of optical trap and x is the sample's displacement.

(a)   (b)
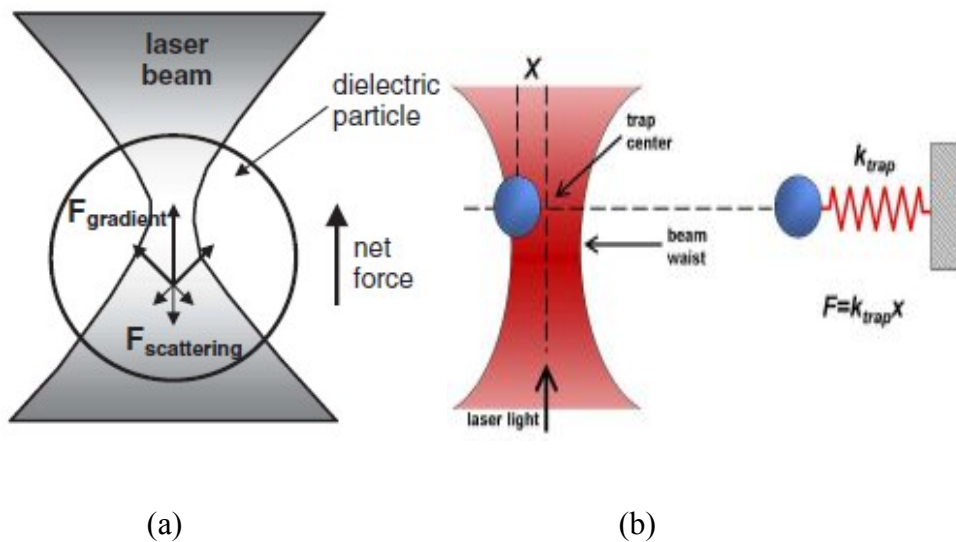
Figure 2.5 (a) Schematic of optical trap (b) Simple spring system to describe the displacement from the trap center [15].

Due to the function principle of optical trap, the object should have a high refractive index compared to the environment and should be as symmetric as possible [16]. Thus, it is most appropriate to study mechanical property of cells in fluid suspension like mechanical response of RBCs at the different developmental stages [17]. Optical trap is also utilized in studying motor protein such as kinesin [18]. The main limitation is that only one particle can be manipulated by a beam of laser at one time.

Micropipette

Micropipette aspiration provide a simple method to probe mechanical property of a cell, it uses a suction pressure to suck a single cell into the micropipette which has a smaller inner diameter than the size of the cell. By measuring the elongation of the cell, we can then evaluate its mechanical property based on the known suction pressure. According to that, several mechanical properties can be analyzed by micropipette. Many experiments have been designed to measure the viscoelastic behavior of erythrocytes, granulocytes and neutrophils [19].

(a)   (b)
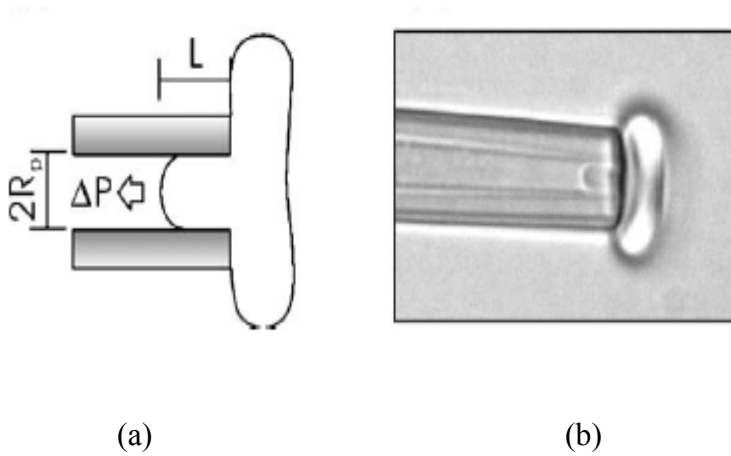
Figure 2.6 (a) Schematic of a micropipette aspiration (MA) technique and (b) image on the aspiration of a RBC [15].

The main disadvantage of MA is the complexity of analyzing stress concentration at the edge of pipette and the friction between micropipette and cell, which, if not take into consideration, will impair the accuracy of measurement.
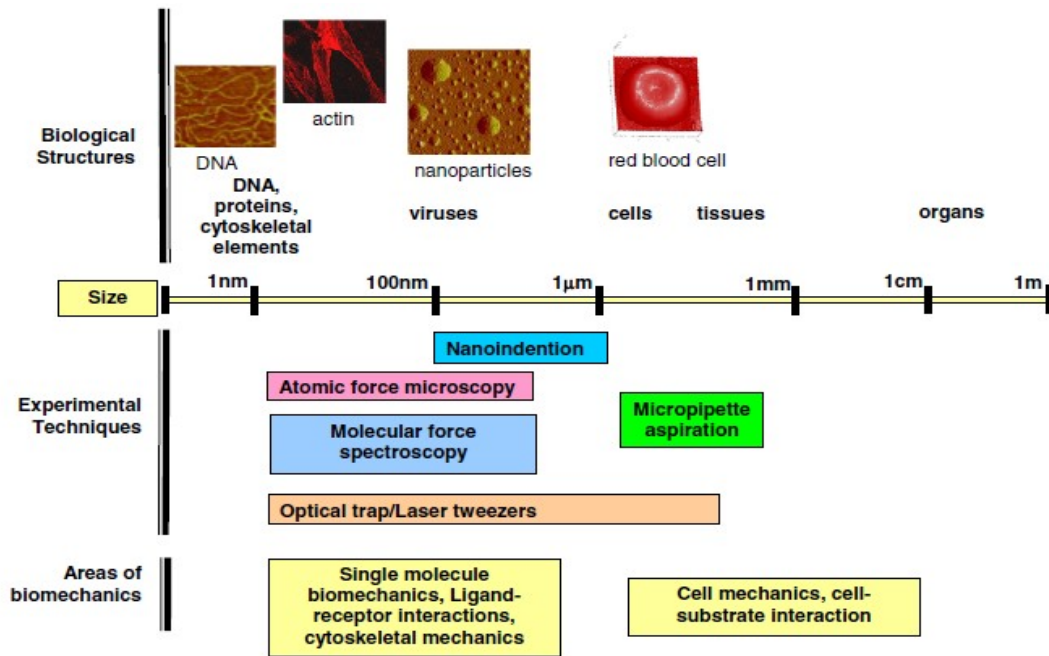
Figure 2.7 Cellular manipulating techniques and the scales for which they are applied [15].

Other imaging techniques used in cell mechanics

As mentioned earlier, in the study of cell mechanics and modeling, imaging techniques are employed to get structure and geometry information of biological sample ranging from single cell to tissue. Commonly, the shape of an object is the first thing we need to consider in building model for any structure. Thus, the imaging part is of great importance in dealing with cell mechanics. As many efforts have been made to develop techniques in imaging, there are many ways to get picture from biological sample depending on the type and size we are interested. Optical microscopy is the standard technique used in the study of biological tissue and cells. Fluorescence microscopy is especially useful as it makes a better contrast between sample we are interested and the

16

environment. Unfortunately, optical techniques are limited in resolution by the

wavelength of light used. Transmission electron microscopy (TEM) and Scanning

electron microscope (SEM) can provide a significantly higher resolution than optical

microscope. However, these techniques have limitation due to sample preparation and

handly.
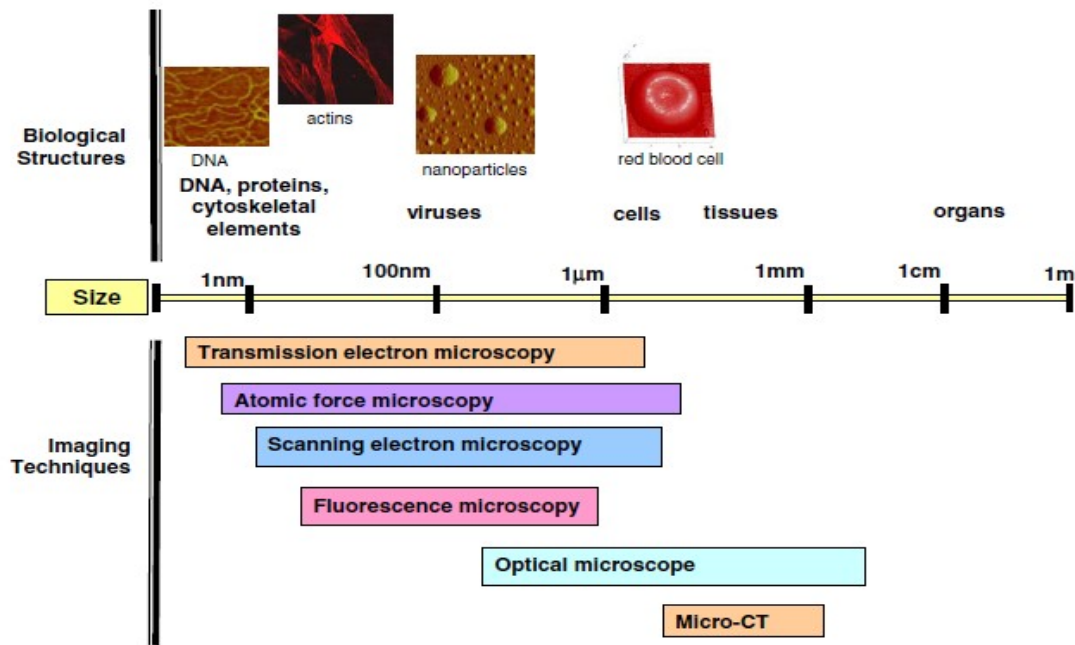
Figure 2.8 Cellular imaging techniques and the scales for which they are applied [15].

2.1.4 Single cell model

As we know, the structural and mechanical property of living cells not only maintains the

integrity of them but also affect their biological function. Any deviation from the normal

condition may result in the dysfunction of cells and even apoptosis. Thus, a quantitative

study of their physical property is needed. Many attempts have been made to build

appropriate model for cells to characterize their mechanical response to transient and

dynamic loads. Generally, these attempts are based either on the structural approach or the continuum approach. Here, we will briefly discuss how these two approaches are applied to single cell mechanics.

Structural based model

Structural based model deems the cytoskeletal structural of cell as the most important component in the single cell mechanics and focus on the role of them in maintaining physical property of cell. While there are many methods for modeling fiber networks [20], few studies have used structural based models for whole cells; cell structure is extremely complex and modeling the whole system would be computationally intractable. Tensegrity model and spectrin level model [21] are among the approaches trying to deal with the equilibrium shape and deformation of cell. Tensegrity model suggests that cell uses tensegrity architecture to maintain their physical shape and process mechanical signal. Ingber's group proposed that the tensegrity structural once used in architecture can be applied to cell mechanics. They demonstrate the cytoskeletal filament as stick and string to resist tension and compression [6]. Spectrin network model was proposed to study for suspended cells such as erythrocytes. It is a network that relaxes shear stress everywhere and generates cytoskeletal structure to predict the large deformation of red

cells [22].
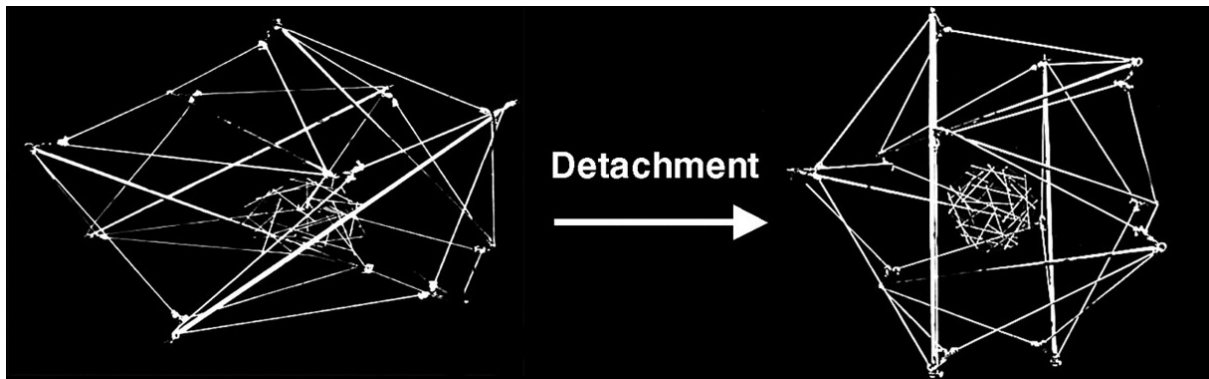
Figure 2.9 The pricture shows how cells in tensegrity model spread on substrate and detach [6].

Continuum based model

The continuum approach treats cell as continuum rather than separate parts. This makes it easier to derive constitutive models to characterize material property and is more straightforward to deal with the mechanical property of cell. Liquid drop model, solid model and biphasic model are in this catalog. The liquid drop model was first developed to investigate the rheological property of neutrophils in micropipette aspiration and was then improved and expanded to different experimental conditions. The main concept is to consider the cell consisting different layers which have different surface tension and

19

viscosity thus resulting in different deformation under pressure [23]

cortex with constant
tension, T₁

nucleus modeled
as a more viscous
Newtonian liquid
droplet

T_1

T_2

μ_1 μ_2

cortex of nucleus
with constant
surface tension,
T_2

cytoplasm modeled
as a less viscous
Newtonian liquid
droplet
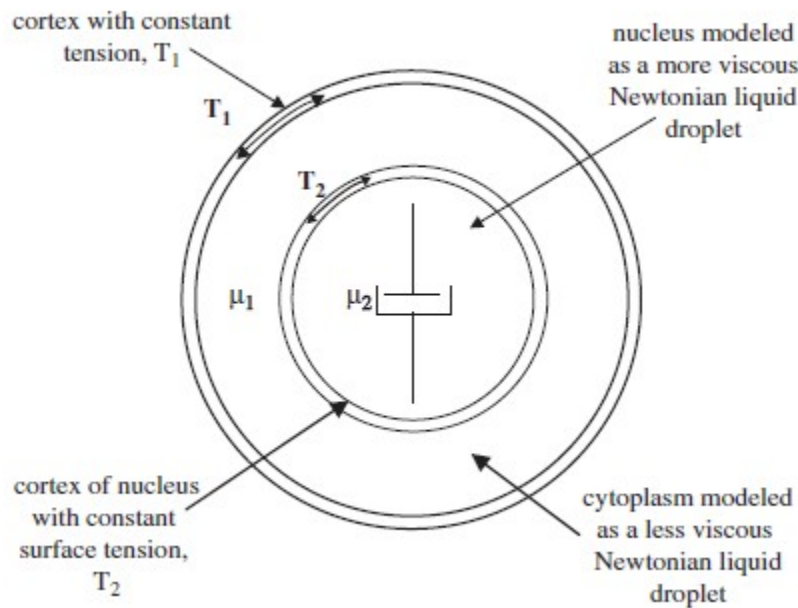
Figure 2.10 The compound liquid drop model [24].

Solid models include both elastic model and viscoelastic models. The most differentiating feature of solid models compared to liquid drop models is that they assume that the whole cell is homogenous and they do not consider different cortical layer. This reduces the parameters needed for modeling. The method to describe the whole cell's mechanical property is achieved by simply using the combination of spring and dashpot to simulate the stress relaxation and the creep function of cell. While liquid drop and solid models both consider cell as a single phase material, the biophasic model treat the cell as a mixture consisting of solid phase and fluid (water) phase. It was first introduced to study biological tissue and then applied at the single cell scale as well. Despite its complexity

compared to viscoelastic model, biophasic property of bone cells and cartilage has been applied to study the mechanotransduction in the dynamic environment of ECM [25].

2.2 Tissue mechanics

Literally, tissue mechanics means applying mechanical principles to biological tissue. Thus, similar to the study of common material such as steel and wood, several aspects are considered when we investigate tissue. First, due to the complexity of our living body, tissues are classified as soft tissue like cardiovascular vessel and hard tissue such as bone. Second, several basic concepts and principles need to be checked before applying to biological tissue. The last but the most important thing is to consider the constitutive relations that describe the mechanical property of tissue and the solution to boundary conditions. As our aim is to find a relation between the mechanical property of cell and tissue, soft tissue is what we are interested. Since soft tissue respect basic concepts (stress and strain) and principles (conservation of mass, momentum and energy), the investigation will be focused mostly on formulating the behavior of soft tissue in constitutive relation and then the solution to initial boundary problems. After that, appropriate model can be achieved to reflect tissue response due to changes in physiological environment.

2.2.1 Soft tissue mechanical characteristic

By definition, soft tissue refers to tissues that connect, support or surround other structures and organs of the body. It has been known for years that soft tissue behave differently from traditional material like metal or wood. Soft tissue is normally

viscoelastic, incompressible and has thermoelastic behavior similar to rubber. While soft tissue exhibits a nonlinear, inelastic, heterogenous and anisotropic behavior, the mechanical property of different tissues differ a lot. This means tissue properties vary a lot from point to point, time to time and individual to individual. Due to the complexity of soft tissue mechanics, characterization of mechanical property is the first step before formulation constitutive relations.
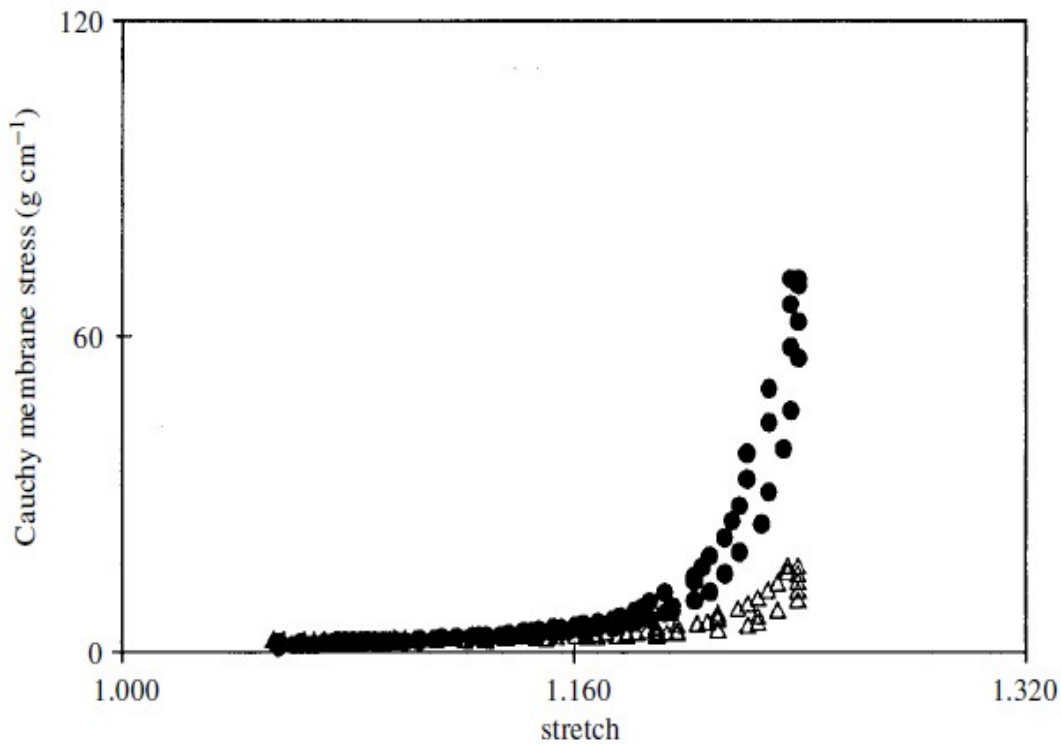
Figure 2.11 Typical stress strain data for soft tissue [26].

Pseudoelasticity

The term pseudoelasticity for soft tissue was first introduced by Fung YC to explain the nonlinear stress and strain relationship. He showed that after some preconditioning

process for soft tissue, it can be independent of strain rate while still present hysteresis

behavior. Fung also suggested an exponential relationship between stress and strain [27].

Equation 2.1. The equation of Green strain tensor and stress tensor

$$S = \frac{\partial W}{\partial E} = ce^Q \frac{\partial Q}{\partial E}$$

In the equation, S represents the stress tensor, W stands for the energy function which

equals to $c(e^Q - 1)$ where Q is a function of the Green strain tensor E and c is just a

material parameter. Based on research data, Fung then found a quadratic relation between

functional form Q and green strain tensor E.

Equation 2.2. The quadratic form of function Q

$$Q = \frac{1}{2}c_{ABCD}E_{AB}E_{CD}$$

Where c_{ABCD} is material constant. Thus, any soft tissue can be described by equation 1

and 2 is called Fung-elastic.
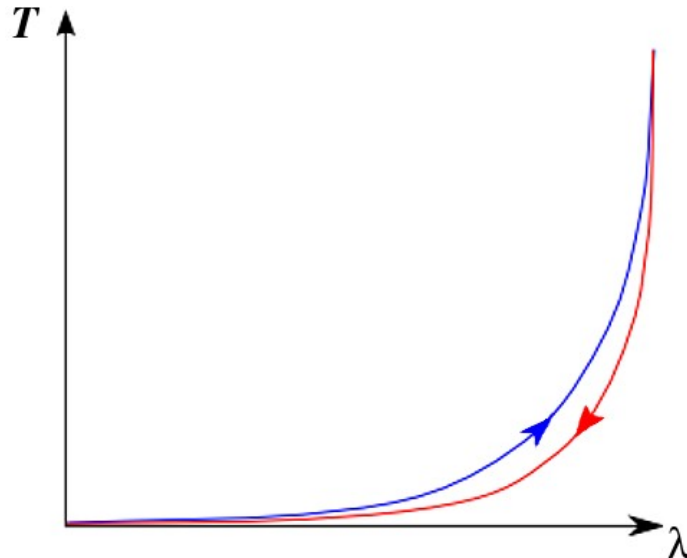
Figure 2.12 Pseudoelastic behavior (Stress T and stretch λ) of preconditioned soft tissue[28].

Viscoelasticity

One of the most important properties of soft tissue is its viscoelasticity. Viscoelasticity means the material exhibit both viscous and elastic behavior when undergoing deformation.Due to the large portion of water contained in soft tissue, it is not hard to understand that it has both solid-like and liquid-like behavior. Typically, a viscoelastic material exhibit hysteresis under cyclic loading, have stress relaxation function under constant strain and behave creep when applied with constant stress. Approaches to describe viscoelastic behavior fall into two types, the differential type (e.g. Maxwell, Voigt and Kelvin models) and the integral type (e.g. Boltzmann models).
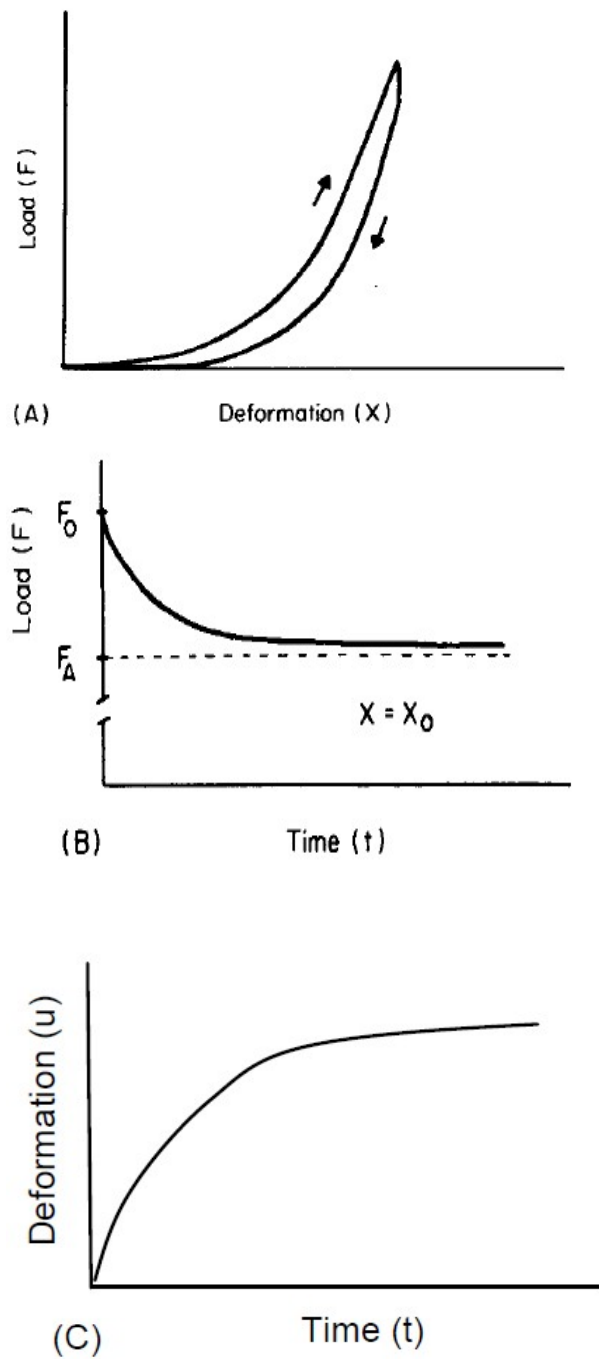
Figure 2.13 Typical mechanical behavior of viscoelastic material (a) hysteresis (b) stress relaxation (c) creep function.

Differential theory deems the response of viscoelastic material to external loading as elastic behavior and viscous behavior. To model the behavior, people use a simple combination of linear spring and dashpots to represent the elastic and viscous component. The elastic component can be represented by spring which can be given as Equation 3.

Equation 2.3. Spring equation where stress(σ) is analogous to force(F), spring constant(k) is analogous to elastic modulus(E) and strain(ε) is analogous to displacement(u)

$$\sigma = k\varepsilon$$

similar to Hooke's Law. The viscous component can be modeled as a dashpot which can be given as

Equation 2.4. Spring equation where stress(σ) is analogous to force(F), η is viscous, strain rate($\frac{d\varepsilon}{dt}$) is analogous to displacement rate($\frac{du}{dt}$)

$$\sigma = \eta \frac{d\varepsilon}{dt}$$

Three common models differ at the arrangement of the two elements are used to describe viscoelastic behavior which is Maxwell model, Voigt model and Kelvin model.

Maxwell Model is composed of a linear spring and a dashpot shown in diagram, in this
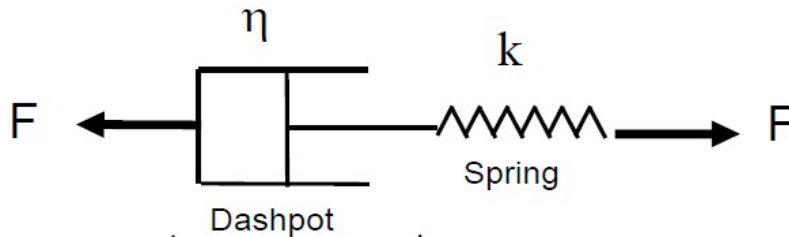
Figure 2.14 Schematic of Maxwell model.

model, same force is transmitted through spring and dashpot, thus a relation of each

elements with the total stress and strain can be concluded as

Equation 2.5. The relation between total stress and strain with each element in Maxwell

model

$$\sigma = \sigma_{spring} + \sigma_{dashpot}, \varepsilon = \varepsilon_{spring} = \varepsilon_{dashpot}$$

The governing equation of the model can be given as

Equation 2.6. Governing equation of Maxwell model

$$\frac{du}{dt} = \frac{1}{k}\frac{dF}{dt} + \frac{F}{\eta}$$

For Voigt model, it consist a spring and dashpot connect in parallel which means they

have the same displacement u.
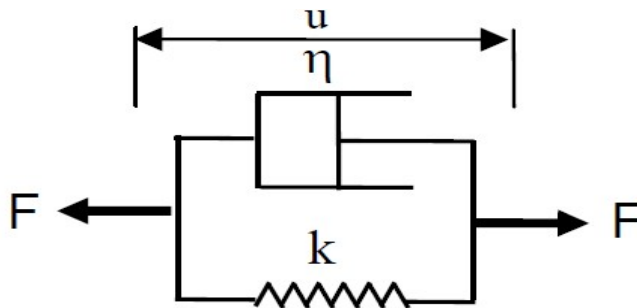
Figure 2.15 Schematic of Vigot model.

Equation 2.7. The relation between total stress and strain with each element in Vigot model

$$\sigma = \sigma_{spring} = \sigma_{dashpot}, \varepsilon = \varepsilon_{spring} + \varepsilon_{dashpot}$$

Equation 8. Governing equation of Vigot model

$$F = ku + \eta \frac{du}{dt}$$

The kelvin model combines a Maxwell model in parallel with a spring which makes it similar to Vigot Model if we consider the Maxwell model as a single component.
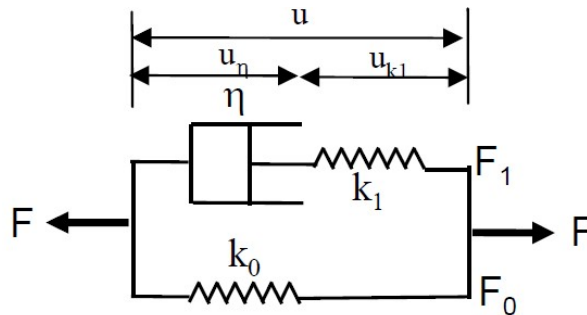
Figure 2.16 Schematic of Kelvin model.

Equation 2.8. The relation between total stress and strain with each element in Kelvin model

$$\sigma = \sigma_{spring} = \sigma_{Maxwell}, \; \varepsilon = \varepsilon_{spring} + \varepsilon_{Maxwell}$$

Equation 2.9. Governing equation of Kelvin model

$$F + \frac{\eta}{k_1}\frac{dF}{dt} = k_0\{u + \frac{\eta}{k_0}\left(1 + \frac{k_0}{k_1}\right)\frac{du}{dt}\}$$

As long as we have got the governing equation of these models, certain analysis for specific condition such as a constant strain (stress relaxation) and constant stress (creep function) can be done. When the model is under either of the stimulus, the spring responds instantaneously while the dashpot responds overtime. Because the inherent nonlinear character of soft tissue, the above linear viscoelasticitymodel cannot apply to all cases in general. It was Fung then, proposed a so called quasi-linear viscoelasticity (QLV) theory. It is composed of an infinite series of Kelvin bodies.
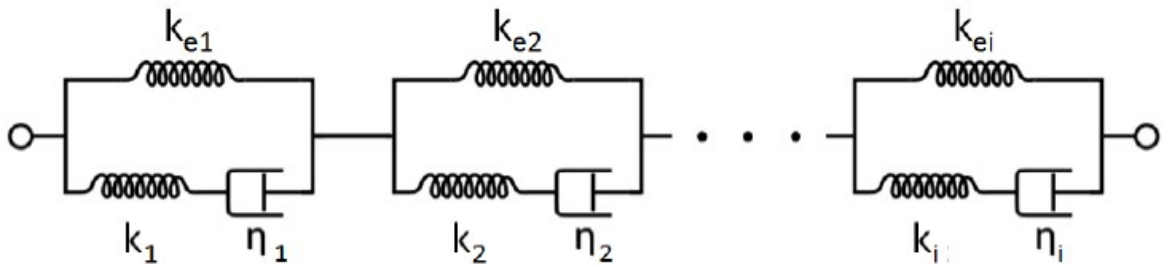
Figure 2.17 Schematic of Kelvin model.

Remodeling and growth of soft tissue

Besides the nonlinear, anisotropic, incompressible (saturated by water) and viscoelastic behavior of soft tissue, another important character elucidated recently is its ability to remodel and growth in response to disease, injury and changes in physiological environment. The first formal framework about kinetic growth was proposed by Rodriguez. He assumed a piece of soft tissue free from external stress and is controlled by a growth tensor Tg, the tissue is divided into many individual pieces which means the responses to the growth tensor in different pieces are not compatible with each other. Due to the internal force assembling individual pieces into a contiguous configuration, residual stress is produced in the process making the tissue still an integrity [29]. However, for soft tissue in our living body, the change in mass (growth) and the change in structure (remodeling) often occur simultaneously. In order to describe the mechanically-based remodeling and growth of soft tissue more accurately, a constrained mixture homogenization theory was proposed. While the mixture theory aims at the separate contributions in mass change by each constituent, the homogenization theory accounts for the stress response to individual constituents [30]. By melding the two theories, we can then able to take advantage of mixture theory and simplify the formulation considering the homogenization.

2.2.2 Imaging techniques in tissue modeling
Since imaging technique is always a powerful method in acquiring anatomical data of soft tissue and reconstructing 3D model, it definitely plays an important role in

investigating tissue mechanics. Here, we will briefly discuss some imaging technique applied in tissue scale.

CT and micro-CT

CT employs an ionizing radiation such as x-ray to go through the sample resulting in a contrast in the absorption of the radiation which is then detected and imaged. The image is 2D and can be further stacked into a 3D representation of the scanned area. The main advantage of CT and micro-CT is the high resolution due to eliminating the superimposition images outside the interested area. Micro-CT has been used to study the structural-function relation of soft tissue and to non-destructively image and quantify the 3D microstructural morphology of samples [31,32]. Moreover, it can be used to quantify regional mechanical properties in lung [33] and employed as an efficacious way to reconstruct bronchial and pulmonary arterial and venous trees in 3D [34]. As the differentiation of different tissue is achieved by contrasting absorption of radiation, the segmentation of tissue is only determined by tissue density which makes it inferior to MRI and optical microscopy in differentiating similar soft tissue density. However, the poor segmentation of different tissue can be addressed to some extent by using contrast agent (e.g., iodine, which is primarily used in angiography). The high radiation exposure is also a limitation of CT which makes a focus on improving low dose CT scan today.
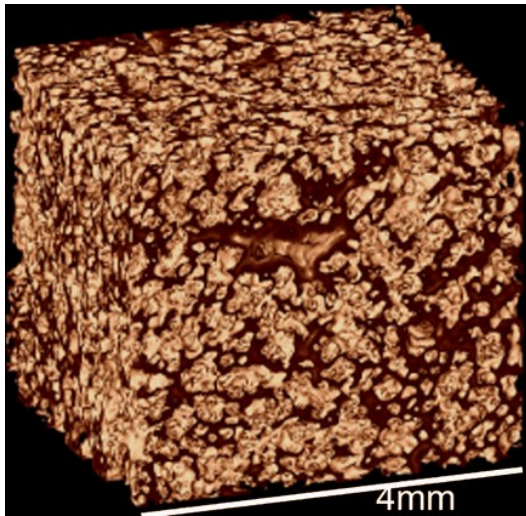
Figure 2.18 Cube of the normal lung specimen, reconstructed in three-dimensions from 286 micro-CT sections (volume of interest, 4 mm per side) [35].

Magnetic resonance imaging (MRI)

Unlike CT scans, MRI does not use ionizing radiation which makes its increasing use in clinical imaging. For MRI, it makes use of a magnetic field to align the magnetization of some atoms in the body and a radio frequency field to further alters the electromagnetic filed. Then, after turning off the filed, we can detect a rotating magnetic field produced by the nuclei which is depended on the strength of magnetic field gradient. The image of MRI is also a 2D picture similar to CT which can be further stacked. The function principle of MRI makes it better at differentiating soft tissue types than CT scans and superior in recognizing soft tissue in similar density. Despite the superior tissue differentiation ability, the resolution of MRI is worse than both CT and optical microscopy. Typical application of MRI in studying soft tissue involves geometry and

motion reconstruction based on MRI image, Cardiac function and anatomy investigated

by analyzing data acquired by MRI [36]. MRI is also a powerful tool in diagnosing tumor

in soft tissue. Besides, since MRI is capable to obtain 2D and 3D images, it has the

potential to track displacement fields within the tissue otherwise the analysis of static

deformation in soft tissue can only be performed at tissue's surface with the help of

external marker or instrumentation [37]. It has been proven the application of MRI to

texture correlation theory in calculating soft tissue (tendon) strain fields is more accurate

than tracking markers placed on the surface of the tissue [38]. Although the accuracy of

MR texture correlation for other types of soft tissue has not been characterized, it is

definitely a promising technique for the study of tissue mechanics in the future.
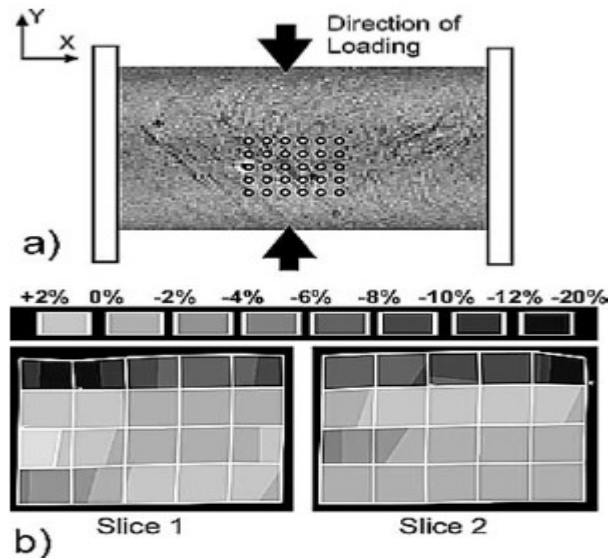
Figure 2.19 Schematic of MRI applied in texture correlation in strain determination [39].

Ultrasound

Ultrasound has been used as a diagnostic imaging technique for a long time and is widely used for its real time application, low cost and non-invasive property. Moreover, it has been employed to noninvasively measure the mechanical property of structure within body based on the principle of ultrasound speckle-tracking [40]. Ultrasound speckle-tracking is to analyze the motion of tissue by tracking the interference pattern and acoustic deflection. The deflections can be then resolved to strain sequences providing quantitatively information about tissue deformation and motion. Such kind of bioelasticity imaging is capable of acquiring the stiffness of soft tissue which is not available with other imaging modalities.
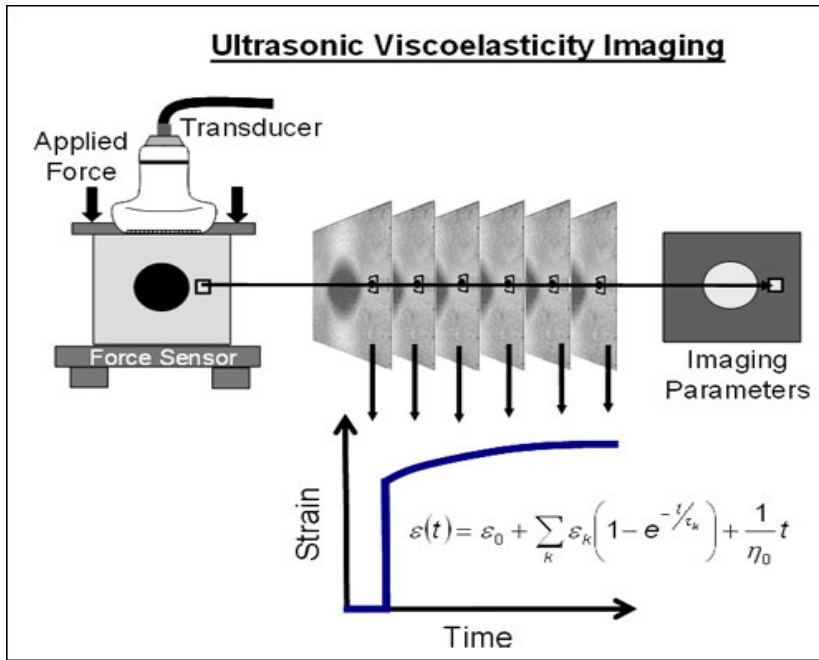
Figure 2.20 Schematic of ultrasounic viscoelasticity imaging [41].

Bioelasticity imaging has been applied to measuring the compliance of artery and diagnosing breast cancer [42]. Previous attempts for peripheral artery include arterial

wall motion estimation, intraparietal strain imaging and pulse wave velocity

measurement. However,vascular vessel wall deforms nonlinearly in three dimensions

which means 1D analysis is not sufficient since only strain information in the radial

direction is obtained. Several 2D and 3D approaches based on blocking matching

technique is applied to address the problem and will remain a research focus in the future.

Optical microscopy

Optical microscopy is a general definition of microscope which uses visible light and

lenses to get images from sample. It includes many types of microscope such as

fluorescence microscope, phase contrast microscope and confocal microscope. Each of

them has its initial superiority and aims at different aspects of imaging tissue. Optical

microscope can also be used to model soft tissue in 3D with the help of theoretical

modeling software in computer to reassemble dissected histological slices together. In

order to get high resolution image of soft tissue, the sample should be sectioned and

placed on slice. Thus making the 3D reconstruction a labor-intensive work due to

hundreds of slices prepared. Despite this limitation, optical microscope does have some

advantages over the other two imaging techniques. Stains can be applied to samples on

slices which make it possible to differentiate even individual cell type in the tissue. It is

superior to CT and MRI because the differentiation is based on the feature of cells not on

the intensity or signal intensity. Recent approach to acquire deep imaging in tissue is

attributed to the development of non-linear optical microscopy. While linear optical

microscope such as confocal microscope involves a single photon and light-matter

interaction to generate contrast which depends linearly on the incident light intensity, non-linear microscope such as two-photon microscope uses multiple photons in the generation of contrast which makes it less sensitive to scattering and thus is better to image in depth. Due to its ability to image biological tissue to the depth of around 1mm, multiphoton microscope has been used to noninvasively study microstructure and to investigate the relation between bulk mechanical property and optical property in collagen gel [43].

2.2.3 Soft tissue modeling

People have always tried building model to describe the structural and function of our living body. For soft tissue modeling, the benefits include knowing injury mechanisms and damage threshold, understanding the diseases related mechanical property change and optimizing the design of tools and instrumentation used in surgery. Due to the complex mechanical behavior of soft tissue, the modeling methods are mainly based on the different mechanical characterization of soft tissue. As continuum mechanics is most often used to serve as a mathematical framework to describe deformation of soft tissue, it will be discussed with basic concepts of linear and nonlinear elasticity and FEM modeling technique.

Continuum mechanics

Continuum mechanics is a branch of mechanics that treat material as continuous. It is a theory that describes the relationships between gross phenomena and deems an

infinitesimal volume of materials as a particle in the continuum. In the field of continuum

mechanics, tensor is often used to describe the equation related to deformation of material.

Linear elastic modeling

Linear elastic modeling assumes the relation between loading and strain is linear and the

deformation of the sample can be recovered completely upon removal of the loading. Due

to its simplicity, linear elasticity theory has been widely used in soft tissue modeling. The

Cauchy stress σ is a function of the infinitesimal strain E. According to Cauchy-Hooke's

law,

$$\sigma_{ij} = C_{ijkl}E_{kl}$$

Where C_{ijkl} is called elasticity tensor. C_{ijkl} is a matrix containing 36 coefficients,

however, since it is symmetric which means $C_{ijkl} = C_{jikl}$, it only has 21 independent

coefficients. The number of independent coefficient can be further reduced if it is more

symmetric (orthotropic, transversely isotropic and isotropic). If the material described is

isotropic, then we only have two independent parameter of C_{ijkl}. We can further

transform the equation and get the relation between Young's modulus E, Poisson's ratio ν

and shear modulus μ

$$\mu = \frac{E}{2(1+v)}$$

Although soft tissue is intrinsically anisotropic, the two parameters ν and μ are in

common use to describe the property of soft tissue in many research. One of the models

based on linear elasticity is Hertz model which is originally used to describe the elastic behavior of two spheres in contact. It is often applied to evaluate the cell's elastic moduli by indenting into the sample using AFM.

$$F = \frac{4}{3}\frac{E}{(1-v^2)}R^{\frac{1}{2}}\delta^{\frac{3}{2}}$$

Where F represents the force, E is the elastic modulus of the sample, v is Poisson's ratio, R is the radius of indenter and δ is the indentation depth.

Linear viscoelastic modeling

Since most soft tissue exhibit viscoelastic behavior which means they have both the property of elastic solid and viscous fluid. Linear viscoelasticity is the kind of theory that deems the creep response and load separable when making the simulation. The linear viscoelastic property can be represented by separating stresses and strains into the hydrostatic (H) and deviatoric (D) components.

$$\sigma = \sigma^H + \sigma^D$$

$$\varepsilon = \varepsilon^H + \varepsilon^D$$

Hydrostatic components result in the change of volume while maintain shape, deviatoric components lead to the deformation of shape but remain the same volume. The hydrostatic stresses and strains have certain relationship given as

$$\sigma^H = 3K\varepsilon^H$$

Where K is the bulk modulus equals to E/3(1-2 ν). Deviatoric stresses and strains can also be related by

$$\sum_{i=0}^{N} p_i \frac{\partial^i \sigma^D}{\partial t^i} = \sum_{j=0}^{M} q_j \frac{\partial^j \varepsilon^D}{\partial t^j}$$

where p_i and q_j are material constants. M and N depends on the number of material constants needed to fit well with the experimental results.

As already mentioned above, stress relaxation and creep function are two specific material behavior of soft tissue. The viscoelastic property is described using models containing linear or parallel combination of spring and dashpot which has been discussed previously.

FEM modeling

The finite element method (FEM) is a numerical technique to find approximate solutions to field equations, especially partial differential equations and has been applied to simulate the deformation of soft tissue by solving equations of continuum mechanics. In order to simulate a structure with FEM, it is first divided into simple parts called elements such as tetrahedrons and quadrilaterals. The point to join one element with an adjacent element is called node, and the assembling of all the elements together create the whole structure. To describe the force and displacement relation at each node, a stiffness term K^n is introduced. The whole structure stiffness matrix K can be derived by reassembling individual elements. When the material is under quasi-static condition, the element behavior can be characterized as

$$Ku = F - R$$

where F and R are the external and internal node forces vector. Based on that, algebraic

equations can be then solved. Although most FEM techniques are optimized for linear

elastic problems, it is applied to simulate the response of biological soft tissue by solving

complex constitutive equations in recent years. Generally, the quality of simulation

largely depends on the generation of mesh but it is a trade-off between time and fine

mesh. Besides, the speed of simulation is also influenced by the constitutive law used,

material property chosen and scale of the deformation. Thus, the pre-process is crucial to

the accuracy and efficiency of FEM modeling.

2.3 The influence of cell and tissue mechanical property on disease states

The relation between biomechanics and human disease has always been a focus of

biomedical research. The application of traditional solid and fluid mechanics concept to

biological tissue and cells has made it possible to quantitatively analyze the

phenomenological responses associated with biological systems. With the rapid advance

in engineering and imaging techniques, we are now be able to make new progress in

studying mechanical property of tissues and even individual cells.

2.3.1 Disease related cell mechanics

Our living body consists of hundreds of different cells and work as a multi-

molecular collective. In order to understand the connections among cellular and

cytoskeletal mechanics, biological function and disease state, the first step is to

investigate the influence of physical forces and mechanical structure change on living cell and tissue and how these factors affect the cellular decision making process. As there are a large number of people suffering from cancer and cardiovascular dysfunction and both of which are diseases among the highest mortality rate, biomechanical studies in these areas are considered of great significance in the development of disease diagnostics, prophylactic and therapeutics. Picture below gives a schematic illustration of relationships among cell structure, biological process and disease states.
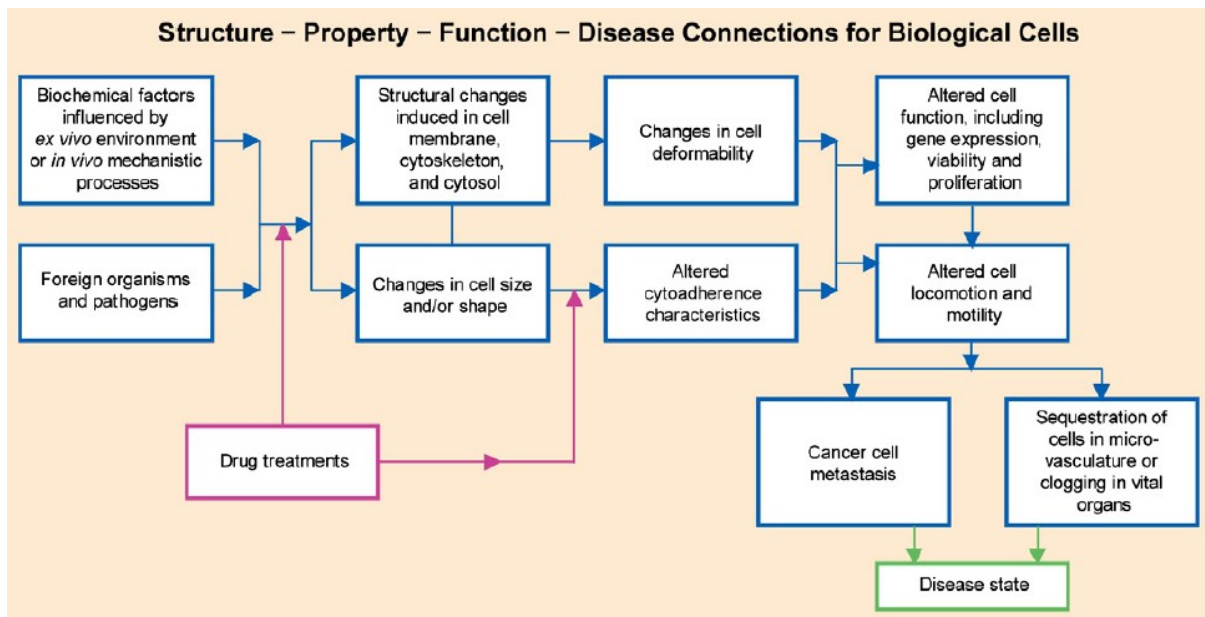
Figure 2.21 Structure-Property-Function-Disease Connections for biological cells [44]

Biomechanics in cancer cells

With the application of continuum mechanics to biological and cellular problem, the study of biomechanical process can now be well categorized and quantified. The research

at individual cell level has also benefited a lot from the concept and result in significant implications of cancer diagnosis and treatment.

Cancer is a disease caused by dysfunction of biological cells, the diseased cells, known as cancer cells, proliferate uncontrollably and result in the disruption of tissue function. The discovery of proto-oncogene that can mutate into oncogene which has a potential to turn normal cell into a cancer cell, has laid the foundation of understanding the roles that molecular and genes play in creating cancer. Figure below gives a demonstration of cell invasion-metastasis cascade.
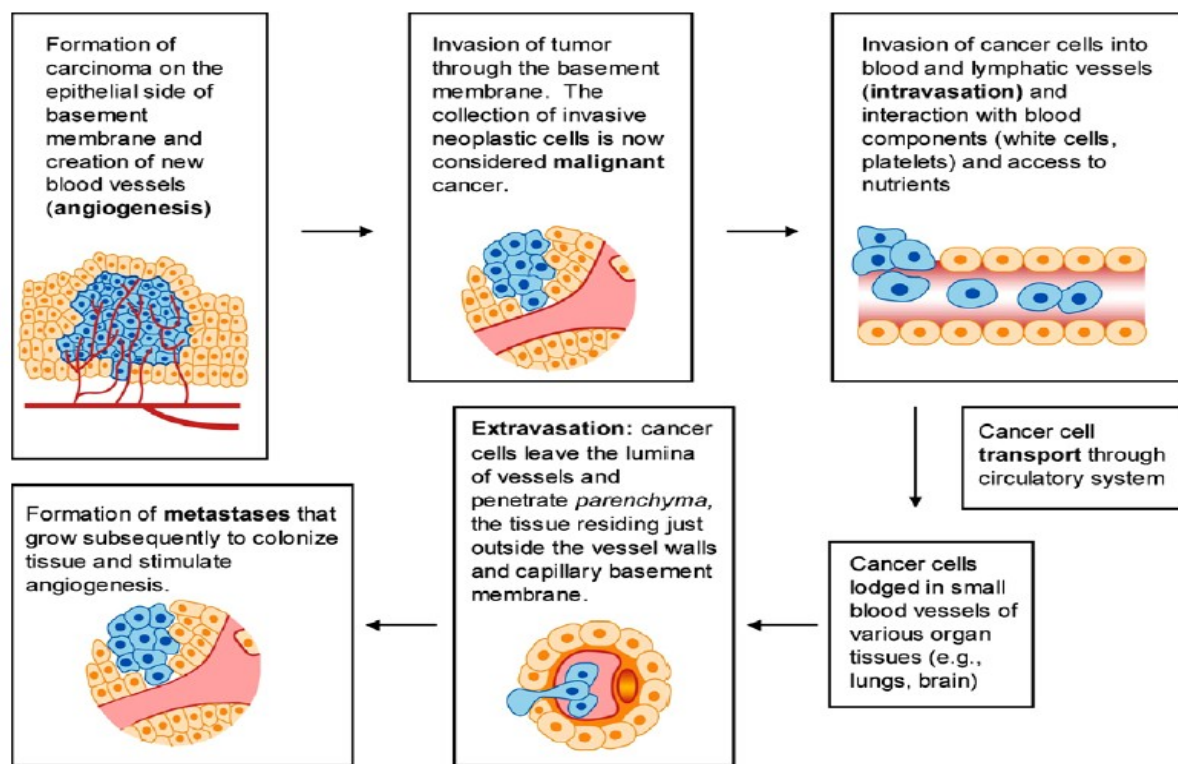
Figure 2.22 Various steps involved in cancer cell invasion-metastasis cascade [45].

Since a cell undergoes a series of genetic changes as it transits to malignancy, there is an increasing interest in understanding the influence of changes in cell structure, mechanics and microenvironment (e.g., cytoskeletal structure, geometry and topology of extracellular matrix (ECM)) on the malignant transformation [45-47]. Alterations in the mechanical interaction between cells and their environment have been proved to contribute to tissue dysplasia result in tumor initiation. Ample examples include transformed epithelia cells which have significantly different cytoskeletal structure than the normal cell which disrupt cell-cell junctional integrity, increase the viability of anchorage-independet cell and enhance invasion [48-50]. Moreover, the stiffening of tissue and ECM accompanied in the cancer formation plainly exist in tumor systems and is well characterized in mammary tumor tissue [51]. The increase in stiffness in turn promote the growth, survival and invasion of tumor cells by increasing tractional force, focal adhesion maturation and signaling through actomyosin contractility [52-54].

A variety of probing techniques have been applied to study the mechanical property of cancer cells. Some techniques are used to apply force on a portion of cell surface which results in nanometer displacement. Such methods include AFM, magnetic twisting cytometry (MTC) and instrumented depth sensing technique. Other methods such as optical tweezer(OT), micro-postarray deformation (mPAD) and micropipette aspiration (MA) induce force on the whole cell while submicrometer displacement can be monitored optically. Among them, AFM can be used with confocal fluorescence imaging to not only get the mechanical property of benign and cancerous cell but also acquire the corresponding information of cytoskeletal structure [55]. Certain study in

43

breast cancer cell is trying to compare cell elasticity and effect of loading rates between benign and malignant cell while investigating the cellular actin cytoskeletal structure [56].

Methods like optical tweezer can be used to efficiently collect abnormal cells based on their deformability [57]. Although the force exerted on the cell is not sufficiently large to result in large deformability, it is still a useful soring method for isolating cells from exfoliative cytology [58].

The availability of techniques to measure the force vs. displacement of cells makes it possible to analyze the mechanical change accompanied with other chemical, biological and genetic pathways through tumor formation. Further investigation in how mechanical responses are influenced by transformation from normal subcellular structure to irregular cytoskeletal network may contribute to a better understanding of cancer at the molecular and cellular level.

Disease related cardiovascular cell mechanics

For cardiovascular system, one of the most thoroughly studied cells is red blood cell. Normal human RBC (red blood cell) is in biconcave shape and has a highly flexible membrane which enables its deformability for circulation. The morphology and mechanics of RBC can be altered by a variety of diseases including hereditary disorders and parasite infections, which may cause the disruption of circulation. Elliptocytosis is an inherited blood cell disease which is characterized by a large amount of blood cells of suffers being elliptical rather than typical disc shape. While the precise cause of the disease is still unclear, sufficient case studies suggest the disruption of horizontal

cytoskeleton interactions may have an influence in HE and leads to reduced elasticity and durability of HE blood cells [59]. Under shear stress, the instability of cytoskeleton result in destabilized network structure and the formation of elliptocytic cell shapes. Sickle cell anemia disease is another inherited blood disorder causing sickle-shaped RBCs. It is believed that the abnormal form of hemoglobin attribute to the disease. Sickle cells exhibit decreased deformability with increased viscosity which causes the decrease in blood flow velocity. Malaria is a wide-spread blood cell disease affecting 500 million people. The disease is induced by parasite modification of RBCs affecting the mechanical property of cells membrane through asexual parasite stages. The deformability change during parasite development has been studied using optical tweezers indicating the role of RESA (ring-infected erythrocyte surface antigen) in deformability of ring stages [60]. The mechanical property of blood cells can also be investigated by ektacytometry [61,62], micropipette aspiration [63] and AFM. Also, biomechanical models were developed to quantitatively predict the motion and deformation of blood cells in vivo [64,65]. The key factor of these models is the preservation of membrane area by lipid bilayer under tension. The newly developed models for RBC can be an efficient support in the biomechanical analysis process. Cardiomyocytes are muscle cells specific to myocardium. These cells contain myofibrils, which are responsible to the contractility of cell. Cardiomyocytes are extremely sensitive to the mechanical environment for their optimal development and function. If they grow on normal matrix condition range from 10-15kPa, they have the capability to differentiate and beat. However, if they are grown on much stiffer substrate (35-70KPa), they will lose their striations and decrease in the frequency of beating [66].

The mechanical property of cardiac muscle is closely related to heart disease. Significantly much stiffer muscle strips were found in those suffering from diastolic heart failure than normal muscle [67]. However it was suggested that the increased stiffness in muscle strips is attributed to the change in matrix rather than cardiac muscle cell due to the fact that the stiffness of muscle strips remain the same even myofibrils and titin were extracted. AFM was used to test the mechanical property of cardiomyocte which may have an influence on left ventricular dysfunction. The result indicates the mechanical property of cardiomyocyte changes with aging as well as the change in ECM participating in the LV diastolic dysfunction [68,69].

Basically, three main cell types play a particularly important role in the biomechanics of arterial wall: endothelial cells, smooth muscle cells and fibroblasts. Endothelial cells make up the interior surface of blood vessel. They alter their shape, size and cytoskeletal structure under the change of flow-induced shear stress [70].Vascular smooth muscle cell is a specific type of muscle cell found in vessels. It is believed to have influence on certain vascular diseases such as atherosclerosis due to its mechanical property and change in phenotype. In atherosclerosis, the vascular smooth muscle cell gradually undergoes a transformation from contractile to synthetic phenotype. The synthetic phenotype of VSMC cannot contract and has a high rate of ECM synthesis [71]. The phenotype shift is not unique to atherosclerosis, the environment change in any other vascular disease may also have an effect on VSMC and result in the alteration in phenotype. Micropipette system has been utilized to study the tensile property of VSMC with the result indicating contractile VSMC has higher elastic modulus than synthetic

VSMC [72,73]. AFM was also used to investigate the mechanical property change in concert with the phenotype shift which can be helpful to elucidate the development of vascular disease [74].

2.3.2 Disease related tissue mechanics

The overall object of tissue mechanics is to illustrate the function of a system by analyzing its geometry, biomechanical property and boundary conditions. When a system suffers from disease, in some cases, the disease will contribute to the alteration in mechanical property of tissue or vice versa. The study of mechanical change arise from certain disease will help us not only better understand the cause of dysfunction but also improve the diagnosis and treatment of the disease.

CV system

The cardiovascular system consists of two major components, the heart and blood vessels. Its function includes supplying blood to organs throughout our body form left heart and circulating blood within right heart and lungs. Blood vessels, in the meantime, serve as the highway for transportation and conserve the blood pressure in diastole. Cardiovascular disease is a class of disease related to cardiovascular system which mainly refers to the dysfunction of heart and peripheral circulation. Atherosclerosis is a disease caused by the thickening of artery wall as a result of accumulation of lipids, calcium, necrotic debris, and excessive matrix and cells. While atherosclerosis is one of the major contributing factors to cardiovascular disease, the endothelial dysfunction is believed largely to affect the development of atherosclerosis [75]. The morphological and

mechanical changes in arterial wall can be deemed as indices of the development of atherosclerosis and further investigation may contribute to the early diagnosis of cardiovascular disease. Since atherosclerosis is a complex disease that can affect the entire vascular wall, studies considering the entire stress field within the wall are needed for biomechanical approach to it. The most regular and common biomechanical test for artery is the cyclic inflation performed on straight segment whose length is maintained near its in vivo value. Extra tests such as cyclic extension and torsion test can be conducted at fixed diameter [76]. Data from these tests reveal a mildly non-linear response in circumferential direction but highly non-linear in axial direction. According to that, it indicates the overall non-linear response of passive vessel to finite deformation.
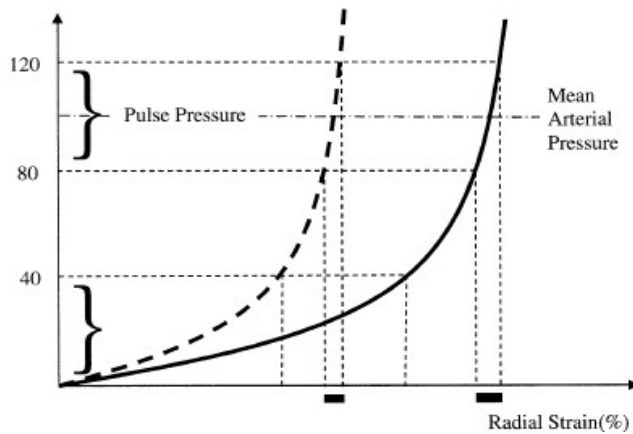
Figure 2.23 Arterial elasticity characteristics at different preloads. Solid curve refers to normal tissue while dashed curve refers to less compliant diseased tissue [77].

Due to the complexity of its mechanical property, multiple constitutive relations are required to describe different behaviors exhibited by the same artery. Pseudoelasticity, viscoelasticity, theory of solid–fluid mixtures, continuum damage mechanics and thermal

damage mechanics are different aspects of mechanical property which may be considered in the analysis of specific condition. In the exploration of atherosclerosis related tissue mechanics, studies of atherosclerotic plaque indicate plaque exhibit a strongly non-linear relationship between stress and finite strain and has a viscoelastic character [78]. Moreover, plaques which are highly calcified turn out to be much stiffer than those primarily consisting matrix proteins [79]. Tensile behavior in the circumferential direction and compressive behavior in the radial direction were measured to acquire physiological characterization of atherosclerotic plaque [80]. The combination of data on plaque behavior and the associated constitutive relations may help in the modeling of disease progression and treatment.

Disease related cartilage mechanics

Cartilage is a load-bearing connective tissue that exists in many areas of human body especially joints between bones. The primary function of cartilage is to support joints and distribute forces loaded on it. Cartilage can also stabilize the motion of joint and contribute to joint lubrication. The study of cartilage mechanics tries to analyze the function-form relationship of cartilage morphology, mechanical behavior and the change of mechanisms associated with disease process.

Osteoarthritis, one of the common cartilage diseases, is a kind of mechanical abnormalities result in progressive degeneration of cartilage. The stiffness of cartilage with osteoarthritis decreases along with a couple of changes in structural and mechanical property such as tensile, compressive and shear behaviors [81]. The degeneration of

cartilage and bone may result in the dysfunction of joint motion and makes patients suffer from disability and pain [82]. The degeneration can be clarified in microscopic level as fibrillation of the articular surface, loss in tissue and occurrence of crack and cleft [83,84]. However, due to the inconsistence of osteoarthritis in human joint, it is often hard to precisely characterize such a disease. Often, the approach to study cartilage mechanics related to osteoarthritis is focused on changes of material behavior as tension, compression and shear. Research result shows the tensile modulus of osteoarthritis affected cartilage can decreases as much as 90% compared to normal tissue which reveals the disrupted collagen fibril network [85]. The compression of cartilage is studied by using a biphasic constitutive law characterized as solid and fluid phases [86]. The degeneration makes the cartilage more compliant and deformable in compression but has less influence on hydraulic permeability [87,88]. Torsional shear testing indicates the loosening in collagen-proteoglycan matrix and a shear behavior dependence on hydration [89,90].
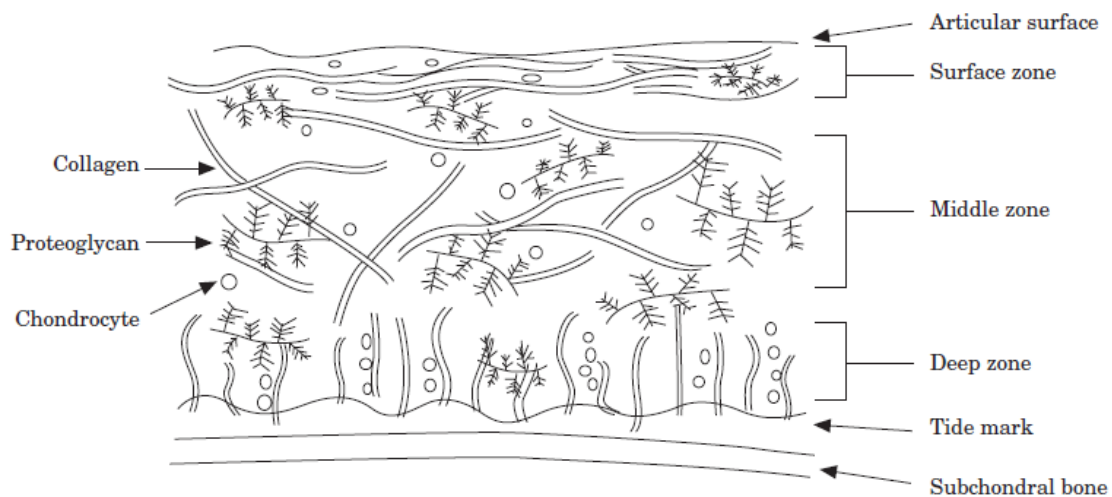
Figure 2.24 Schematic of articular cartilage [81].

The analysis of cartilage degeneration is advanced by applying appropriate model and imaging technique. Anterior cruciate ligament transection model (ACLT) is the most widely used model for the study of cartilage degeneration. ACLT produces increased anterior drawer in the knee joint at extension and at 90°of flexion reflecting the morphological and histological changes [91]. MRI is introduced in the quantitatively analysis of cartilage morphology, structure and function in health and disease [92]. Experimental osteoarthritis models as well as imaging technique used in post-processing have been successful in reporting the cartilage changes associated with the disease and lay the foundation of studying the degeneration progress.

2.4 Tissue mechanics based on multi-cellular network

The advancing experimental abilities nowadays make it possible to gather a large number of biophysical and biological data in cellular level. An efficient transformation of the information from the cellular scale to the whole tissue where multiple cell types are involved to describe the tissue behavior associated with cellular change influenced by disease progression. The mechanical property of a cell is controlled in many ways and largely affected by the communication with its environment. Thus, in order to describe multi-cellular system based on cells, a thorough consideration of network among cells and the environment is needed. Moreover, to integrate cellular information gathered into complex system, computational technique and appropriate model is essential. Agent-based model seeks to study the multicellular interactions important in tissue patterning

which allows investigation of properties emerging from the collective behavior of individual units.

2.4.1 Cell-cell interaction and many cell interaction

Cell-cell interaction refers to the interaction between neighboring cells that play an important role in controlling both the fate and function of individual cells as well as governing the emergent properties of associated tissue. Cell-cell interactions are fundamental and widespread character in tissue and organ. Some cell-cell interactions are temporary, such as the interaction between immune system and cell, while in other cases, stable cell-cell junction occurs and regulate the organization of cells in tissue. Study reveals cell proliferation is closely related to intercellular communication across gap junction and the disruption of such communication is believed to link to several pathologies [93]. It has been indicated that gap-junctional intercellular communication plays an important role in the maintenance of homeostasis in the process of embryogenesis, differentiation, growth, and regeneration [94]. Previous research shows the interconnection of granulation tissue fibroblasts due to extensive cell-cell contact. Fibroblast was found to cultivate and operate in proliferation of tumor cells in nude mice which indicates the essential role fibroblast plays to initiate a tumor in host [95]. Force exerted between interconnection fibroblast was measured by isolating and pairing them to acquire contractile force [96]. Experimental result suggests the inhibition of gap junction is associated with the inhibition of wound contraction and is directly related to the role of cell-cell interaction which can result in reorganization of matrix. The study of force map indicate around 10-8 N can be generated by single cell [97]. Such forces can cause

reasonable deformation of other individual cells and in the surrounding matrix to about 30-50μm. To measure the mechanical parameters of cell, it is either suspended in a spherical shape or spread on a 2-D substrate [98,99]. Certain models such as JKR model(Johnson–Kendall–Roberts) can be applied to describe the mechanical property of spherical shape cells in suspension [100]. MEMS-based techniques are developed to quantify the mechanical interaction between cells which requires the resolution in force and displacement of picoNewtons and nanometers. However, cells in the tissue are surrounding each other which means a single cell is compressed by its surrounding cells not only in contact with another individual cell. This leads to a refinement of the model by considering the volume conservation based on the relaxing force generated by strongly compression of surrounding cells. The idea of interactions among cells has made significant progress in understanding tissue dysfunction and diseases. It has becoming clear that cell-cell interaction is a critical component in tumor progression for instance [101]. Cell-Cell contact status has been characterized as a necessary property to understand in order to fully describe a more complex system.

2.4.2 Cell-Matrix interaction

In our human body, there are around 1013 cells and approximately 200 types of different cells. ECM serves as a residence for each one of these cell types. It is defined as the extracellular part of tissue which provides support to cells and performs other important functions. It has also been known that cells exert forces on their matrix and the elasticity of matrix have an influence on the forces of cells and their motility. Many cell types including fibroblasts, smooth muscle cells and endothelial cells are proved to contract

collagen matrices. The contraction of matrix is a highly conserved feature of cell motile

behavior and has the potential to change the structure of tissue [102]. Therefore, a

thorough knowledge of the mechanism of cell-matrix interaction is indispensable for

tissue mechanics and tissue engineering. The force exerted on the matrix by the cell

which is often termed tractional force is believed to be responsible for the organization of

the matrix in early studies. However, it is a complex and interactive mechanical system

including several variables such as cell-matrix tension states, tractional force relative to

matrix stiffness and growth factor environment that regulate the interaction between cells

and protein matrices. It is also possible for cells to penetrate and move through the matrix

due to its porosity and the geometry of the matrix has an influence on cell adhesion which

is one of the major design principles to guide cell behavior and tissue formation [103].

Experiment results shows the stiffness of matrix can alter the nature of cell-cell

interaction. Cells tend to remain in contact on compliant substrate while migrate away

from each other on stiffer substrates [104]. In both the tissue and cell level, many

activities in our body largely depend on the property of the matrix. Angiogenesis is the

process of growing new blood vessel from pre-existing vascular network. According to

its vital role in wound healing and tumor formation, many researches have focused on

how to control angiogenesis in the engineering of most tissues and how to inhibit tumor

growth by limiting blood supply related to angiogenesis. Most of these studies require a

better understanding of the influence of matrix mechanics and cell-matrix interaction.

Studies reveal that endothelial cells can generate new vasculature if plated on collagen

gels, fibrin gels or matrigel scaffolds; otherwise, they will form tubules given enough

time for secreting their own matrix [105,106]. Obviously, these gels are relatively

compliant compared to glass and tissue culture polystyrene. Thus, mechanical property of

the extracellular matrix seems to be a determinant in angiogenesis and require further

investigation. Although the mechanism of how cell sense each other is still not clear,

endothelial cells are observed to undergo shape changes during network formation by

time-lapse microscopy. Previous hypothesis points out that there is a balance between

cell-cell and cell-matrix adhesion placed on different matrices. The more cell-cell contact

on more compliant substrate is believed to arise from cells unable to adhere well

to the substrate. Based on that, to find an appropriate balance between cell-matrix and

cell-cell adhesion may be an effective way to control angiogenesis. Besides, cell-cell

adhesion may in turn affect the substrate by exerting traction force communicating

through matrix which results in the deformation of substrate. As it is well established that

cells exert more traction force on stiffer substrate while the disturbance field on a stiff

substrate is less than a compliant one, the two competing factors result in an uncertain

relationship between the average distance of deformation and the compliance of substrate.

However, result shows cells on compliant substrate induce larger displacement of the

substrate than on stiff substrate even they exert weaker forces [107]. Further investigation

suggests that cell can have a mechanical influence on its neighboring cell by extending

stress through substrate [108]. A better understanding of cell-matrix interactions could

help us to better control the formation of tissue by mediating cells associated with each

other.

2.4.3 Agent based model

Biological tissue is a composite of cellular and acellular material arranged in certain structures and is considered as a complex system due to its specific temporal and spatial dynamic behavior based on multifaceted composition. Understanding the complex biological system requires the integration of the autonomous entities interactions with each other and the system environment to predict higher level emergent patterns. Four dispensable elements are involved in the elucidation of tissue pattern, 1) Characterize all the autonomous entities within tissue such as molecular and cellular components; 2) Comprehend the way all the components act with each other; 3) Integrate the temporal and spatial dynamic behavior of components into system 4) Simulate the phenomena of system considering all these events. Agent based-modeling (ABM) has been recently applied to biomedical research [109]. ABM is characterized as a "bottom-up" modeling technique assuming the integration of simple rules governing agent reactions can generate a complex higher level outcomes observed in a certain system. Such concept is highly compatible with biological system such as tissue which is largely affected by cellular behavior and its environment. Typically, in the process of modeling biological phenomena, the individual agent represents a single cell and certain tissue can be composed of several different agents. As different agents have individual attributes and state variables, these characters are corresponding to cellular dynamic behavior and phenotypic state. The most important part in agent-based modeling is the establishement of rules governing individual agents. It defines initial conditions, boundary conditions as well as agent-agent interactions and agent-environment

interaction. The rules determines how the individual agent will change related to the given information and these agent behaviors aggregat to produce emergent phenomena.
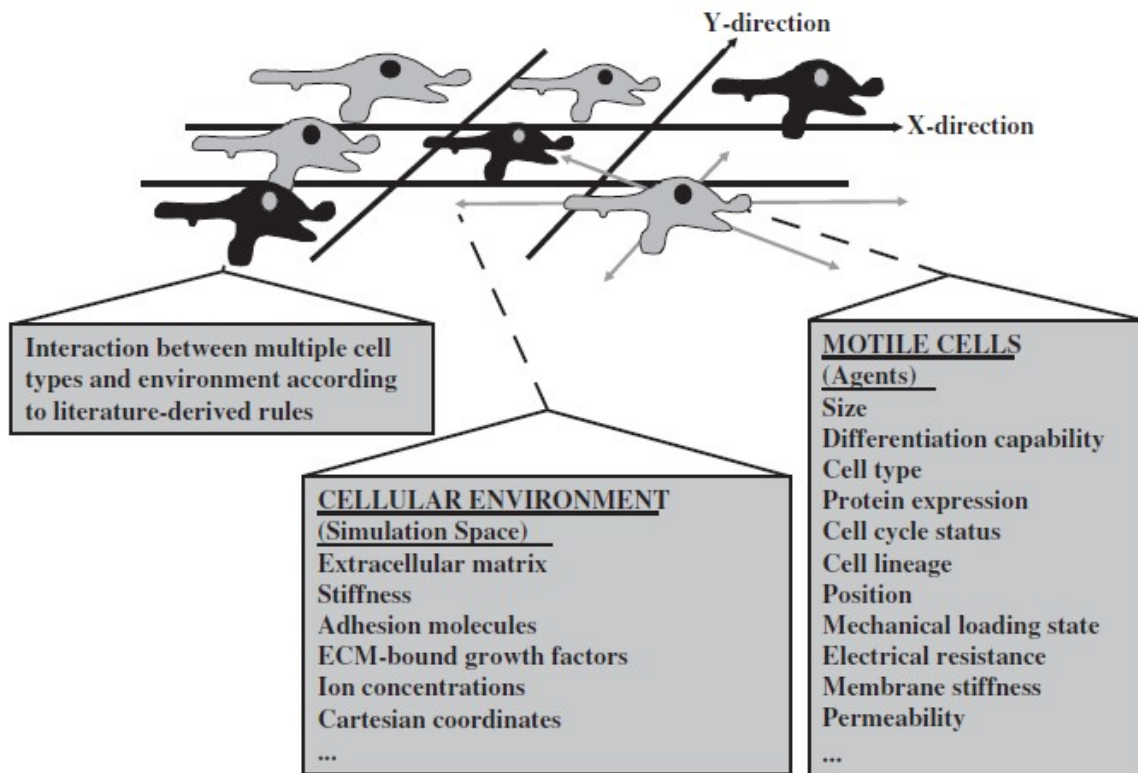
Figure 2.25 Schematic of agent based model [109].

As shown above, the attributes of cells and environment can be described by a variety of parameters. However, if we only care about changes in certain aspects such as the tissue dysfunction affected by mechanical change, then we can simply focus on parameters which have an influence on the interested apsect. ABM can not only simplify the process but also deal with spatio-temporal interplay which enables the observation of growning phenomena. Some areas of biomedical research has already employed ABM for

investigation. Ample examples include tumor formation which is a complex process depending on many cell types, their mechanical behavior and gene expression. Some tumor models are trying to determine the contributing factors to tumor progression [110]. Other processes highly depend on cell-cell interactions and cell-matrix interactons can also utilize ABM as an efficient way for analysis. Thus, ABM can also be applied to physiological and pathological events as well as morphogenesis of tissues. In order to ensure the realism of the complex biological system, the ABM should be integrated with experiments. First, we need to derive the govering rules for agents from published literature or new experiments. Second, the rules should be parameterized to make the model output matrix fit with experiment data. Third, validating the ABM output by comparing it with experiment data which were not used in the parameter fitting process, finally we can use the validated ABM model for predictions. Because cell-based mechanics measurements are relatively recent, this type of approach as not yet been

applied to cell-tissue biomechanical systems.
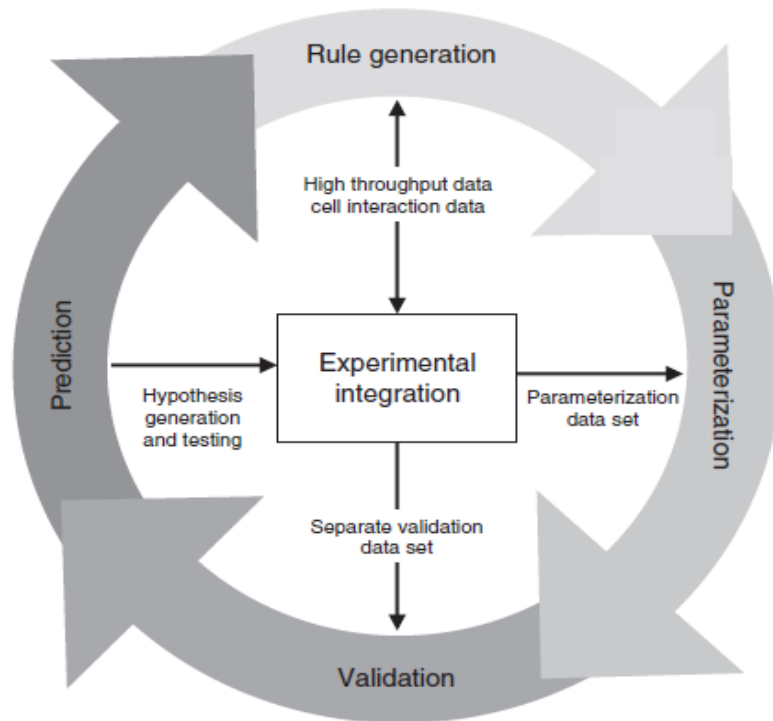
Figure 2.26 Integration of ABM into experimetal data [109]

2.5 References

[1] Cooper, G. M. (1997). The cell a molecular approach (Washington, DC: ASM Press).

[2] Charras, G. T., and Horton M. A. *Single cell mechanotransduction and its modulation analyzed by atomic force microscope indentation*. Biophysical Journal, 2002. 82: 2970-2981.

[3] Wu, H. W., Kuhn T., and Moy V. T. *Mechanical properties of l929 cells measured by atomic force microscopy: Effects of anticytoskeletal drugs and membrane crosslinking*. Scanning, 1998. 20: 389-397.

[4] Humphrey, J. D. *On mechanical modeling of dynamic changes in the structure and properties of adherent cells*. Mathematics and Mechanics of Solids, 2002. 7: 521-539.

[5] Janmey, P. A., Euteneuer U., Traub P., and Schliwa M. *VISCOELASTIC PROPERTIES OF VIMENTIN COMPARED WITH OTHER FILAMENTOUS BIOPOLYMER NETWORKS*. Journal of Cell Biology, 1991. 113: 155-160.

[6] Ingber, D. E. *Tensegrity: The architectural basis of cellular mechanotransduction*. Annual Review of Physiology, 1997. 59: 575-599.

[7] Ingber, D. E. *Mechanobiology and diseases of mechanotransduction*. Annals of Medicine, 2003. 35: 564-577.

[8] Bhushan, B., and Li X. D. *Nanomechanical characterisation of solid surfaces and thin films*. International Materials Reviews, 2003. 48: 125-164.

[9] Zhu, C., Bao G., and Wang N. *Cell mechanics: Mechanical response, cell adhesion, and molecular deformation*. Annual Review of Biomedical Engineering, 2000. 2: 189-226.

[10] Radmacher, M. *Measuring the elastic properties of living cells by the atomic force microscope*. Atomic Force Microscopy in Cell Biology, 2002. 68: 67-90.

[11] Costa, K. (2006). Imaging and Probing Cell Mechanical Properties With the Atomic Force Microscope. In Cell Imaging Techniques, D. Taatjes, and B. Mossman, eds. (Humana Press), pp. 331-361.

[12] Rotsch, C., and Radmacher M. *Drug-induced changes of cytoskeletal structure and mechanics in fibroblasts: An atomic force microscopy study*. Biophysical Journal, 2000. 78: 520-535.

[13] Benoit, M. *Cell adhesion measured by force spectroscopy on living cells*. Atomic Force Microscopy in Cell Biology, 2002. 68: 91-114.

[14] Willemsen, O. H., Snel M. M. E., Cambi A., Greve J., De Grooth B. G., and Figdor C. G. *Biomolecular interactions measured by atomic force microscopy*. Biophysical Journal, 2000. 79: 3267-3281.

[15] Lim, C. T., Zhou E. H., Li A., Vedula S. R. K., and Fu H. X. *Experimental techniques for single cell and single molecule biomechanics*. Materials Science & Engineering C-Biomimetic and Supramolecular Systems, 2006. 26: 1278-1288.

[16] Smith, S. B., Cui Y. J., and Bustamante C. (2003). Optical-trap force transducer that operates by direct measurement of light momentum. In Biophotonics, Pt B, G. Marriott, and I. Parker, eds., pp. 134-162.

[17] Mohanty, K., Mohanty S., Monajembashi S., and Greulich K. O. *Orientation of erythrocytes in optical trap revealed by confocal fluorescence microscopy*. Journal of Biomedical Optics, 2007. 12.

[18] Kuo, S. C., and Sheetz M. P. *FORCE OF SINGLE KINESIN MOLECULES MEASURED WITH OPTICAL TWEEZERS*. Science, 1993. 260: 232-234.

[19] Hochmuth, R. M. *Micropipette aspiration of living cells*. Journal of Biomechanics, 2000. 33: 15-22.

[20] Sander, E. A., Stylianopoulos T., Tranquillo R. T., and Barocas V. H. *Image-based multiscale modeling predicts tissue-level and network-level fiber reorganization in stretched cell-compacted collagen gels*. Proceedings of the National Academy of Sciences of the United States of America, 2009. 106: 17675-17680.

[21] Ingber, D. E. *Tensegrity I. Cell structure and hierarchical systems biology*. Journal of Cell Science, 2003. 116: 1157-1173.

[22] Li, J., Dao M., Lim C. T., and Suresh S. *Spectrin-level modeling of the cytoskeleton and optical tweezers stretching of the erythrocyte*. Biophysical Journal, 2005. 88: 3707-3719.

[23] Kan, H. C., Udaykumar H. S., Shyy W., and Tran-Son-Tay R. *Hydrodynamics of a compound drop with application to leukocyte modeling*. Physics of Fluids, 1998. 10: 760-774.

[24] Lim, C. T., Zhou E. H., and Quek S. T. *Mechanical models for living cells - A review*. Journal of Biomechanics, 2006. 39: 195-216.

[25] Guilak, F., and Mow V. C. *The mechanical environment of the chondrocyte: a biphasic finite element model of cell-matrix interactions in articular cartilage*. Journal of Biomechanics, 2000. 33: 1663-1673.

[26] Humphrey, J. D. *Continuum biomechanics of soft biological tissues*. Proceedings of the Royal Society a-Mathematical Physical and Engineering Sciences, 2003. 459: 3-46.

[27] Fung, Y. C., Fronek K., and Patitucci P. *PSEUDOELASTICITY OF ARTERIES AND THE CHOICE OF ITS MATHEMATICAL EXPRESSION*. American Journal of Physiology, 1979. 237: H620-H631.

[28] Fung, Y. C. (1993). Biomechanics : mechanical properties of living tissues (New York: Springer-Verlag).

[29] Humphrey, J. D., and Rajagopal K. R. *A constrained mixture model for growth and remodeling of soft tissues*. Mathematical Models & Methods in Applied Sciences, 2002. 12: 407-430.

[30] Lin, A. S. P., Barrows T. H., Cartmell S. H., and Guldberg R. E. *Microarchitectural and mechanical characterization of oriented porous polymer scaffolds*. Biomaterials, 2003. 24: 481-489.

[31] Lal, P., and Sun W. *Computer modeling approach for micro sphere-packed bone scaffold*. Computer-Aided Design, 2004. 36: 487-497.

[32] Simon, B. A. *Non-invasive imaging of regional lung function using X-ray computed tomography*. Journal of Clinical Monitoring and Computing, 2000. 16: 433-442.

[33] Taylor, C. A., and Draney M. T. *Experimental and computational methods in cardiovascular fluid mechanics*. Annual Review of Fluid Mechanics, 2004. 36: 197-231.

[34] Watz, H., Breithecker A., Rau W. S., and Kriete A. *Micro-CT of the human lung: Imaging of alveoli and virtual endoscopy of an alveolar duct in a normal lung and in a lung with centrilobular emphysema - Initial observations*. Radiology, 2005. 236: 1053-1058.

[35] Stevens, C., Remme E., LeGrice I., and Hunter P. *Ventricular mechanics in diastole: material parameter sensitivity*. Journal of Biomechanics, 2003. 36: 737-748.

[36] Augenstein, K. F., McVeigh E. R., and Young A. A. *Magnetic resonance imaging and ventricle mechanics*. Philosophical Transactions of the Royal Society a-Mathematical Physical and Engineering Sciences, 2001. 359: 1263-1275.

[37] Einarsdottir, H., Karlsson M., Wejde J., and Bauer H. C. F. *Diffusion-weighted MRI of soft tissue tumours*. European Radiology, 2004. 14: 959-963.

[38] Gilchrist, C. L., Xia J. Q., Setton L. A., and Hsu E. W. *High-resolution determination of soft tissue deformations using MRI and first-order texture correlation*. Ieee Transactions on Medical Imaging, 2004. 23: 546-553.

[39] Helmchen, F., and Denk W. *Deep tissue two-photon microscopy (vol 2, pg 932, 2005)*. Nature Methods, 2006. 3: 235-235.

[40] Wang, P., and Olbricht W. L. *Fluid and solid mechanics in a poroelastic network induced by ultrasound*. Journal of Biomechanics, 2011. 44: 28-33.

[41] Coussot, C., Kalyanam S., Yapp R., and Insana M. F. *Fractional Derivative Models for Ultrasonic Characterization of Polymer and Breast Tissue Viscoelasticity*. Ieee Transactions on Ultrasonics Ferroelectrics and Frequency Control, 2009. 56: 715-726.

[42] Weitzel, W. F., Kim K., Rubin J. M., Xie H., and O'Donnell M. *Renal advances in ultrasound elasticity imaging: Measuring the compliance of arteries and kidneys in end-stage renal disease*. Blood Purification, 2005. 23: 10-17.

[43] Raub, C. B., Suresh V., Krasieva T., Lyubovitsky J., Mih J. D., Putnam A. J., Tromberg B. J., and George S. C. *Noninvasive assessment of collagen gel microstructure and mechanics using multiphoton Microscopy*. Biophysical Journal, 2007. 92: 2212-2222.

[44] Suresh, S. *Biomechanics and biophysics of cancer cells*. Acta Biomaterialia, 2007. 3: 413-438.

[45] Lelievre, S. A., Weaver V. M., Nickerson J. A., Larabell C. A., Bhaumik A., Petersen O. W., and Bissell M. J. *Tissue phenotype depends on reciprocal interactions*

between the extracellular matrix and the structural organization of the nucleus. Proceedings of the National Academy of Sciences of the United States of America, 1998. 95: 14711-14716.

[46] Nelson, C. M., and Bissell M. J. *Modeling dynamic reciprocity: Engineering three-dimensional culture models of breast architecture, function, and neoplastic transformation.* Seminars in Cancer Biology, 2005. 15: 342-352.

[47] Paszek, M. J., and Weaver V. M. *The tension mounts: Mechanics meets morphogenesis and malignancy.* Journal of Mammary Gland Biology and Neoplasia, 2004. 9: 325-342.

[48] Kokkinos, M. I., Wafai R., Wong M. K., Newgreen D. F., Thompson E. W., and Waltham M. *Vimentin and epithelial-mesenchymal transition in human breast cancer - Observations in vitro and in vivo.* Cells Tissues Organs, 2007. 185: 191-203.

[49] Pagan, R., Martin I., Alonso A., Llobera M., and Vilaro S. *Vimentin filaments follow the preexisting cytokeratin network during epithelial-mesenchymal transition of cultured neonatal rat hepatocytes.* Experimental Cell Research, 1996. 222: 333-344.

[50] Willipinski-Stapelfeldt, B., Riethdorf S., Assmann V., Woelfle U., Rau T., Sauter G., Heukeshoven J., and Pantel K. *Changes in cytoskeletal protein composition indicative of an epithelial-mesenchymal transition in human micrometastatic and primary breast carcinoma cells.* Clinical Cancer Research, 2005. 11: 8006-8014.

[51] Paszek, M. J., Zahir N., Johnson K. R., Lakins J. N., Rozenberg G. I., Gefen A., Reinhart-King C. A., Margulies S. S., Dembo M., Boettiger D., Hammer D. A., and

Weaver V. M. *Tensional homeostasis and the malignant phenotype*. Cancer Cell, 2005. 8: 241-254.

[52] Croft, D. R., Sahai E., Mavria G., Li S. X., Tsai J., Lee W. M. F., Marshall C. J., and Olson M. F. *Conditional ROCK activation in vivo induces tumor cell dissemination and angiogenesis*. Cancer Research, 2004. 64: 8994-9001.

[53] O'Brien, L. E., Jou T. S., Pollack A. L., Zhang Q. H., Hansen S. H., Yurchenco P., and Mostov K. E. *Rac1 orientates epithelial apical polarity through effects on basolateral laminin assembly*. Nature Cell Biology, 2001. 3: 831-838.

[54] Wang, F., Weaver V. M., Petersen O. W., Larabell C. A., Dedhar S., Briand P., Lupu R., and Bissell M. J. *Reciprocal interactions between beta 1-integrin and epidermal growth factor receptor in three-dimensional basement membrane breast cultures: A different perspective in epithelial biology*. Proceedings of the National Academy of Sciences of the United States of America, 1998. 95: 14821-14826.

[55] Li, Q. S., Lee G. Y. H., Ong C. N., and Lim C. T. *AFM indentation study of breast cancer cells*. Biochemical and Biophysical Research Communications, 2008. 374: 609-613.

[56] Kumar, S., and Weaver V. *Mechanics, malignancy, and metastasis: The force journey of a tumor cell*. Cancer and Metastasis Reviews, 2009. 28: 113-127.

[57] Kuo, S. C. *Using optics to measure biological forces and mechanics*. Traffic, 2001. 2: 757-763.

[58] Guck, J., Schinkinger S., Lincoln B., Wottawah F., Ebert S., Romeyke M., Lenz D., Erickson H. M., Ananthakrishnan R., Mitchell D., Kas J., Ulvick S., and Bilby C. *Optical*

deformability as an inherent cell marker for testing malignant transformation and metastatic competence. Biophysical Journal, 2005. 88: 3689-3698.

[59] Intengan, H. D., and Schiffrin E. L. *Structure and mechanical properties of resistance arteries in hypertension - Role of adhesion molecules and extracellular matrix determinants*. Hypertension, 2000. 36: 312-318.

[60] Diez-Silva, M., Dao M., Han J. Y., Lim C. T., and Suresh S. *Shape and Biomechanical Characteristics of Human Red Blood Cells in Health and Disease*. Mrs Bulletin, 2010. 35: 382-388.

[61] Cranston, H. A., Boylan C. W., Carroll G. L., Sutera S. P., Williamson J. R., Gluzman I. Y., and Krogstad D. J. *PLASMODIUM-FALCIPARUM MATURATION ABOLISHES PHYSIOLOGIC RED-CELL DEFORMABILITY*. Science, 1984. 223: 400-403.

[62] Dondorp, A. M., Angus B. J., Hardeman M. R., Chotivanich K. T., Silamut K., Ruangveerayuth R., Kager P. A., White N. J., and Vreeken J. *Prognostic significance of reduced red blood cell deformability in severe falciparum malaria*. American Journal of Tropical Medicine and Hygiene, 1997. 57: 507-511.

[63] Glenister, F. K., Coppel R. L., Cowman A. F., Mohandas N., and Cooke B. M. *Contribution of parasite proteins to altered mechanical properties of malaria-infected red blood cells*. Blood, 2002. 99: 1060-1063.

[64] Gov, N. S., and Safran S. A. *Red blood cell membrane fluctuations and shape controlled by ATP-induced cytoskeletal defects (vol 88, pg 1859, 2005)*. Biophysical Journal, 2005. 89.

[65] Paulitschke, M., and Nash G. B. *MEMBRANE RIGIDITY OF RED-BLOOD-CELLS PARASITIZED BY DIFFERENT STRAINS OF PLASMODIUM-FALCIPARUM*. Journal of Laboratory and Clinical Medicine, 1993. 122: 581-589.

[66] Engler, A. J., Carag-Krieger C., Johnson C. P., Raab M., Tang H. Y., Speicher D. W., Sanger J. W., Sanger J. M., and Discher D. E. *Embryonic cardiomyocytes beat best on a matrix with heart-like elasticity: scar-like rigidity inhibits beating*. Journal of Cell Science, 2008. 121: 3794-3802.

[67] Chaturvedi, R. K., Blaise M., Verdon J., Iqbal S., Ergina P., Cecere R., Devarennes B., and Lachapelle K. *Cardiac Surgery in Octogenarians: Long-Term Survival, Functional Status, Living Arrangements, and Leisure Activities*. Annals of Thoracic Surgery, 2010. 89: 805-810.

[68] Lakatta, E. G., and Levy D. *Arterial and cardiac aging: Major shareholders in cardiovascular disease enterprises - Part II: The aging heart in health: Links to heart disease*. Circulation, 2003. 107: 346-354.

[69] Lieber, S. C., Aubry N., Pain J., Diaz G., Kim S. J., and Vatner S. F. *Aging increases stiffness of cardiac myocytes measured by atomic force microscopy nanoindentation*. American Journal of Physiology-Heart and Circulatory Physiology, 2004. 287: H645-H651.

[70] Davies, P. F. *FLOW-MEDIATED ENDOTHELIAL MECHANOTRANSDUCTION*. Physiological Reviews, 1995. 75: 519-560.

[71] Owens, G. K., Kumar M. S., and Wamhoff B. R. *Molecular regulation of vascular smooth muscle cell differentiation in development and disease*. Physiological Reviews, 2004. 84: 767-801.

[72] Matsumoto, T., Sato J., Yamamoto M., and Sato M. *Smooth muscle cells freshly isolated from rat thoracic aortas are much stiffer than cultured bovine cells: Possible effect of phenotype*. Jsme International Journal Series C-Mechanical Systems Machine Elements and Manufacturing, 2000. 43: 867-874.

[73] Miyazaki, H., Hasegawa Y., and Hayashi K. *Tensile properties of contractile and synthetic vascular smooth muscle cells*. Jsme International Journal Series C-Mechanical Systems Machine Elements and Manufacturing, 2002. 45: 870-879.

[74] Qiu, H. Y., Zhu Y., Sun Z., Trzeciakowski J. P., Gansner M., Depre C., Resuello R. R. G., Natividad F. F., Hunter W. C., Genin G. M., Elson E. L., Vatner D. E., Meininger G. A., and Vatner S. F. *Vascular Smooth Muscle Cell Stiffness As a Mechanism for Increased Aortic Stiffness With Aging*. Circulation Research, 2010. 107: 615-U117.

[75] Cai, H., and Harrison D. G. *Endothelial dysfunction in cardiovascular diseases - The role of oxidant stress*. Circulation Research, 2000. 87: 840-844.

[76] Humphrey, J. D., Kang T., Sakarda P., and Anjanappa M. *COMPUTER-AIDED VASCULAR EXPERIMENTATION - A NEW ELECTROMECHANICAL TEST SYSTEM*. Annals of Biomedical Engineering, 1993. 21: 33-43.

[77] Lee, R. T., Grodzinsky A. J., Frank E. H., Kamm R. D., and Schoen F. J. *STRUCTURE-DEPENDENT DYNAMIC MECHANICAL-BEHAVIOR OF FIBROUS*

CAPS FROM HUMAN ATHEROSCLEROTIC PLAQUES. Circulation, 1991. 83: 1764-1770.

[78] Loree, H. M., Grodzinsky A. J., Park S. Y., Gibson L. J., and Lee R. T. *STATIC CIRCUMFERENTIAL TANGENTIAL MODULUS OF HUMAN ATHEROSCLEROTIC TISSUE*. Journal of Biomechanics, 1994. 27: 195-204.

[79] Huang, H., Virmani R., Younis H., Burke A. P., Kamm R. D., and Lee R. T. *The impact of calcification on the biomechanical stability of atherosclerotic plaques*. Circulation, 2001. 103: 1051-1056.

[80] Humphrey, J. D. *Mechanics of the arterial wall: Review and directions*. Critical Reviews in Biomedical Engineering, 1995. 23: 1-162.

[81] Setton, L. A., Elliott D. M., and Mow V. C. *Altered mechanics of cartilage with osteoarthritis: human osteoarthritis and an experimental model of joint degeneration*. Osteoarthritis and Cartilage, 1999. 7: 2-14.

[82] Cicuttini, F. M., and Spector T. D. *THE EPIDEMIOLOGY OF OSTEOARTHRITIS OF THE HAND*. Revue Du Rhumatisme, 1995. 62: S3-S8.

[83] Dijkgraaf, L. C., Debont L. G. M., Boer G., and Liem R. S. B. *THE STRUCTURE, BIOCHEMISTRY, AND METABOLISM OF OSTEOARTHRITIC CARTILAGE - A REVIEW OF THE LITERATURE*. Journal of Oral and Maxillofacial Surgery, 1995. 53: 1182-1192.

[84] Nesic, D., Whiteside R., Brittberg M., Wendt D., Martin I., and Mainil-Varlet P. *Cartilage tissue engineering for degenerative joint disease*. Advanced Drug Delivery Reviews, 2006. 58: 300-322.

[85] Akizuki, S., Mow V. C., Muller F., Pita J. C., Howell D. S., and Manicourt D. H. *TENSILE PROPERTIES OF HUMAN KNEE-JOINT CARTILAGE .1. INFLUENCE OF IONIC CONDITIONS, WEIGHT BEARING, AND FIBRILLATION ON THE TENSILE MODULUS*. Journal of Orthopaedic Research, 1986. 4: 379-392.

[86] Mow, V. C., Kuei S. C., Lai W. M., and Armstrong C. G. *BIPHASIC CREEP AND STRESS-RELAXATION OF ARTICULAR-CARTILAGE IN COMPRESSION - THEORY AND EXPERIMENTS*. Journal of Biomechanical Engineering-Transactions of the Asme, 1980. 102: 73-84.

[87] Hayes, W. C., and Mockros L. F. *VISCOELASTIC PROPERTIES OF HUMAN ARTICULAR CARTILAGE*. Journal of Applied Physiology, 1971. 31: 562-**&**.

[88] Kempson, G. E., Swanson S. A. V., Spivey C. J., and Freeman M. A. R. *PATTERNS OF CARTILAGE STIFFNESS ON NORMAL AND DEGENERATE HUMAN FEMORAL HEADS*. Journal of Biomechanics, 1971. 4: 597-**&**.

[89] Quinn, T. M., and Morel V. *Microstructural modeling of collagen network mechanics and interactions with the proteoglycan gel in articular cartilage*. Biomechanics and Modeling in Mechanobiology, 2007. 6: 73-82.

[90] Zhu, W. B., Mow V. C., Koob T. J., and Eyre D. R. *VISCOELASTIC SHEAR PROPERTIES OF ARTICULAR-CARTILAGE AND THE EFFECTS OF GLYCOSIDASE TREATMENTS*. Journal of Orthopaedic Research, 1993. 11: 771-781.

[91] Setton, L. A., Mow V. C., and Howell D. S. *MECHANICAL-BEHAVIOR OF ARTICULAR-CARTILAGE IN SHEAR IS ALTERED BY TRANSECTION OF THE*

ANTERIOR CRUCIATE LIGAMENT. Journal of Orthopaedic Research, 1995. 13: 473-482.

[92] Eckstein, F., Reiser M., Englmeier K. H., and Putz R. *In vivo morphometry and functional analysis of human articular cartilage with quantitative magnetic resonance imaging - from image to data, from data to theory*. Anatomy and Embryology, 2001. 203: 147-173.

[93] Evans, W. H., and Boitano S. *Connexin mimetic peptides: specific inhibitors of gap-junctional intercellular communication*. Biochemical Society Transactions, 2001. 29: 606-612.

[94] Spanakis, S. G., Petridou S., and Masur S. K. *Functional gap junctions in corneal fibroblasts and myofibroblasts*. Investigative Ophthalmology & Visual Science, 1998. 39: 1320-1328.

[95] Picard, O., Poupon M. F., and Escande J. P. *FIBROBLAST COOPERATION FOR THE GRAFT OF TUMOR-CELLS IN ATHYMIC MICE*. Comptes Rendus De L Academie Des Sciences Serie Iii-Sciences De La Vie-Life Sciences, 1984. 298: 387-&.

[96] Mariappan, M. R., Williams J. G., Prager M. D., and Eberhart R. C. *"Engineering" the wound-healing process - The association of Chitosan-mediated inhibition of wound-model contraction with inhibition of gap junctions*. Ieee Engineering in Medicine and Biology Magazine, 1999. 18: 22-26.

[97] Roy, P., Petroll W. M., Cavanagh H. D., Chuong C. J., and Jester J. V. *An in vitro force measurement assay to study the early mechanical interaction between corneal fibroblasts and collagen matrix*. Experimental Cell Research, 1997. 232: 106-117.

[98] Bausch, A. R., Moller W., and Sackmann E. *Measurement of local viscoelasticity and forces in living cells by magnetic tweezers*. Biophysical Journal, 1999. 76: 573-579.

[99] Chu, Y. S., Dufour S., Thiery J. P., Perez E., and Pincet F. *Johnson-Kendall-Roberts theory applied to living cells*. Physical Review Letters, 2005. 94.

[100] Jaasma, M. J., Jackson W. M., and Keaveny T. M. *Measurement and characterization of whole-cell mechanical behavior*. Annals of Biomedical Engineering, 2006. 34: 748-758.

[101] Ramtani, S. *Mechanical modelling of cell/ECM and cell/cell interactions during the contraction of a fibroblast-populated collagen microsphere: theory and model simulation*. Journal of Biomechanics, 2004. 37: 1709-1718.

[102] Reinhart-King, C. A., Dembo M., and Hammer D. A. *Cell-Cell Mechanical Communication through Compliant Substrates*. Biophysical Journal, 2008. 95: 6044-6051.

[103] Guo, W. H., Frey M. T., Burnham N. A., and Wang Y. L. *Substrate rigidity regulates the formation and maintenance of tissues*. Biophysical Journal, 2006. 90: 2213-2220.

[104] Grinnell, F., and Petroll W. M. (2010). Cell Motility and Mechanics in Three-Dimensional Collagen Matrices. In Annual Review of Cell and Developmental Biology, Vol 26, R. Schekman, L. Goldstein, and R. Lehmann, eds., pp. 335-361.

[105] Davis, G. E., Bayless K. J., and Mavila A. *Molecular basis of endothelial cell morphogenesis in three-dimensional extracellular matrices*. Anatomical Record, 2002. 268: 252-275.

[106] Vailhe, B., Ronot X., Tracqui P., Usson Y., and Tranqui L. *In vitro angiogenesis is modulated by the mechanical properties of fibrin gels and is related to alpha(v)beta(3) integrin localization*. In Vitro Cellular & Developmental Biology-Animal, 1997. 33: 763-773.

[107] Califano, J. P., and Reinhart-King C. A. *A Balance of Substrate Mechanics and Matrix Chemistry Regulates Endothelial Cell Network Assembly*. Cellular and Molecular Bioengineering, 2008. 1: 122-132.

[108] Reinhart-King, C. A. *How Matrix Properties Control the Self-Assembly and Maintenance of Tissues*. Annals of Biomedical Engineering, 2011. 39: 1849-1856.

[109] Thorne, B. C., Bailey A. M., and Peirce S. M. *Combining experiments with multi-cell agent-based modeling to study biological tissue patterning*. Briefings in Bioinformatics, 2007. 8: 245-257.

[110] Abbott, R. G., Forrest S., and Pienta K. J. *Simulating the hallmarks of Cancer*. Artificial Life, 2006. 12: 617-634.

CHAPTER THREE

MECHANICAL PROPERTIES OF STEM CELLS FROM DIFFERENT SOURCES

DURING VASCULAR SMOOTH MUSCLE CELL DIFFERENTIATION

3.1 Introduction

Stem cell therapy has been under intensive research in recent years due to its potential in regenerating tissue and treating injury. Vascular smooth muscle cell (VSMC), as one of the crucial constituents in human vascular regeneration, can be derived from a variety of stem cell sources including bone-marrow progenitor cells [1], skin-derived precursors [2] and adipose stem cells [3]. Although it is known that VSMC and stem cells both can undergo significant phenotype shift in response to environment including mechanical stimuli [4], no comparison of mechanical property change has been made between different stem cell sources during differentiation. A better understanding of the mechanical property change during VSMC differentiation will not only indicate the differentiation status the cell is undergoing but also guide us to better design cell-cultured scaffold based on the optimal environment it requires during differentiation.

Bone marrow-derived mesenchymal stem cells (BMSCs) have been shown to have the capacity to differentiate towards a variety of cell types, including vascular smooth muscle cell lineages [5], and thus, have shown great potential in tissue repair application [6]. Previous studies showed a high similarity between native smooth muscle cell and mesenchymal stem cell differentiated towards a vascular smooth muscle lineage, which include expression of specific smooth muscle cell cytoskeleton protein during the

differentiation of MSC following SMC pathway [7]. Mesenchymal stem cells are also believed to stimulate angiogenesis in certain condition and are reported to stabilize vascular structure when co-cultured with other cells. These features together with their low immunogenicity make BMSCs a promising resource in vascular tissue repair [7-9].

Adipose tissue derived stem cells (ADSCs) have a mesenchymal-like morphology and are capable of differentiating to form different kinds of tissue-specific cells [10]. Some groups have hypothesized that ADSCs may not be inherent to adipose tissue and that they are instead floating mesenchymal or blood peripheral stem cells passing into adipose tissue [11]. However, there is no doubt that these cells isolated from adipose tissue, can be potentially useful stem cells for tissue repairing and disease treatment [12]. ADSCs have been confirmed having the capability to differentiate to functional SM-like cells; many smooth muscle cell specific markers were observed upon differentiation [13,14]. In addition, ADSCs are easier to harvest and purify compared to bone marrow derived stem cell. Thus, ADSCs are also considered as a competitive candidate in repairing vascular tissue.

Vascular smooth muscle cell, as one of the main constituents of the media layer in blood vessel, is under consistently mechanical loading from changes in blood pressure. As cellular mechanical behavior is highly associated with tissue level function, it is very important to investigate and understand the mechanical behavior of VSMCs and VSMC-like cells before applying them to any tissue level application [15]. Given the limited study of mechanical behavior of cells undergoing vascular smooth muscle cell

76

differentiation, the overall goal of this study was to investigate the differences in cellular mechanical properties of BMSCs and ADSCs during VSMC differentiation using AFM nanoindentation. VSMC-related cell markers were further visualized by immunofluorescence and the gene expression was assessed using PCR. Researchers have suggested that ADSCs can be differentiated to contractile VSMCs induced by TGF-β1.[16] However, they do so more slowly than their bone marrow counterparts. Studies show that it may take up to 6 weeks for ADSCs to differentiate into VSMC-like cells with the same level of differentiation markers as what is achieved by cells differentiated from BMSCs within 7 days. [14,17] Our hypothesis is that since BMSCs can be more quickly differentiated to functional SMC-like cells compared to ADSCs, they will also achieve more VSMC-like mechanical properties. This study will help elucidate the potential of using different sources of stem cells to differentiate into functional VSMC with certain mechanical strength.

3.2 Materials and Method

3.2.1 Cell Culture

For these studies, human bone marrow and adipose derived cells were purchased from commercial sources. Mesenchymal stromal cells isolated from human red bone marrow (BMSCs, Thermo Scientific HyClone, SV30110.01) were seeded at 1×10^4 cells/ cm^2 in Φ 35-mm dishes (Fluorodish FD35-100) resuspended in Dulbecco's modified low glucose Eagle medium (LG-DMEM, Gibco) supplemented with 20% FBS (Atlanta Biologicals, Lawrenceville, GA, USA) and 1% 100× penicillin-streptomycin (Fisher

Scientific, Pittsburgh, PA, USA). After cells were adhered to plates (1 day culture in incubator), we added differentiation media containing 10ng/ml TGF-β1 to induce differentiation towards VSMC. BMSCs were cultured for 7 days and used for following study at different time points. Human adipose derived stem cells (ADSCs) isolated from human lipoaspirate tissue (Thermo Scientific HyClone, SV30102.01) were cultured in Φ 35-mm dishes with 1×10^4 cells/ cm^2 in LG-DMEM (Gibco) supplemented with 10% FBS and 1% 100× penicillin-streptomycin. Similarly, culture media with 10ng/ml TGF-β1 was added to induce differentiation after cells adhere to plates. According to the manufacture, bone marrow derived stem cell was acquired from single donor while adipose derived stem cell was obtained from multiple donors. Since many factors, including substrate stiffness and culture conditions, can affect cell mechanical properties [18], The two cell types were maintained in standard cell culture condition on tissue culture plastic dish to minimize potential confounding factors due to culture substrate selection. As a comparison positive control group, primary VSMCs were isolated from rat aortic tissue using standard methods. It should be noted that the Young's modulus of human VSMC is characterized in 10-100kPa which lies within the same range of rat VSMC [19,20]. Procedures were approved by the Clemson University Institutional Animal Use and Care Committee. The cells were cultured for 1 day in LG-DMEM with 10% FBS and 1% 100× penicillin-streptomycin.

3.2.2 AFM indentation

For AFM indentation, an Asylum Research MFP-3D AFM mounted on an Olympus IX-81 spinning disc confocal microscope placed on a vibration isolation table was used.

Borosilicate spherical probes (radius = 2.5μm, Bruker Nano Inc) with a nominal spring

constant of 0.06N/m were utilized to indent into cells. Cells were kept in 35-mm culture

dishes with growth media throughout the experiment. Prior to loading with the AFM, a

thermal fluctuation test is performed in air to calculate the actual spring constant of the

cantilever [21]. Single cells were randomly chosen by the optical microscope with a 20X

objective lens while morphologically abnormal and overlapped cells were excluded.

AFM tests were performed on one dish at a time while the rest of dishes were stored in an

incubator until just prior to use. Normally, each test takes less than 30mins for one dish.

This is similar to the time cells are out of the incubator for other cell culture maintenance

protocols (e.g., media changes, microscopy images). Similar to past studies using the

same system [22], the tempature does not fluctuate by more than 8°C over 30mins while

no noticeable changes in cell behavior and mechanical properties were observed over the

30mins time the cells were in the AFM. The AFM probe was positioned over the central

part of the cell and was adjusted to avoid the edge of the cell. Each cell was indented 5

times to a depth of at least 1μm into the cell with a loading rate of 1μm/s in 5μm force

distance. At each time point, 10 representative cells from each sample were chosen for

evaluation and their elastic modulus were then analyzed based on at least 50 replicates

per sample.
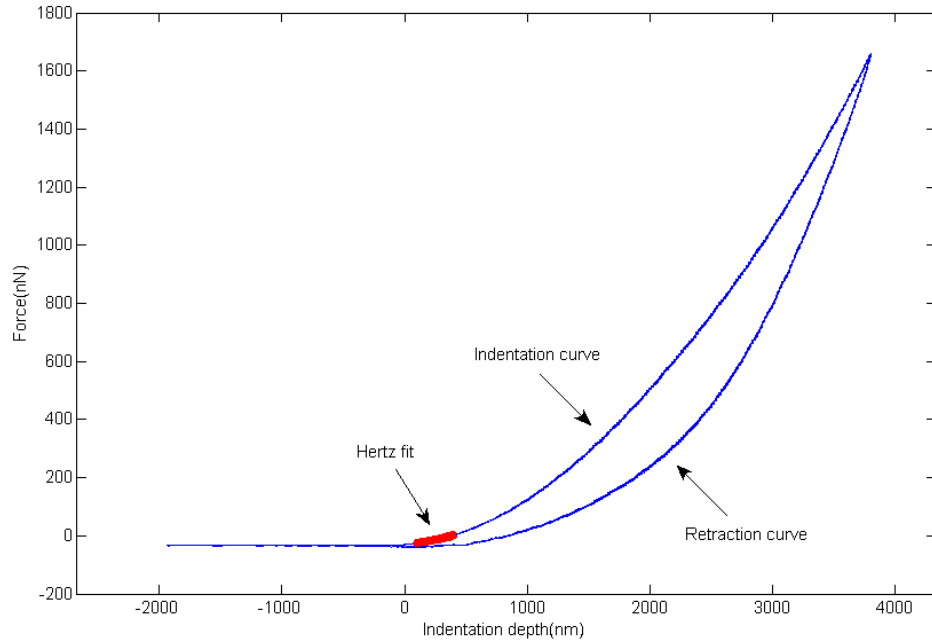
Figure 3.1 Representative AFM indentation consisting both an indent and retract curve. The contact point was determined by a certain degree of upwards shift while the Hertz model fit to the data over the indentation curve from 30nm to a 300nm indentation depth.

3.2.3 Indentation curve analysis

The Hertz contact model [23] was used to estimate the elastic modulus values from the indentation curves acquired from the contact between AFM spherical tip and cell. A MATLAB script was used to determine the contact point of the force curves by identifying the point at which force shifts upwards above the baseline noise level [24]. The modulus was calculated using the Hertz model fit to the data over the indentation curve from 30nm to a 300nm indentation depth, a range over which the Hertz contact

model still remain accurate [25]. The Hertz contact model is used to simulate the elastic

behavior between a spherical indenter (AFM probe) and an elastic half plane (cell) [26].

$$F = \frac{4}{3} \frac{E}{(1-v^2)} R^{\frac{1}{2}} \delta^{\frac{3}{2}}$$ (1)

Where F represents the force, E is the elastic modulus of the cell, v is Poisson's ratio

(v=0.5 as the cell cytoplasm is assumed incompressible [27]), R is the radius of indenter,

and δ is the indentation depth. The Hertz model has two major assumptions: linear

elasticity and infinite sample thickness. These can result in significant errors if the

experiments are far from these approximations. However, by using microsphere tips and

the small indentation depth, the approximations of the Hertz model remain close to major

assumptions and have reasonable accuracy in the calculation of elastic modulus for cells

[28]. As validation of model assumptions, the point-wise calculated elastic modulus was

found to be nearly constant over the 30-300nm indentation range. This indicates that the

conditions of the Hertz model are fairly well met in this indentation range [23].

3.2.4 Immunofluorescence

We fixed cells in 24-well plates with 4% Paraformaldehyde (PFA, Sigma-Aldrich) at

37°C for 10 minutes and rinsed cells with phosphate buffered saline (PBS) two times for

30 minutes. PBS with 0.01 M Glycine and 0.1% Triton-X was placed on the cells for 30

minutes. Cells were then rinsed with 5% BSA/PBS and 1% BSA/PBS followed by

incubation with primary antibodies against SMα-actin (αSMA) (Sigma-Aldrich),

calponin (Abcam) and SM myosin heavy chain (SM-MHC) (Abcam) at 4°C. Fluorescein

isothiocyanate (FITC)-conjugated goat anti-rabbit secondary antibody (Millipore) was

added the following day to detect the localization of anti-calponin antibodies while FITC-conjugated goat anti-mouse secondary antibody (Millipore) was used to detect the localization of antiαSMA and anti-SM-MHC antibodies. Images were visualized using a Nikon Eclipse TE2000-S fluorescence microscope (Nikon USA, Melville, New York, USA)

3.2.5 RNA Isolation and RT-PCR

We extracted total RNA using TRIzol (Invitrogen) from cells cultured during different differentiation time points to investigate if there is any correlation between the expression of αSMA and cellular mechanical property. The isolated RNA was further purified using RNeasy Kit (Qiagen, Valencia, CA) according to the instructions of the manufactures. RNA quantity was assessed using Take3 micro-volume plates (BioTek) and 1 μg was used for each reverse-transcription. DNA denaturation was performed in PCR by 3 minutes heating at 70 while Complementary DNA (cDNA) was synthesized using QuantiTect reverse transcription kit (QiaGen) and equal volume of synthesized cDNA was then added to a master mix containing specifically designed primers for αSMA and β-actin. Reverse transcription was conducted consisting 1 hour heating at 44°C followed by a 10 minutes Rtease inactivation a 92°C. The amplification efficiency of primers was tested first to ensure the number of PCR cycles for amplification is in a linear range. The primer sequences for αSMA are designed as 5'- GGTGATGGTGGGAATGGG-3' and 5'-GCAGGGTGGGATGCTCTT-3′to generate a 188 fragment size PCR product [3] and the primer sequences for β-actin are 5'- TGGGTCAGAAGGATTCCTATGT-3' and 5'-CAGCCTGGATAGCAACGTACA-3′ to generate PCR product [29]

3.2.6 Quantitative Real-Time PCR analysis

For quantitative PCR analysis, the expression of αSMA and β-actin was assessed during

the differentiation of both BMSCs and ADSC. We performed RT-PCR on Rotor-Gene

(RG-3000, Corbett Research) using QuantiTect SYBR Green PCR Kit (QiaGen) to have

a final reaction volume of 25ml. The expression of αSMA was normalized based on the

transcript level of β-actin to determine the differentiated portion of total amount of stem

cells.

3.2.7 Statistical analysis

ANOVA with Tukey multi comparison test using SAS software were performed to

determine if there are significant differences among samples during differentiation.

Student's t-tests were used to examine significant differences between samples on a given

day and across all time points. P value less than 0.05 were considered statistically

significant based on the significant level of 5%. The statistical analysis was conducted on

the elastic modulus of both two stem cells over differentiation.

3.3 Results

3.3.1 Elastic modulus of single cell during differentiation

The modulus values obtained from the 1-day cultured VSMCs were consistent with those

from previously published studies of similar in vitro cultured VSMCs [30]. Generally, the

resulting elastic modulus of both BMSCs and ASCs gradually increased during

differentiation (Figure 3.2) and both stem cells reach 80% confluency at day 7. We found

a significant increase in the mechanical properties of day 3 BMSCs while observing a

relatively steady raise in the Young's modulus of ASCs over 7 days differentiation. Force

curves were then plotted according to each time point during differentiation (Figure 3.3).

Both BMSCs and ASCs exhibit an increasing force vs. indentation trend with time in

culture.
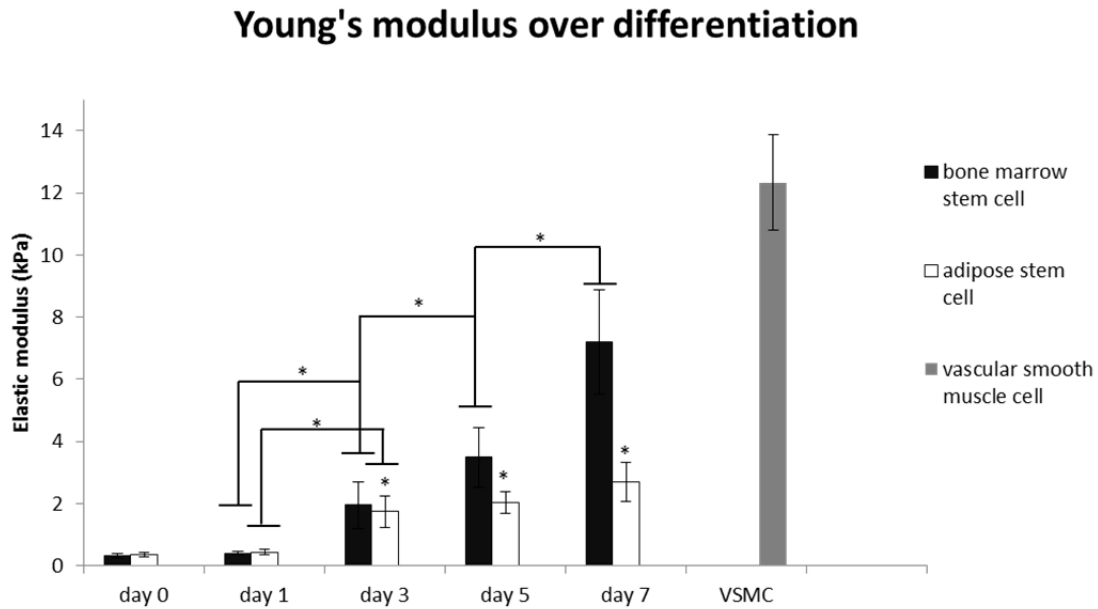
Figure 3.2 Apparent elastic modulus of BMSCs and ADSCs measured with a

borosilicate spherical AFM probes of 5μm diameter at 1μm/s approaching speed with

indentation depth from 30nm to 300nm for calculation (10cells per day). Data are

presented as mean ± standard error (*Significant difference between two groups

(p<0.05)).

Indentation (nm) vs Froce (nN) for adipose derived stem cell

Indentation (nm) vs Force (nN) for mesenchymal stem cell derived from bone marrow

Figure 3.3 Averaged force vs. indentation curves of BMSCs and ADSCs. Curves shown in the figure are averaged at different time points over differentiation (control is undifferentiated cell at day 0). Generally BMSCs generate higher force in response to indentation compared to ADSCs.

3.3.2 Gene expression of SMC-specific markers
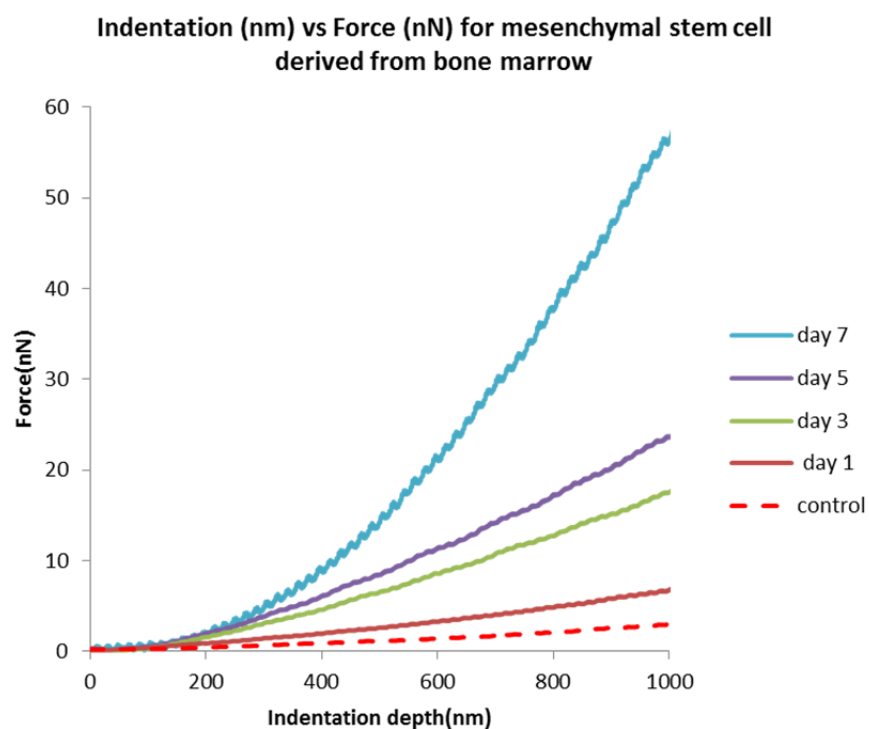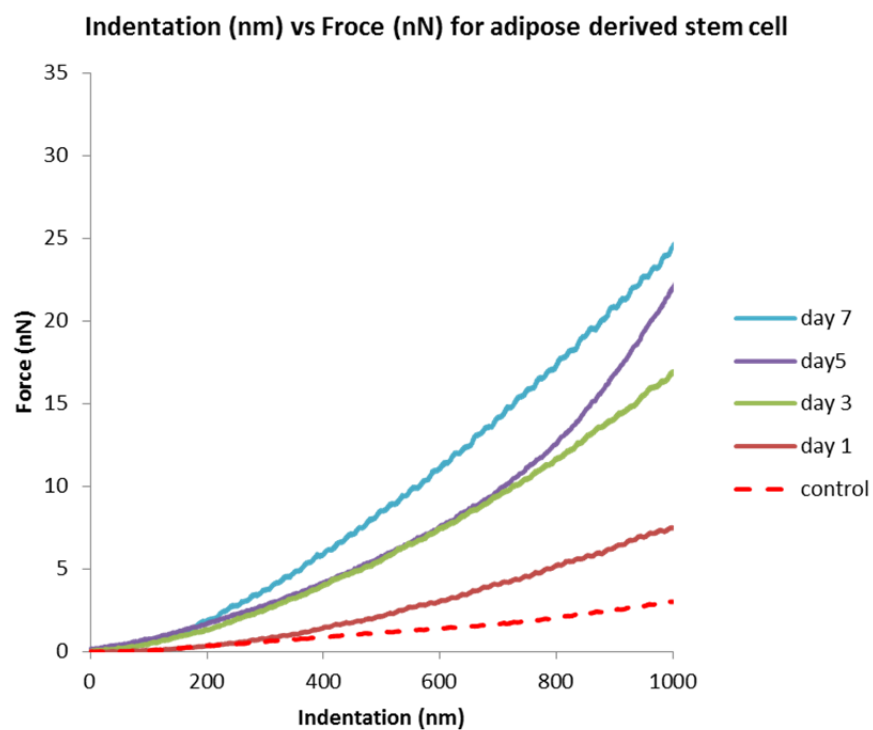
The main objective of this work is to determine whether the expression of specific SMC markers match the change in mechanical property during differentiation (Figure 4). Early and late SMC markers including αSMA, calponin and SM-MHC are detected by fluorescent staining and αSMA is further quantified by real time PCR. We found that for ADSCs, the expression of specific SMC markers gradually increased during differentiation while for BMSCs, the increase of the gene expression can be merely observed after three to five days differentiation. In addition, not all ADSCs showed positive staining for calponin and SM-MHC at day 3 while all the BMSCs imaged stained for calponin and SM-MHC at day 3 (Figure 4). We found a baseline expression of αSMA in both undifferentiated stem cells. The expression of αSMA has a significant increase at day 3 for both stem cell types. Although the relative gene expression of αSMA for ADSCs is slightly higher than that of the BMSCs, the quantity of αSMA in terms of RNA level for ADSCs is still much lower than BMSCs based on the absolute number of their PCR cycles, which might be the reason why ADSCs exhibit lower elastic modulus than BMSCs (Figure 3.4).
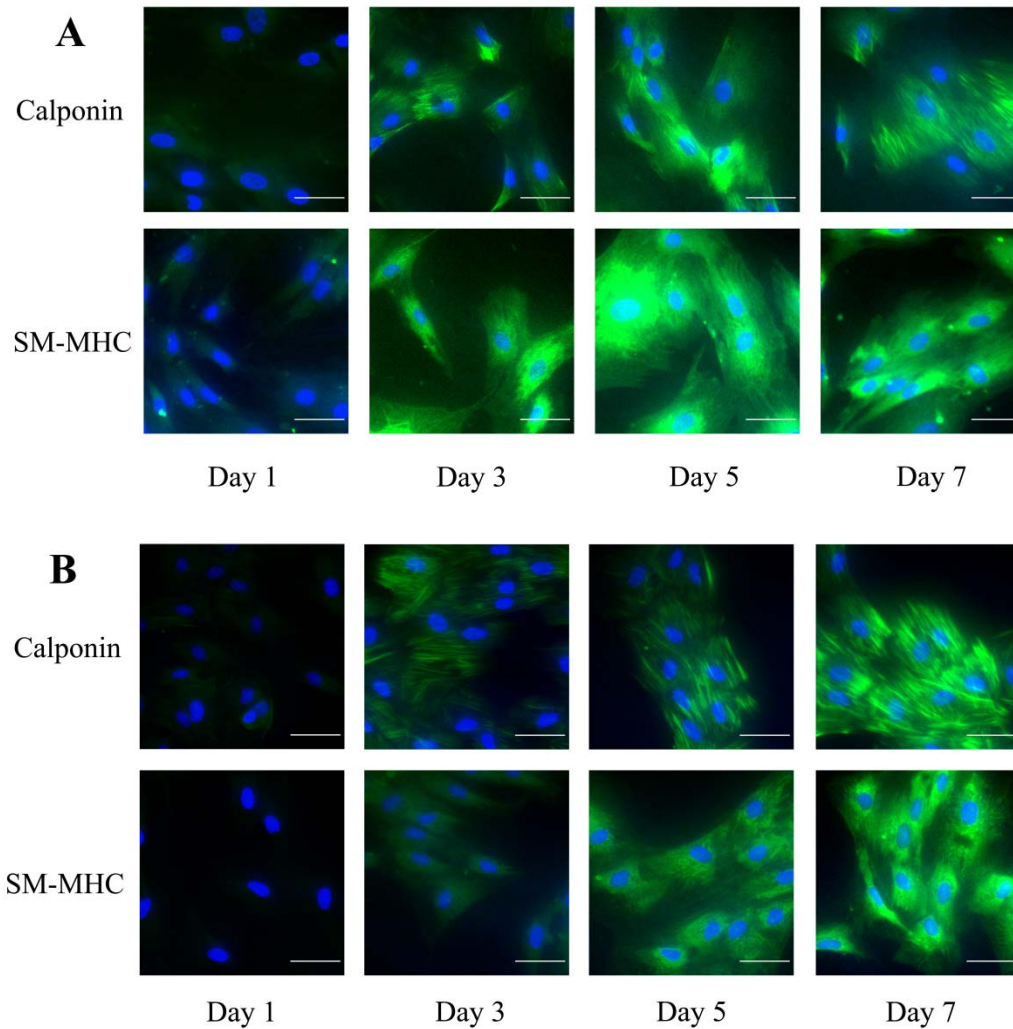
Figure 3.4 The immunofluorence staining of SMC-specific marker calponin and SM-MHC over 7 day differentiation from (A) BMSCs and (B) ADSCs. Nucleus were stained with DAPI while antibodies against calponin and SM-MHC were used for immunostaining (scale bar=50μm).
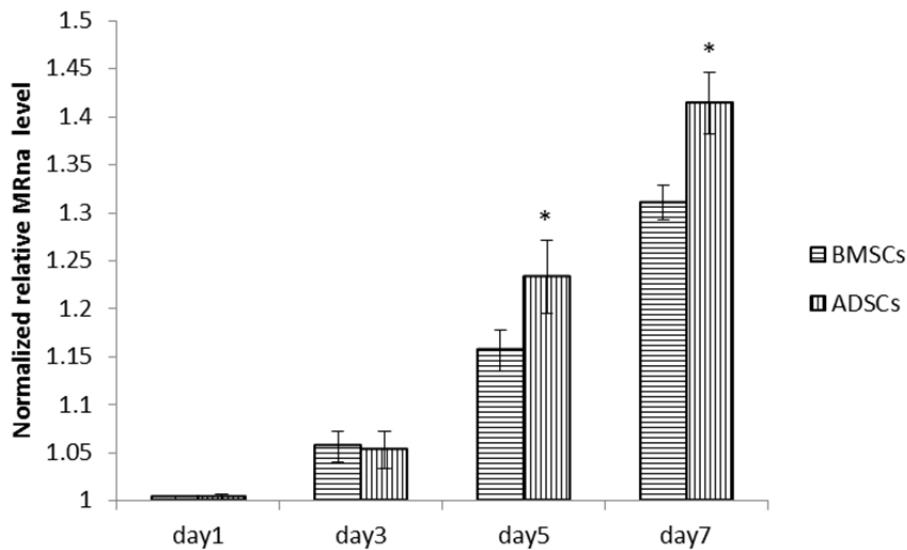
Figure 3.5 Expression of αSMA normalized to control gene β-actin during SMC differentiation for 7 days using real-time PCR (*Significant difference between two groups ($p<0.05$)). Data are presented as mean ± standard error.

3.4 Discussion

One of the major challenges in the development of cell therapy for vascular disease is to validate a reliable cell source in order to translate the progress from cell study to clinical application. Since mature SMCs cultured in vitro can easily lose their ability to proliferate and contract if used as seeded cells for blood vessel construction [31]. Recent research has been focused on exploring alternative cell source which can be served as donor for cardiovascular cells. It has been shown that BMSCs have the ability to differentiate into cells characteristic of blood vessels [32,33] and are believed to help stabilize vascular structure when co-cultured with other type of cells [34]. On the other hand, ADSCs have been shown to be capable of differentiating into smooth muscle like

cells expressing both early and late SMC markers [3] and are believed to improve vasculogenesis for cell therapy in adult [35]. Thus, in our study, we analyzed the progression of the mechanical properties of these two types of stem cells during differentiation towards a vascular smooth muscle cell lineage. This data can help to determine the cells suitability as a source for vascular smooth muscle repair.

The mechanical behavior of a vascular smooth muscle cell not only suggests its ability to contract and relax but also indicates tissue level function. However, limited research has been done to analyze the mechanical property change during vascular smooth muscle cell differentiation, let alone any comparison between different stem cell sources. In the present study, we investigated if the process of vascular smooth muscle cell differentiation varies given different sources of stem cells. The results show the mechanical property of differentiating stem cells changes significantly depending on the cell source. The Hertz model was utilized in our study to evaluate cell's elastic modulus. Although Hertz model makes several simplifying assumptions, it can still provide good qualitatively comparison of the elastic modulus between different cells during differentiation. Previous research shows the result of cell's modulus remains reasonable if the indentation depth used in Hertz fit is small before significant non-linearity occurs with the increase of indentation depth [36].

In our current study, a significant increase in elastic modulus was observed from day 3 BMSCs during differentiation. In the following days, the value reaches its peak at day 7 which is very close to the elastic modulus of vascular smooth muscle cell in control

group (Figure 2). Cells in both groups reached 80% confluency at day 7. Since cells are known to stiffen when in confluent cultures[37], it is not clear whether any additional increases in modulus that can be observed after day 7 are due to the cells differentiating further or from the additional cell-cell contacts that occur in very confluent cell cultures. Compared to BMSCs, the overall elastic modulus of ADSCs was much lower and underwent a smoother increase during differentiation. As has previously been established [1], there is a high similarity between the expression of certain genes in BMSCs and smooth muscle cells; therefore, we are not surprised to discover that BMSCs eventually have the similar elastic modulus as in vitro 1-day cultured vascular smooth muscle cell after differentiation. However, the differentiation potential of BMSCs into different vascular lineages is still not fully understood [38]. Due to the variable nature and incomplete characterization of isolated mesenchymal stem cells, both the culture condition and isolation method are highly variable [39]. In our research, we found that BMSCs from a commercial cell line source have the potential to differentiate into smooth muscle-like cells with mechanical properties similar to native VSMCs, which is crucial in clinical use. However, our current experiments are not sufficient to characterize the whole mechanical behavior of cells and thus further investigation is required to determine if the differentiated stem cells are functional given a physiological loading condition. However, considering the difficulty in obtaining large number of mesenchymal stem cells from bone marrow for clinical use, ADSCs provide an attractive alternative cell source, as they can be harvested in relatively large quantities with minimal compensation of tissue morbidity. While the elastic modulus of ADSCs increased more slowly over time

during differentiation compared to BMSCs, the results show ADSCs still have the potential to gradually acquire higher elastic modulus during differentiation induced by TGF-beta 1. Thus, these cells could be a promising cell source for tissue repair. However, further study is required to determine if the elastic modulus of ADSCs can get closer to fully differentiated vascular smooth muscle cells if given different conditions including the combination of growth factor, co-culture with different cells, and cyclic mechanical loading.

To further establish that cells differentiated are functional smooth muscle cell, the expression of SMC-specific markers were examined by PCR and fluorescent staining. Fluorescent microscopic images of FITC-labeled αSMA reveals that cells differentiated from both stem cell sources have a baseline level of αSMA with minor but constant increase over differentiation. After 7 days culture, most cells appear to be elongated with highly expressed αSMA throughout the cells. As previous research suggests the relationships between the existence of αSMA and cellular contractility along with the fact that contractile VSMCs having more αSMA are stiffer than synthetic VSMCs with less αSMA [30,40] we believe that the increase of αSMA along with morphological and adhesive alterations, result in the change of elastic modulus measured in our AFM experiments. Our work shows that there is a correlation between the level of αSMA in the cell and the cellular mechanical properties. The gene expression of αSMA was analyzed by PCR. Consistent with fluorescent staining, αSMA has a baseline expression for both undifferentiated BMSCs and ADSCs along with the increase in baseline expression over differentiation.

However, the expression of αSMA alone does not definitely suggest the cells are fully differentiated, other groups have found that the mid-differentiation marker calponin and late stage differentiation marker SM-MHC may have more SMC lineage correlativity than   SMA [41]. In our study, both of the two markers were found to be significantly enhanced after 7 days culture compared to the merely detection at day 1 culture. There is also an increase in the levels of both markers over time during differentiation which correlates with the change in elastic modulus. All the results suggest that when induced by TGF-beta 1, both of the two stem cell types differentiate down a SMC lineage while acquiring basic SMC functionality reflected by the increase of elastic modulus. Although TGF-beta 1 activation is not completely understood [42], it has been well documented to be responsible for the induction of mural cell (pericytes or smooth muscle cell) differentiation which are crucial in modulating blood flow and vasculargensis..

Functional VSMC plays an important role in blood circulation by contracting and relaxing. Previous studies showed that there is a difference in the mechanical properties of vascular smooth muscle cells as they shift between synthetic/proliferative and contractile/quiescent phenotypes VSMC [30,43,44]. While cells are naturally viscoelastic, the elastic property measured previously still provides some insight into the mechanical property of VSMC. In our study, we utilized AFM to analyze the mechanical properties of live cells undergoing differentiation down a smooth muscle cell lineage. Based on that, we demonstrate both stem cells used in our study stiffen when differentiating down

VSMC lineages as induced by TGF-beta 1. This change in mechanical properties is also correlated to the change in αSMA expression. Taken together, these results help to analyze the functionality of differentiated cells that may have potential use in clinical application. In addition, while it is possible to assess individual cell mechanical properties in 2D cultures, it will be very difficult to do so when the cells are cultured inside 3D matrices for potential tissue engineering or regenerative medicine applications. The results from this study, which show the correlation between aSMA expression and cellular mechanical properties, could help researchers to assess, at least qualitatively, the mechanical properties of differentiating cells in setups where direct cell probing cannot be performed.

3.5 Conclusion

In vitro 7-day culture of BMSCs induced by TGF-beta 1 exhibited greater elastic modulus than ADSCs. We also found that BMSCs can acquire the mechanical property close to VSMC cultured in vitro. This result indicates BMSCs may be a better candidate in differentiating to functional VSMC in terms of mechanical strength. However, further research is required to determine if the differentiation can be affected by environmental change including cyclic loading and combination of growth factor. Optimization of such differentiation can have potential use in clinical application in future.

3.6 References

[1] Han, J. H., Liu J. Y., Swartz D. D., and Andreadis S. T. *Molecular and functional effects of organismal ageing on smooth muscle cells derived from bone marrow mesenchymal stem cells*. Cardiovascular Research, 2010. 87: 147-155.

[2] Steinbach, S. K., El-Mounayri O., DaCosta R. S., Frontini M. J., Nong Z. X., Maeda A., Pickering J. G., Miller F. D., and Husain M. *Directed Differentiation of Skin-Derived Precursors Into Functional Vascular Smooth Muscle Cells*. Arteriosclerosis Thrombosis and Vascular Biology, 2011. 31: 2938-U2452.

[3] Wang, C., Yin S., Cen L., Liu Q. H., Liu W., Cao Y. L., and Cui L. *Differentiation of Adipose-Derived Stem Cells into Contractile Smooth Muscle Cells Induced by Transforming Growth Factor-beta 1 and Bone Morphogenetic Protein-4*. Tissue Engineering Part A, 2010. 16: 1201-1213.

[4] Beamish, J. A., He P., Kottke-Marchant K., and Marchant R. E. *Molecular Regulation of Contractile Smooth Muscle Cell Phenotype: Implications for Vascular Tissue Engineering*. Tissue Engineering Part B-Reviews, 2010. 16: 467-491.

[5] Kaveh, K., Ibrahim R., Abu Bakar M. Z., and Ibrahim T. A. *Mesenchymal Stem Cells, Osteogenic Lineage and Bone Tissue Engineering: A Review*. Journal of Animal and Veterinary Advances, 2011. 10: 2317-2330.

[6] Rezai, N., Podor T. J., and McManus B. M. *Bone marrow cells in the repair and modulation of heart and blood vessels: Emerging opportunities in native and engineered tissue and biomechanical materials*. Artificial Organs, 2004. 28: 142-151.

[7] Galmiche, M. C., Koteliansky V. E., Briere J., Herve P., and Charbord P. *Stromal Cells from Human Long-Term Marrow Cultures Are Mesenchymal Cells That Differentiate Following a Vascular Smooth-Muscle Differentiation Pathway*. Blood, 1993. 82: 66-76.

[8] Au, P., Tam J., Fukumura D., and Jain R. K. *Bone marrow-derived mesenchymal stem cells facilitate engineering of long-lasting functional vasculature*. Blood, 2008. 111: 4551-4558.

[9] Choong, C. S. N., Hutmacher D. W., and Triffitt J. T. *Co-culture of bone marrow fibroblasts and endothelial cells on modified polycaprolactone substrates for enhanced potentials in bone tissue engineering*. Tissue Engineering, 2006. 12: 2521-2531.

[10] Zuk, P. A., Zhu M., Mizuno H., Huang J., Futrell J. W., Katz A. J., Benhaim P., Lorenz H. P., and Hedrick M. H. *Multilineage cells from human adipose tissue: Implications for cell-based therapies*. Tissue Engineering, 2001. 7: 211-228.

[11] Chong, P. P., Selvaratnam L., Abbas A. A., and Kamarul T. *Human peripheral blood derived mesenchymal stem cells demonstrate similar characteristics and chondrogenic differentiation potential to bone marrow derived mesenchymal stem cells*. Journal of Orthopaedic Research, 2012. 30: 634-642.

[12] Mizuno, H., Tobita M., and Uysal A. C. *Concise Review: Adipose-Derived Stem Cells as a Novel Tool for Future Regenerative Medicine*. Stem Cells, 2012. 30: 804-810.

[13] Marra, K. G., Brayfield C. A., and Rubin J. P. *Adipose Stem Cell Differentiation into Smooth Muscle Cells*. Adipose-Derived Stem Cells: Methods and Protocols, 2011. 702: 261-268.

[14] Rodriguez, L. V., Alfonso Z., Zhang R., Leung J., Wu B., and Ignarro L. J. *Clonogenic multipotent stem cells in human adipose tissue differentiate into functional smooth muscle cells*. Proceedings of the National Academy of Sciences of the United States of America, 2006. 103: 12167-12172.

[15] Janmey, P. A. *The cytoskeleton and cell signaling: Component localization and mechanical coupling*. Physiological Reviews, 1998. 78: 763-781.

[16] Park, W. S., Heo S. C., Jeon E. S., Hong D. H., Son Y. K., Ko J. H., Kim H. K., Lee S. Y., Kim J. H., and Han J. *Functional expression of smooth muscle-specific ion channels in TGF-beta(1)-treated human adipose-derived mesenchymal stem cells*. American Journal of Physiology-Cell Physiology, 2013. 305: C377-C391.

[17] Narita, Y., Yamawaki A., Kagami H., Ueda M., and Ueda Y. *Effects of transforming growth factor-beta 1 and ascorbic acid on differentiation of human bone-marrow-derived mesenchymal stem cells into smooth muscle cell lineage*. Cell and Tissue Research, 2008. 333: 449-459.

[18] Byfield, F. J., Reen R. K., Shentu T.-P., Levitan I., and Gooch K. J. *Endothelial actin and cell stiffness is modulated by substrate stiffness in 2D and 3D*. Journal of Biomechanics, 2009. 42: 1114-1119.

[19] Lynn Ray, J., Leach R., Herbert J.-M., and Benson M. *Isolation of vascular smooth muscle cells from a single murine aorta*. Methods in Cell Science, 2001. 23: 185-188.

[20] Wuyts, F. L., Vanhuyse V. J., Langewouters G. J., Decraemer W. F., Raman E. R., and Buyle S. *ELASTIC PROPERTIES OF HUMAN AORTAS IN RELATION TO AGE*

AND ATHEROSCLEROSIS - A STRUCTURAL MODEL. Physics in Medicine and Biology, 1995. 40: 1577-1597.

[21] Butt, H. J., and Jaschke M. *Calculation of Thermal Noise in Atomic-Force Microscopy*. Nanotechnology, 1995. 6: 1-7.

[22] Deitch, S., Gao B. Z., and Dean D. *Effect of matrix on cardiomyocyte viscoelastic properties in 2D culture*. Molecular & cellular biomechanics : MCB, 2012. 9: 227-249.

[23] Kuznetsova, T. G., Starodubtseva M. N., Yegorenkov N. I., Chizhik S. A., and Zhdanov R. I. *Atomic force microscopy probing of cell elasticity*. Micron, 2007. 38: 824-833.

[24] Crick, S. L., and Yin F. C. P. *Assessing micromechanical properties of cells with atomic force microscopy: importance of the contact point*. Biomechanics and Modeling in Mechanobiology, 2007. 6: 199-210.

[25] Dimitriadis, E. K., Horkay F., Maresca J., Kachar B., and Chadwick R. S. *Determination of elastic moduli of thin layers of soft material using the atomic force microscope*. Biophysical Journal, 2002. 82: 2798-2810.

[26] Rico, F., Roca-Cusachs P., Gavara N., Farre R., Rotger M., and Navajas D. *Probing mechanical properties of living cells by atomic force microscopy with blunted pyramidal cantilever tips*. Physical Review E, 2005. 72: 10.

[27] Radmacher, M. *Measuring the elastic properties of living cells by the atomic force microscope*. Atomic Force Microscopy in Cell Biology, 2002. 68: 67-90.

[28] Mahaffy, R. E., Shih C. K., MacKintosh F. C., and Kas J. *Scanning probe-based frequency-dependent microrheology of polymer gels and biological cells*. Physical Review Letters, 2000. 85: 880-883.

[29] Heydarkhan-Hagvall, S., Helenius G., Johansson B. R., Li J. Y., Mattsson E., and Risberg B. *Co-culture of endothelial cells and smooth muscle cells affects gene expression of angiogenic factors*. Journal of Cellular Biochemistry, 2003. 89: 1250-1259.

[30] Hemmer, J. D., Dean D., Vertegel A., Langan E., and LaBerge M. *Effects of serum deprivation on the mechanical properties of adherent vascular smooth muscle cells*. Proceedings of the Institution of Mechanical Engineers Part H-Journal of Engineering in Medicine, 2008. 222: 761-772.

[31] Lagna, G., Ku M. M., Nguyen P. H., Neuman N. A., Davis B. N., and Hata A. *Control of phenotypic plasticity of smooth muscle cells by bone morphogenetic protein signaling through the myocardin-related transcription factors*. Journal of Biological Chemistry, 2007. 282: 37244-37255.

[32] Kashiwakura, Y., Katoh Y., Tamayose K., Konishi H., Takaya N., Yuhara S., Yamada M., Sugimoto K., and Daida H. *Isolation of bone marrow stromal cell-derived smooth muscle cells by a human SM22 alpha promoter - In vitro differentiation of putative smooth muscle progenitor cells of bone marrow*. Circulation, 2003. 107: 2078-2081.

[33] Minguell, J. J., Erices A., and Conget P. *Mesenchymal stem cells*. Experimental Biology and Medicine, 2001. 226: 507-520.

[34] Sorrell, J. M., Baber M. A., and Caplan A. I. *Influence of Adult Mesenchymal Stem Cells on In Vitro Vascular Formation*. Tissue Engineering Part A, 2009. 15: 1751-1761.

[35] Miranville, A., Heeschen C., Sengenes C., Curat C. A., Busse R., and Bouloumie A. *Improvement of postnatal neovascularization by human adipose tissue-derived stem cells*. Circulation, 2004. 110: 349-355.

[36] Chizhik, S. A., Huang Z., Gorbunov V. V., Myshkin N. K., and Tsukruk V. V. *Micromechanical properties of elastic polymeric materials as probed by scanning force microscopy*. Langmuir, 1998. 14: 2606-2609.

[37] Efremov, Y. M., Dokrunova A. A., Bagrov D. V., Kudryashova K. S., Sokolova O. S., and Shaitan K. V. *The effects of confluency on cell mechanical properties*. Journal of Biomechanics, 2013. 46: 1081-1087.

[38] Ramkisoensing, A. A., Pijnappels D. A., Askar S. F. A., Passier R., Swildens J., Goumans M. J., Schutte C. I., de Vries A. A. F., Scherjon S., Mummery C. L., Schalij M. J., and Atsma D. E. *Human Embryonic and Fetal Mesenchymal Stem Cells Differentiate toward Three Different Cardiac Lineages in Contrast to Their Adult Counterparts*. PLoS ONE, 2011. 6: 11.

[39] Roobrouck, V. D., Ulloa-Montoya F., and Verfaillie C. M. *Self-renewal and differentiation capacity of young and aged stem cells*. Experimental Cell Research, 2008. 314: 1937-1944.

[40] Kinner, B., Zaleskas J. M., and Spector M. *Regulation of smooth muscle actin expression and contraction in adult human mesenchymal stem cells*. Experimental Cell Research, 2002. 278: 72-83.

[41] Lee, S. H., Hungerford J. E., Little C. D., and IruelaArispe M. L. *Proliferation and differentiation of smooth muscle cell precursors occurs simultaneously during the development of the vessel wall*. Developmental Dynamics, 1997. 209: 342-352.

[42] Abe, M., Harpel J. G., Metz C. N., Nunes I., Loskutoff D. J., and Rifkin D. B. *AN ASSAY FOR TRANSFORMING GROWTH-FACTOR-BETA USING CELLS TRANSFECTED WITH A PLASMINOGEN-ACTIVATOR INHIBITOR-1 PROMOTER LUCIFERASE CONSTRUCT*. Analytical Biochemistry, 1994. 216: 276-284.

[43] Matsumoto, T., Sato J., Yamamoto M., and Sato M. *Smooth muscle cells freshly isolated from rat thoracic aortas are much stiffer than cultured bovine cells: Possible effect of phenotype*. Jsme International Journal Series C-Mechanical Systems Machine Elements and Manufacturing, 2000. 43: 867-874.

[44] Miyazaki, H., Hasegawa Y., and Hayashi K. *Tensile properties of contractile and synthetic vascular smooth muscle cells*. Jsme International Journal Series C-Mechanical Systems Machine Elements and Manufacturing, 2002. 45: 870-879.

CHAPTER FOUR

DIFFERENTIATION OF HUMAN ADIPOSE DERIVED STEM CELL INTO

FUNCTIONAL VASCULAR SMOOTH MUSCLE CELL UNDER BIOCHEMICAL

AND BIOMECHANICAL SIGNALS

4.1 Introduction

Tissue engineering of small-diameter blood vessels holds great promise in treating

peripheral arterial disease. However, several major obstacles have severely limited the

use of combining biomaterials and vascular cells. [1-3] Among all of them, finding a

reliable source of VSMCs that can be made functional over the time has proven to be a

formidable task. Terminally differentiated SMCs, which have been used previously, lack

the ability to proliferate extensively. In addition, they are limited in supply due to the fact

that there are no obvious arteries that can be removed from the body to isolate arterial

SMCs. These disadvantages make it necessary to explore alternative cell source to

provide large number of functional VSMCs that can be used in blood vessel engineering.

Stem cell therapy has been under intensive research in recent years due to its potential in

regenerating tissue and treating injury. Vascular smooth muscle cells (VSMCs), as one of

the crucial constituents in human vascular regeneration, can be derived from a variety of

stem cell sources including bone-marrow progenitor cells,[4] skin-derived precursors[5]

and adipose stem cells.[6] Among them, adipose stem cells (ADSCs) are capable of

differentiating toward osteogenic, chondrogenic adipogenic and cardiomyogenic lineages

under appropriate conditions [7,8] and have several advantages such as easy obtainability,

lower donor site morbidity, and higher harvest frequency. Thus, ADSCs are considered a competitive candidate in blood vessel engineering.

Phenotype regulation of vascular smooth muscle cell differentiated by stem cell is a key point in vascular replacement. Fast proliferation of synthetic VSMCs are preferred to populate vascular constructs initially in order to provide mechanical strength and tissue architecture at the first stage while contractile VSMCs are eventually needed to prevent stenosis and attain contractility. Many efforts have been made to study environmental cues that can control the differentiation and proliferation of VSMCs. Soluble factors have been believed to promote VSMCs differentiation in different ways. More proliferative, synthetic SMCs were achieved from stem cells by using platelet-derived growth factor (PDGF), insulin-like growth factors (IGFs)[9,10] while contractile phenotype were promoted with transforming growth factor β1 (TGF-β1) and Ang-II.[11,12] It has also been shown that VSMC phenotype can be controlled by the composition and physical structure of ECM.[13] There is also an increased focus on fabricating substrates with different topography to study specific cellular behaviors.[14] Previous studies show that microchannel scaffolds with discontinuous walls not only support VSMC proliferation but also transform the cell phenotype towards greater contractility and promote cell alignment when the cells reach confluence.[15] Mechanical environment has been assumed to play an important role in determining SMC phenotype as well. However, inconsistent results have been observed in the phenotypic response of SMCs to cyclic strain.[16-19] It has been suggested that the cell state before mechanical strain as well as the magnitude and duration of the strain might contribute to the outcome of phenotype

102

response.[20,21] Given the complexity and variety of stimuli that can regulate VSMCs phenotype shift, there is not yet a conclusion on how we should differentiate and control the environment of VSMCs seeded for vascular engineering.

In our study, we evaluated the influence of combining multiple biomechanical and chemical factors to control proliferation, phenotype, and mechanical behavior of VSMC differentiated from ADSCs. The phenotype of VSMCs will be assessed by the expression of intermediate and late SMC markers and functionally based on its mechanical properties. Our goal is to investigate the potential of utilizing environmental signals to promote VSMCs differentiation and proliferation while regulate their phenotype to meet the need for vascular engineering. The finding of this research could be useful to guide the optimization of VSMCs culture condition for vascular replacement purpose.

4.2 Materials and Method

4.2.1 Micro-patterning of PDMS substrate

Micropatterns were designed using AutoCAD and printed on a photomask film (CAD/Art Services, USA). The size of the individual discontinued wall on PDMS was 30μm×300μm with a 300μm space between walls (see supplemental SEM image). SU-8 2025 (Microchem, USA) master was first fabricated using photolithography steps for PDMS replication. SU-8 photoresist was spin-coated on 350μm thick circular silicon wafer with 50.8mm diameter (University wafer, USA). To harden the photoresist, silicon wafer was soft baked at 65°C for 5mins and then at 95°C for 5mins after photoresist was spread uniformly on silicon wafer. After pre-baking, the silicon wafer was brought to UV

exposure through the designed photomask followed by baking at 65°C and 95°C again. The wafer was then developed using SU-8 developer (Microchem, USA), rinsed with isopropyl alcohol and dried with nitrogen gun. The SU-8 wafer was then ready to be used as a negative mold for PDMS patterning.

Sylgard 184 silicone elastomer base and curing agent were mixed and stirred at 10 : 1 ratio (Sylgard184 kit, Dow Corning, Midland, MI, USA). The mixture was vacuumized for 60mins to remove air bubbles. The degassed mixture was then poured onto silicon wafer and spinned at 1000rpm for 1min followed by soft bake at 65°C for 6 mins. After cooling down the wafer, patterned PDMS was peeled off by blazer and resonated in 100% ethanol and DI water for 30mins followed by chemical treatment in triethylamine, ethyl acetate and acetone each for 2 hours. PDMS was then immersed in 70% ethanol with overnight UV sterilization before it can be used for cell culture. Fibronectin I was coated to the substrate at 10µg/mL prior to cell culture.

4.2.2 Cell culture

ADSCs were obtained from commercially available cell line, which is isolated and expanded from human lipoaspirate from multiple donors (Thermo Scientific HyClone, SV3010201); characterized and tested with stromal, stem, and hematopoietic markers. The passage number of ADSCs used in these experiments was 2-5. ADSCs were differentiated toward SMC lineage via soluble factor along with mechanical stimuli. Differentiating media consisted of LG-DMEM (Gibco) supplemented with 10% FBS (Atlanta Biologicals, Lawrenceville, GA, USA), 1% 100× penicillin-streptomycin (Fisher

Scientific, Pittsburgh, PA, USA) and 10ng/ml TGF-β1(R&D systems, Inc. Minneapolis, MN). Cells were seeded on patterned PDMS substrate layered on the bottom of 6-well flexcell culture plates. At day 3 of cell culture, some groups were exposed to mechanical stretch for 24hrs to simulate pulsatile blood flow.

4.2.3 In vitro mechanical stretch

The Flexcell system FX-2000 (Flexcell, Hillsborough, NC) was used to apply cyclic stretch to ADSCs cultured on patterned PDMS substrate. Due to the intrinsic adhesion between PDMS substrate and silicon membrane of Bioflex plate, mechanical stretch applied at the bottom of the plate can be transmitted to PDMS layered on the silicon membrane. Verification test was performed to check the strain distribution of PDMS substrate by marking dots on both the bottom of the plate and the PDMS. The dots marked on both sides matched up with each other when deformation was applied on silicon membrane indicating same strain field was experienced on PDMS and the bottom of Bioflex plate. ADSCs cultured on patterned PDMS were subjected to 10% strain at 1 Hz at day 3 for 24hrs to simulate the effect of pulsatile blood flow.
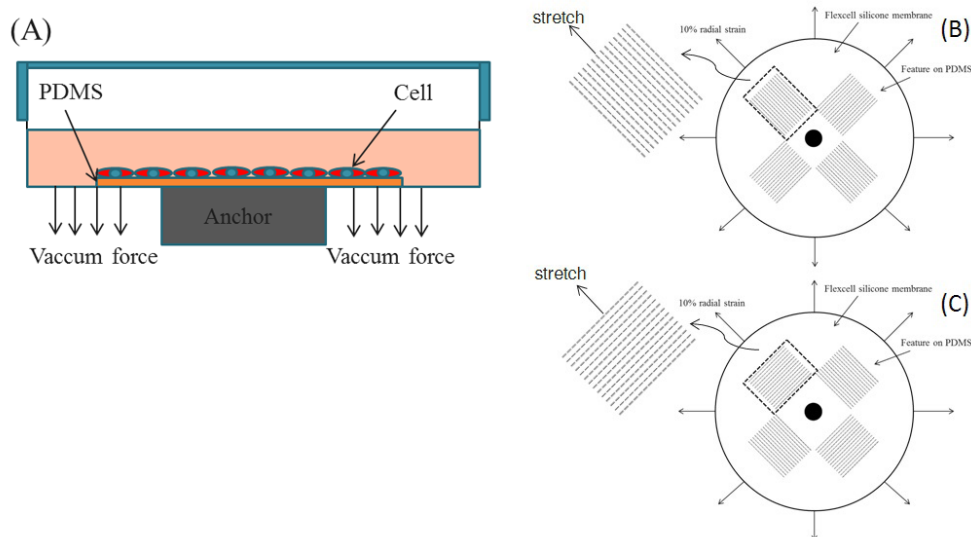
Figure 4.1 Schematic diagram of the Flexcell system : (A) ADSCs on flexcell membrane (B) Discontinued wall on PDMS parallel to mechanical stretch (C) Discontinued wall on PDMS perpendicular to mechanical stretch.

4.2.4 Controls and conditions

Four varied conditions were investigated in this study to evaluate the effect of a chemical growth factor, substrate topography, mechanical stretch on the behavior of differentiating cells. The negative control group was ADSCs seeded on PDMS substrate without differentiating media. Without the induction of TGF-β1, ADSCs proliferated during 7 days culture but did not follow specific differentiation pathway. The positive control group was ADSCs cultured on PDMS substrate with differentiating media. Similar to previous study, ADSCs in this group differentiated into smooth muscle like cell with positive protein and gene expression of VSMC specific markers. For mechanical stretch groups, ADSCs were seeded in two different conditions including (1) PDMS with

features parallel to the direction of mechanical stretch (2) PDMS with features perpendicular to the direction of mechanical stretch

4.2.5 AFM indentation and stress relaxation

For AFM indentation and stress relaxation, an Asylum Research MFP-3D AFM mounted on an Olympus IX-81 spinning disc confocal microscope placed on a vibration isolation table was used. Borosilicate spherical probes (radius = 2.5μm, Nanoandmore corp) with a nominal spring constant of 0.12N/m were utilized to indent into cells. PDMS substrates with cells on it were transferred to fluorodish (WPI) with growth media throughout the experiment to undergo indentation. Prior to loading with the AFM, a thermal fluctuation test is performed in air to calculate the actual spring constant of the cantilever.[22] Single cells were randomly chosen by the optical microscope with a 20× objective lens while morphologically abnormal and overlapped cells were excluded. The AFM probe was positioned over the central part of the cell and was adjusted to avoid the edge of the cell. Each cell was indented 5 times to a depth of more than 1μm with a loading rate of 1μm/s. At each time point, 10 representative cells from each sample were chosen for evaluation and their elastic modulus were then analyzed. Stress relaxation was performed to assess the non-elastic response of single cell. In contrast to indentation, the AFM tip was held within cell for 60 seconds and then retracts back to its original spot. Two relaxation curves were acquired from each cell for further evaluation.

4.2.6 Force curve analysis

The force curves were exported from AFM software (Igor pro, USA) and loaded by

MATLAB with a custom script to determine the contact point of the force curves by

identifying the point at which force shifts upwards above the baseline noise level.[23]

The elastic modulus values from individual cell were calculated by fitting the Hertz

contact model[24] to exported force curve data. This model was fit to the data over the

indentation curve from 30nm to a 300nm indentation depth, a range over which the Hertz

contact model still remain accurate.[25] The Hertz contact model is used to simulate the

elastic behavior between a spherical indenter (AFM probe) and an elastic half plane.[26]

$$F = \frac{4}{3}\frac{E}{(1-v^2)}R^{\frac{1}{2}}\delta^{\frac{3}{2}} \qquad (1)$$

Where F represents the force, E is the elastic modulus of the cell, v is Poisson's ratio

(v=0.5 as the cell cytoplasm is assumed incompressible[27]), R is the radius of indenter,

and δ is the indentation depth. The Hertz model has two major assumptions: linear

elasticity and infinite sample thickness. These can result in significant errors if the

experiments are far from these approximations. However, by using microsphere tips and

the small indentation depth, we can remain close the approximations of the Hertz model

and have reasonable accuracy in the calculation of elastic modulus for cells.[28]

4.2.7 Stress relaxation curve analysis

Stress relaxation curves were also exported from AFM software (Igor pro, USA) and

shifted along y-axis to set the baseline force value to 0. Curves were then normalized to

the maximum force to obtain a starting normalized force value of 1.0 and making all the

stress relaxation curves fit into a 0 to 1 force range. In order to describe the viscosity of the normalized data, the percentage of relaxation was used and calculated with a reduced relaxation function G (t) as

Percent relaxation=1-G (t=60sec)

The reduced relaxation function G(t) can be calculated with various relaxation models. In our study, Quasilinear Viscoelastic (QLV) model was used to fit the data. The QLV reduced relaxation function G (t) contains 3 parameters (c, τ_1, and τ_2) with a continuous relaxation spectrum (S (τ) = c / τ) between τ_1 and τ_2:

$$G\ (t) = \frac{1+c \int_{\tau_1}^{\tau_2} \frac{e^{\frac{-t}{\tau}}}{\tau} d\tau}{1+c \int_{\tau_1}^{\tau_2} \frac{1}{\tau} d\tau} \qquad (2)$$

The constant c is unitless and represents a relative measure of viscous energy dissipation while τ_1 and τ_2 are time constants governing short and long term relaxation behavior, respectively.

4.2.8 Cell proliferation assay

The proliferation of cells cultured under different conditions were analyzed at day 1, 3, 5 and 7 by using CellTiter AQ proliferation assay kit (Promega). The detection of viable cells was based on the bioreduction of a tetrazolium compound (MTS) by cells into a colored formazan product that is soluble in tissue culture medium. Assays were performed by adding 1:5 ratio of CellTiter reagent to medium into cell culture wells containing PDMS substrate, the absorbance of the formazan product on PDMS at 490 nm was recorded by BioTek plate reader. The cell proliferation index was read directly from

the absorbance data as an arbitrary number. All data presented in results are the average of three independent experiments.

4.2.9 Analysis of cell alignment

The alignment of a single cell with respect to the feature on PDMS substrate was measured by calculating the angle between the long axis of the cell nucleus to the long axis of the micropatterned discontinued wall on PDMS with the use of ImageJ software.[29] According to that, the alignment of cell has a value ranges from 0° to 90°. An angle of 0° indicates that the cell is highly aligned to the discontinued wall while an angle of 90°indicates that the cell is aligned perpendicular to the discontinued wall. A wide range of cell angles within a sample means cells are randomly oriented.

4.2.10 Immunofluorescence

Immunostaining was carried out in 6-well flexcell plate with PDMS substrate in it. Cells seeded on PDMS were fixed with 4% Paraformaldehyde (PFA, Sigma-Aldrich) at 37°C for 10 minutes and rinsed with phosphate buffered saline (PBS) two times for 30 minutes. PBS with 0.01 M Glycine and 0.1% Triton-X was used as permeabilization buffer to treat cells for 30 minutes. Cells were then rinsed with 5% BSA/PBS and 5% donkey serum followed by the incubation with primary antibodies against αSM-actin (αSMA) (Sigma-Aldrich), calponin (Abcam), SM22-α (Thermo scientific) and SM myosin heavy chain (SM-MHC) (Signma-Aldrich) at 4°C. Cells were washed three times in 1%BSA-PBS solution and incubated in secondary antibody at 37°C for 2 hours. Images were visualized

using a Nikon Eclipse TE2000-S fluorescence microscope (Nikon USA, Melville, New York, USA)

4.2.11 RNA Isolation and RT-PCR

Expression of smooth muscle cell markers were identified by isolating total RNA from differentiated cells after 1 week culture. Total RNA was extracted using TRIzol (Invitrogen) from cells and further purified using RNeasy Kit (Qiagen, Valencia, CA) according to the instructions of the manufactures. RNA quantification was conducted by using Take3 micro-volume plates (BioTek) and 1 μg RNA of each sample was used for reverse-transcription. Complementary DNA (cDNA) was synthesized using QuantiTect reverse transcription kit (QiaGen) and equal volume of synthesized cDNA was amplified by PCR using primers shown in Table 1. PCR was carried out for 40 cycles of denaturing (94 °C, 15 s), annealing (56°C, 20 s), and extension (72°C, 20s). The amplification efficiency of primers was tested first to ensure the number of PCR cycles for amplification is in a linear range. Human GAPDH was used as internal control for standardization.

Table 4.1 Primer sequence for RT-PCR

Targets	Forward primer	Reverse primer
αSMA	5'-CCAGCTATGTGAAGAAGAAGAGG-3'	5'-GTGATCTCCTTCTGCATTCGGT-3'
SM22-α	5'-CGCGAAGTGCAGTCCAAAATCG-3'	5'-GGGCTGGTTCTTCTTCAATGGGG-3'
Calponin	5'-GGCGAAGACGAAAAGGAAA-3'	5'-GGGTACTCGGGAGTCAGACAG-3'
SM-MHC	5'-GGACGACCTGGTTGTTGATT-3'	5'-GTAGCTGCTTGATGGCTTCC-3'

GAPDH	5'-AGCCACATCGCTCAGACACC-3'	5'-GTACTCAGCGCCAGCATCG-3'

4.2.12 Statistics

ANOVA with Tukey multi comparison test using SAS software were performed to determine if there are significant differences among samples during differentiation. Student's t-tests were used to examine significant differences between samples on a given day and across all time points. P value less than 0.05 were considered statistically significant based on the significant level of 5%. The statistical analysis was conducted among samples in various conditions of all the studies.

4.3 Results

4.3.1 Proliferation

The viability of ADSCs cultured on PDMS in different conditions was evaluated by the MTS assay. The result shows ADSCs induced by differentiating media TGF-β1 proliferate faster than ADSCs without TGF-β1. Mechanical stretch downregulates the proliferation of ADSCs a little while the alignment of features on PDMS did not

influence cell proliferation.

MTS cell viability assay (normlized)
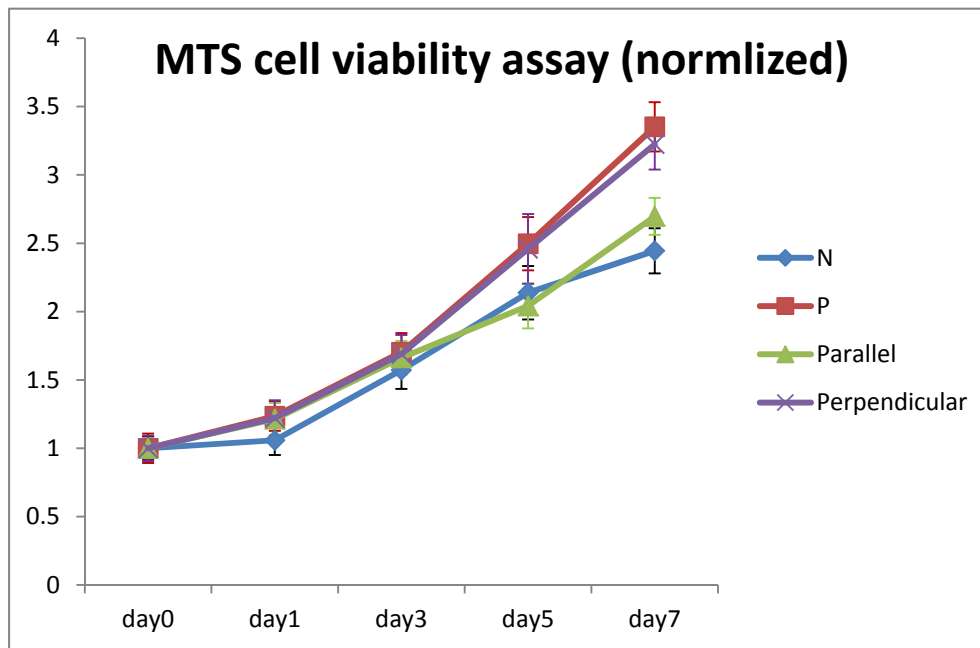
Figure 4.1 The viability of ADSCs cultured in different conditions evaluated by MTS assay. Data are presented as mean ± standard error.

4.3.2 ADSCs alignment on PDMS

The orientation of cell was measured by calculating the angle between the longer axis of cellular nucleus and the longer axis of discontinued wall. ADSCs seeded on PDMS without feature were unorganized and randomly aligned. In contrast, for ADSCs cultured on PDMS with discontinued wall, they were organized and their alignment varied with respect to different culturing conditions. The average cell angle of negative and positive control group was 24.379°±18.291° and 20.029°±18.904° indicating ADSCs with differentiating media aligned better inside discontinued wall. The average cell angle of ADSCs cultured on 1) PDMS with features parallel and (2) perpendicular to 1 day

mechanical stretch were 43.01°±24.75° and 14.03°±10.1° suggesting that the orientation

of feature to mechanical stretch plays a major role in cellular alignment.
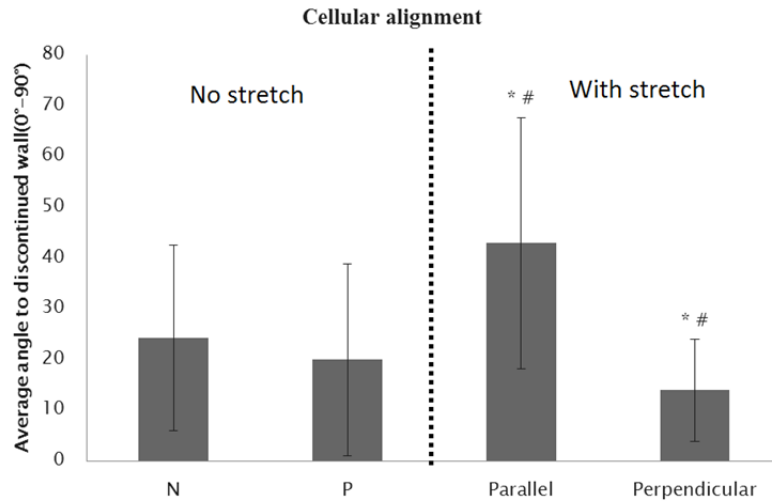
Figure 4.2 Cellular alignment was measured by ImageJ. The average angle of ADSCs

seeded in various conditions was calculated between the longer axis of cellular nucleus

and the discontinued wall. * p<0.05 compared to negative control, # p<0.05 compared to

positive control. Data are presented as mean ± standard error.

4.3.3 Elastic modulus

AFM indentation and stress relaxation were aimed at investigating the effect of substrate

topography, mechanical stretch and 3D culture on cellular mechanical behavior. The

elastic modulus obtained from negative control group of cells without differentiating

media were 0.45±0.08kPa which is significantly lower than the rest of the groups while

the elastic modulus of cells found in positive control group was 2.75±0.22kPa which is

similar to our previous study of ADSCs differentiated by TGF-β1 in vitro. The

distribution of elastic modulus for various conditions is shown in Figure 4. The elastic

modulus of ADSCs cultured on (1) PDMS with features parallel and (2) PDMS with

feature perpendicular to 1 day mechanical stretch were 3.03±0.41kPa and 3.47±0.25kPa

indicating that cells cultured on features perpendicular to mechanical stretch were stiffer

than seeded on features parallel to mechanicals stretch.
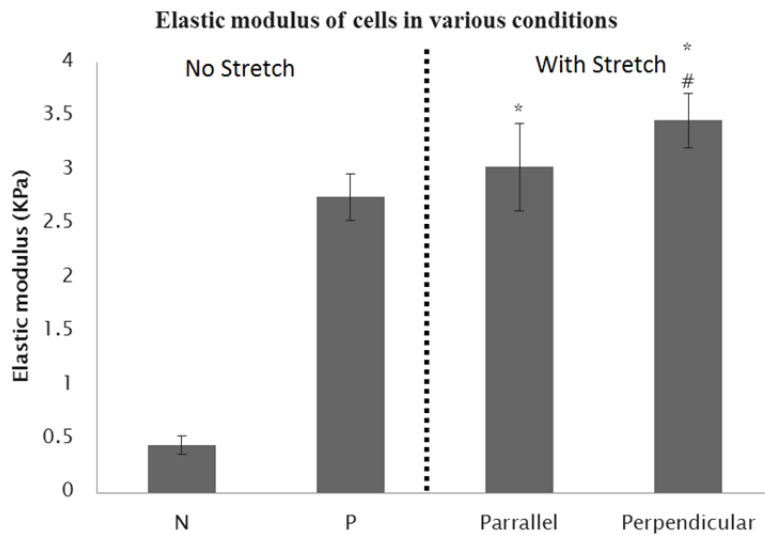
Figure 4.3 Apparent elastic modulus of ADSCs measured with a borosilicate spherical

AFM probes of 5μm diameter at 1μm/s approaching speed with indentation depth from

30nm to 300nm for calculation (10cells per sample). * p<0.05 compared to negative

control, # p<0.05 compared to positive control. Data are presented as mean ± standard

error.

4.3.4 Stress Relaxation

Stress relaxations were performed to estimate the viscoelastic behavior of cells in various

conditions. The average percent stress relaxed of cells over 7 days culture are shown in

table2 The coefficient of determination (R^2) for QLV has an overall 99% value indicating that the model fit the ADSCs relaxation data well. On day 7 in culture, generally ADSCs in mechanical stretch groups have lower value of percent stress relaxed compared to ADSCs cultured in in control groups. There were no significant differences between negative and positive control groups.

Table 4.2 Percent stress relaxed over 60 seconds hold for ADSCs 7 days culture in different conditions. QLV model was used to fit stress relaxation curves with R2 listed. Data from all samples were averaged with standard error.

	Samples	Percent Stress Relaxed (%)	Coefficient of determination on R^2 (%)	τ_1 (fast relaxation)	τ_2 (longer relaxation)	C(energy dissipation)
No stretch	N	58.65±2.37	99.76	0.47±0.13	368.80±18.46	0.18±0.04
	P	57.83±3.78	98.13	0.26±0.01	123.41±25.91	0.13±0.005
	Parallel	49.52±3.92	98.71	0.31±0.04	141.83±78.46	0.21±0.02

With Stretch

Perpendicular   50.26±3.46   99.65   0.29±0.08   217.50±70.28   0.17±0.04
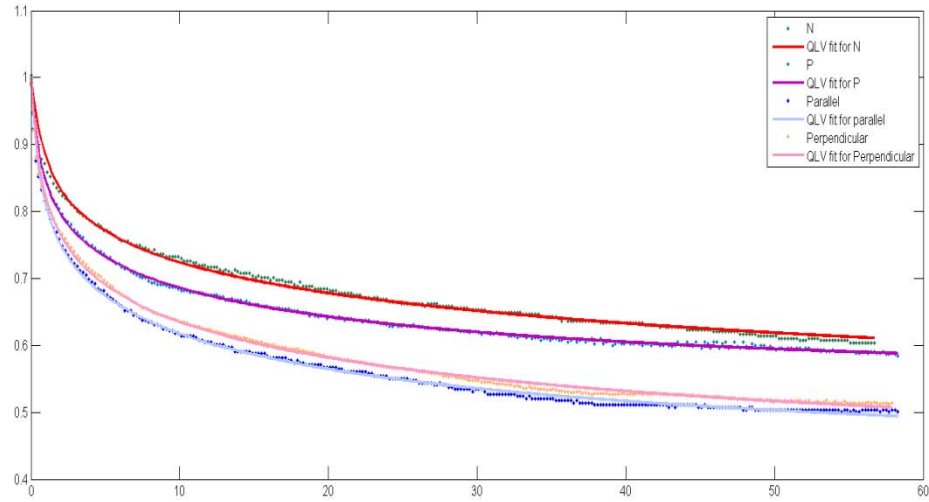
Figure 4.4 Sample stress relaxation curve with QLV fit.

4.3.5 Immunofluorescence

To determine the role of multiple stimuli in the differentiation of ADSCs to SM-like cells,

we investigate the expression of SMC specific markers including αSMA, SM22α,

calponin and SM-MHC detected by fluorescent staining. Figure 6 shows the marker

expression among various conditions.

| α-SMA | SM22α | calponin | SM-MHC |
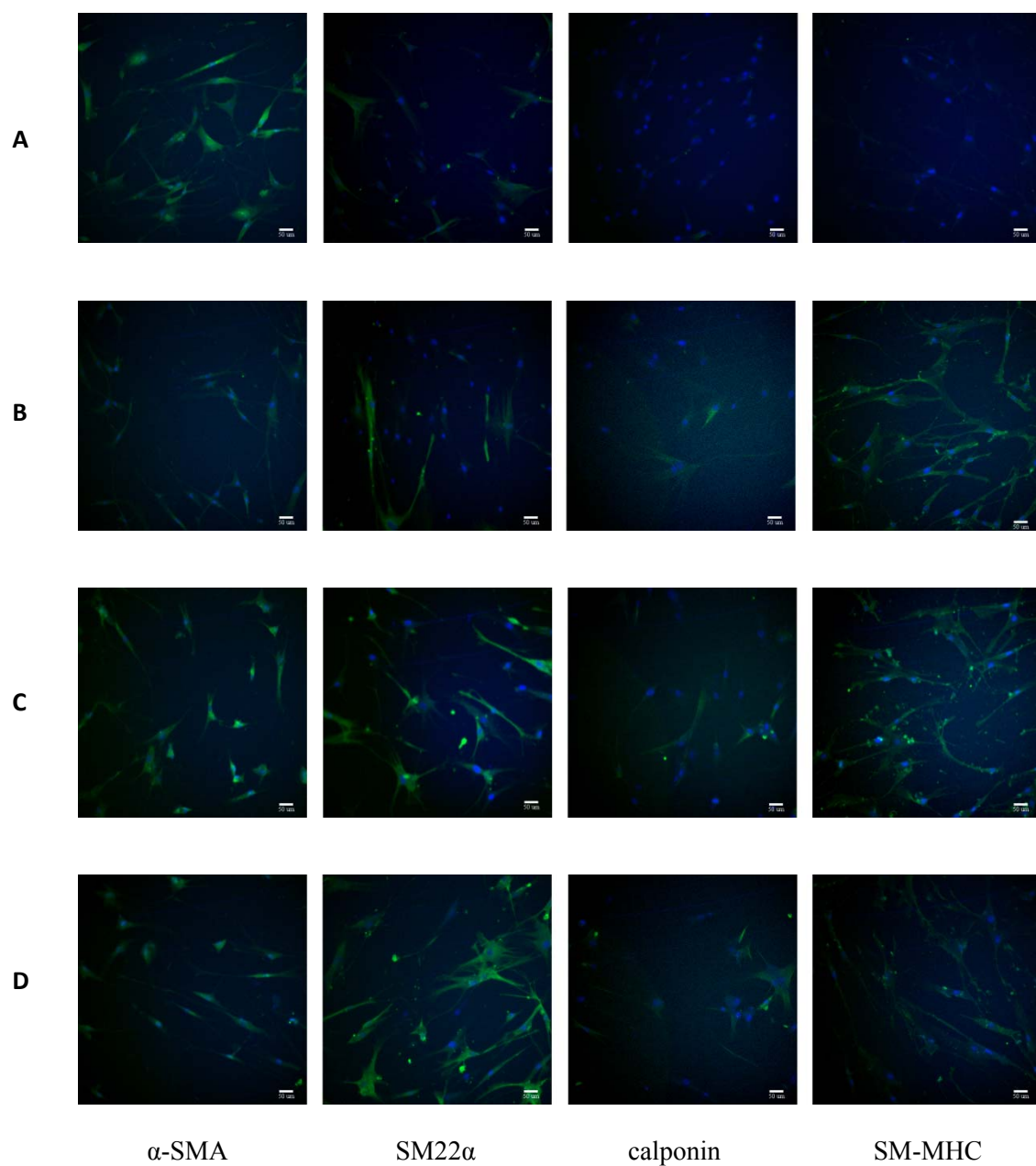
Figure 4.5 Expression of SMC-specific proteins (a-SMA, SM22α, calponin, SM-MHC) under (A) negative control group (B) positive control group (C) parallel group (D) perpendicular group by immunofluorescent staining. Nucleus were stained with DAPI

while FITCS conjugated antibodies against a-SMA, SM22α, calponin, SM-MHC were used for immunostaining (scale bar=50μm).

4.3.6 RT-PCR

In order to corroborate our findings of SMC-specific protein expression under different culture conditions, RT-PCR was performed to assess SMC-specific gene expression regulated by multiple biomechanical signals. By comparing gene expressions including αSMA, SM22α, calponin and SM-MHC between cells in negative and positive control group, we found TGF-β1 upregulated SMC-specific gene expression similar to previous study [12]. Although all these genes were elevated compared to control group, differences in gene expression were observed among these conditions. Higher fold change in gene expressions of ADSCs cultured on PDMS with features perpendicular to mechanical stretch was found compared to ADSCs cultured on parallel feature. The expression of αSMA and SM22α were also downregulated slightly as a result of 10% mechanical strain for 24 hours if compared to positive no stretch control group. Gene expression of ADSCs in various groups was shown in Figure 7.
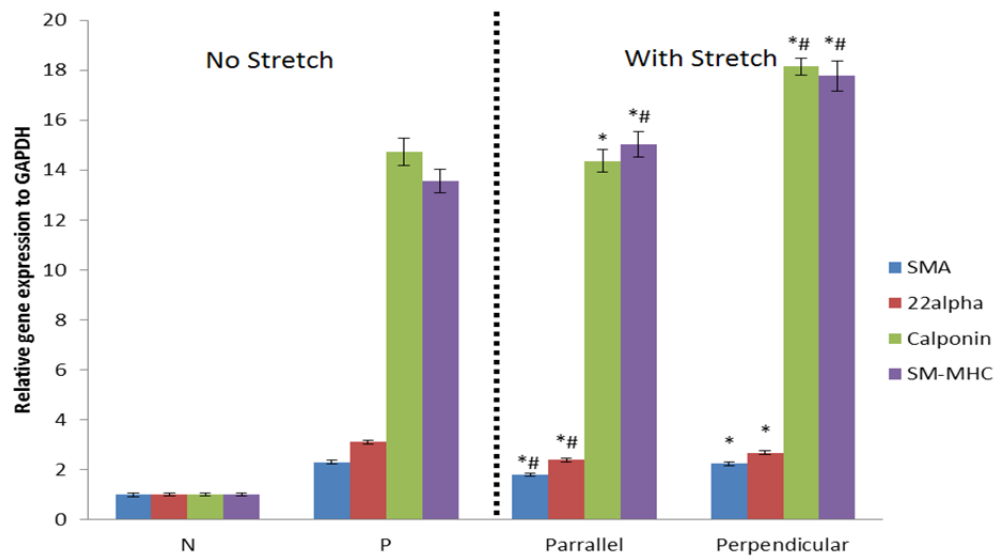
Figure 4.6 RT-PCR was performed to measure the expression of αSMA, SM22α, calponin and SM-MHC of ADSCs cultured for 7 days in different conditions with control gene GAPDH. * p<0.05 compared to negative control, # p<0.05 compared to positive control. Data presented as mean ± standard error.

4.4 Discussion and Conclusion

The results of our study indicate that the migration, mechanical property and differentiation of VSMC can be regulated by diverse mechanical signals including substrate topography and mechanical stretch. Distinct differences were observed among cells cultured in different conditions. An important finding of this study is the potential of combining different chemical and mechanical signals in modulating VSMC differentiation and phenotype change. This could be extremely helpful in obtaining

functional VSMC from stem cell source by promoting the proliferation and differentiation at first followed with cellular phenotype and growth control.

The excessive proliferation and unexpected phenotype shifts that can result in vessel restenosis has always been one of the major concerns of reconstructing VSMCs layer into tissue-engineered vessel construct.[30,31] It has been known that cyclic strain can be a key factor in VSMCs behavior.[21,32] Our findings suggest that 24hr 10% cyclic strain has a minor effect in repressing the proliferation. Literatures also report that the pathological cyclic strain largely increase VSMCs proliferation while physiological strain decrease VSMCs proliferation.[33,34] Thus, we believe the proper use of mechanical stretch can help control VSMCs proliferation as well as keep the cells in a quiescent state.

In vascular structure, endothelial cells (ECs) are oriented longitudinally in the intima while the VSMCs are aligned circumferentially in the media.[35,36] One of the main tasks in tissue engineering is to mimic the vascular architecture. Thanks to the introduction of microfabrication techniques, the shape and orientation of VSMCs can now be regulated by micropattern or microchannel on a given surface.[15,37,38] In our study, we utilize soft lithography to fabricate discontinued microwalls on PDMS to study cellular alignment under different conditions. Our finding that cellular alignment is highly correlated with the orientation of features on substrate suggests that the direction of features on substrate to cyclic loading is almost as important as the shape of features. In our study, cells close to microwall tend to adhere to the wall thus they aligned parallel to the feature. However, cells in the middle of two walls tend to align perpendicular to the

direction of mechanical stretch if not restricted by walls. Therefore, cells cultured on

PDMS with microwalls perpendicular to mechanical stretch had a significant better

alignment than cells in parallel group (Figure 4.8). The limitation of this study is that

cells were not allowed to proliferate to fully confluency which could result in even better

cellular alignment as observed by other group.[15]
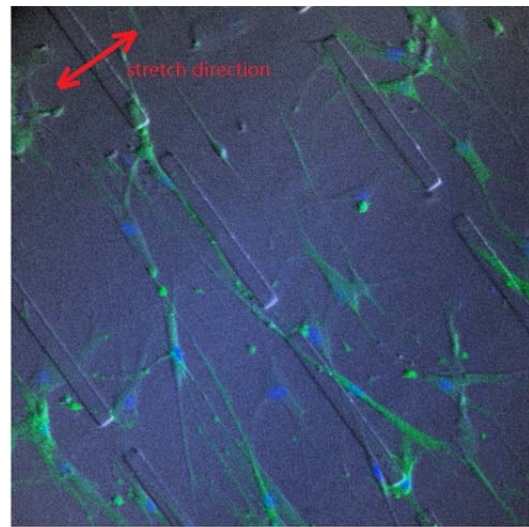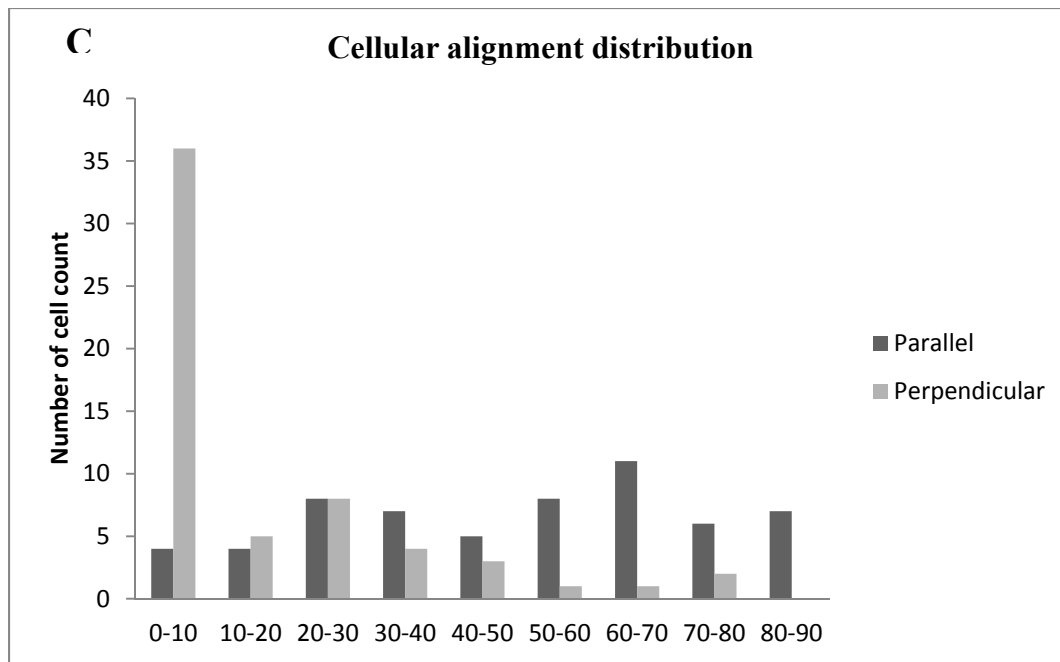

A   B

Figure 4.7 Sample confocal images to calculate cellular alignment (A) cells in parallel group (B) cells in perpendicular group and distribution of cellular alignment based on the angle of cellular nucleus and longer axis of discontinued wall (C) number of cells count in parallel and perpendicular group.

The mechanical behavior of a vascular smooth muscle cell not only suggests its ability to contract and relax but also indicates tissue-level function. However, limited research has been done to analyze the effect of combining biochemical and biomechanical signals on VSMCs behavior. TGF-β1 has been found to induce smooth muscle differentiation from adult stem cell according to many research groups.[39-41] Micropatterned substrates have also been reported to induce and maintain the differentiated VSMC phenotype in vitro.[15,42] In addition, past studies have shown that the phenotype of differentiated VSMCs can be modulated by mechanical strain [19]. In our study, we investigated the

mechanical behavior of ADSCs following VSMC differentiation under different conditions. We found that the topography of substrates and the mechanical strain both have impact on the mechanical properties of VSMCs differentiated from ADSCs. When these environmental factors are combined, they contribute differently to the mechanical property change of cells which could be used to guide the optimization of culture environment in order to achieve functional VSMCs.

Cellular mechanical propeties were characterized in two different mechanical tests: elastic modulus of cells tested by AFM nanoindentation provided the overall mechanical property of single cell for comparison among different conditions while percent stress relaxation of cells analyzed by dwelling the AFM tip for 60s gave the viscoelastic information of cell. ADSCs cultured in the perpendicular group shows the highest elastic modulus among all conditions followed by cells in parallel group and positive no stretch control group. Cyclic stretch has been shown to increase the expression of contractile differentiation markers in VSMCs[43,44] and cells in contractile phenotype are stiffer than cells in synthetic phenotype[45] thus the increase of stiffness of cells in perpendicular group may due to the upregulation of contractile phenotype in response to cyclic strain. Stress relaxation experiments have been used to determine viscoelastic property of cells recently.[46-48] Under 60s static strain, the least percent stress relaxed was observed among cells with collagen top layer followed by cells in parallel and perpendicular group and then the control groups. Since it has been conjectured that the viscoelastic behavior of biological tissue is closely related to the smooth muscle content,[49] our study sheds light on how environmental signals affect the viscoelastic

behavior of differentiated smooth muscle cell, which can be helpful in designing tissue engineered construct.

Our findings are generally consistent with previous studies of how smooth muscle cell respond to different environmental signals. It has been reported that airway smooth muscle cells exposed to chronic mechanical strain have increased cytoskeletal stiffness[50] and vascular smooth muscle cell under cyclic equibiaxial stretching at 0.25hz can have a time dependent significant increase in cell stiffness[51] which is similar to the increase of elastic modulus of the ADSCs cells in response to cyclic strain observed in our study. However, currently, there are no standards of how to apply mechanical strain to VSMCs which might be the reason why some different effects have been observed in VSMCs in response to mechanical strain.[52-54]

The Hertz contact model was utilized in our study to evaluate cell elastic modulus. Although Hertz model makes several simplifying assumptions, it can still provide good qualitatively comparison of the elastic modulus between different cells during differentiation. Previous research shows the result of cell modulus remains reasonable if the indentation depth used in Hertz fit is small before significant non-linearity occurs with the increase of indentation depth.[55] The QLV model has been used extensively to model tissue behavior, but was only recently applied to cellular data.[56,57] In our study, QLV model provided a good fit with an average R^2 of 0.99 and remains consistent among cells in all four conditions.

To further establish that cells differentiated from ADSCs are functional smooth muscle cell, the expression of SMC-specific markers were examined by PCR and fluorescent staining. ADSCs cultured in all conditions induced by TGF-β1 were stained positive for SMC specific protein αSMA, SM22α, calponin and SM-MHC compared to negative control group. The gene expression analyzed by PCR reveals a baseline expression of αSMA, SM22α in negative control group with a generally 2 fold increase found in other groups after 7 days differentiation. The expression of SMC late marker calponin and SM-MHC had more than 14 fold increase among positive, parallel and perpendicular group compared to negative control group. According to the result, it suggests that when induced by TGF-β1, ADSCs differentiate down a SMC lineage and such differentiation can be modulated by different environmental factors in terms of the expression of specific markers.

In conclusion, TGF-β1 promoted the VSMC differentiation of ADSCs with the increase of mechanical strength and SMC specific marker expression of cells. 10% Cyclic strain at 1hz for 24hrs slightly inhibit cell proliferation but upregulate SMC marker expression. Among all the conditions, ADSCs cultured on discontinued walls perpendicular to mechanical strain had the best cellular alignment along with highest elastic modulus and marker expression. Based on our findings, ADCSs as one of the most abundant stem cell in our body can be a competitive candidate in providing functional smooth muscle cell if modulated with proper environmental signals. However, further research is required to determine the best way to combine biochemical and biophysical stimuli to achieve large quantity of functional VSMCs without excessive proliferation and phenotype shift.

4.5 Reference

[1] Hoerstrup, S. P., Zund G., Sodian R., Schnell A. M., Grunenfelder J., and Turina M. I. *Tissue engineering of small caliber vascular grafts*. European Journal of Cardio-Thoracic Surgery, 2001. 20: 164-169.

[2] Dahl, S. L. M., Koh J., Prabhakar V., and Niklason L. E. *Decellularized native and engineered arterial scaffolds for transplantation*. Cell Transplantation, 2003. 12: 659-666.

[3] Wu, H. C., Wang T. W., Kang P. L., Tsuang Y. H., Sun J. S., and Lin F. H. *Coculture of endothelial and smooth muscle cells on a collagen membrane in the development of a small-diameter vascular graft*. Biomaterials, 2007. 28: 1385-1392.

[4] Han, J. H., Liu J. Y., Swartz D. D., and Andreadis S. T. *1.Molecular and functional effects of organismal ageing on smooth muscle cells derived from bone marrow mesenchymal stem cells*. Cardiovascular Research, 87: 147-155.

[5] Steinbach, S. K., El-Mounayri O., DaCosta R. S., Frontini M. J., Nong Z. X., Maeda A., Pickering J. G., Miller F. D., and Husain M. *2Directed Differentiation of Skin-Derived Precursors Into Functional Vascular Smooth Muscle Cells*. Arteriosclerosis Thrombosis and Vascular Biology, 31: 2938-U2452.

[6] Wang, C., Yin S., Cen L., Liu Q. H., Liu W., Cao Y. L., and Cui L. *3.Differentiation of Adipose-Derived Stem Cells into Contractile Smooth Muscle Cells Induced by Transforming Growth Factor-beta 1 and Bone Morphogenetic Protein-4*. Tissue Engineering Part A, 16: 1201-1213.

[7] Huang, J. I., Zuk P. A., Jones N. F., Zhu M., Lorenz H. P., Hedrick M. H., and Benhaim P. *Chondrogenic potential of multipotential cells from human adipose tissue*. Plastic and Reconstructive Surgery, 2004. 113: 585-594.

[8] Zuk, P. A., Zhu M., Ashjian P., De Ugarte D. A., Huang J. I., Mizuno H., Alfonso Z. C., Fraser J. K., Benhaim P., and Hedrick M. H. *Human adipose tissue is a source of multipotent stem cells*. Molecular Biology of the Cell, 2002. 13: 4279-4295.

[9] Hayashi, K., Saga H., Chimori Y., Kimura K., Yamanaka Y., and Sobue K. *Differentiated phenotype of smooth muscle cells depends on signaling pathways through insulin-like growth factors and phosphatidylinositol 3-kinase*. Journal of Biological Chemistry, 1998. 273: 28860-28867.

[10] Moussallem, M. D., Olenych S. G., Scott S. L., Keller T. C. S., and Schlenoff J. B. *Smooth Muscle Cell Phenotype Modulation and Contraction on Native and Cross-Linked Polyelectrolyte Multilayers*. Biomacromolecules, 2009. 10: 3062-3068.

[11] Potta, S. P., Liang H. M., Pfannkuche K., Winkler J., Chen S. H., Doss M. X., Obernier K., Kamisetti N., Schulz H., Hubner N., Hescheler J., and Sachinidis A. *Functional Characterization and Transcriptome Analysis of Embryonic Stem Cell-Derived Contractile Smooth Muscle Cells*. Hypertension, 2009. 53: 196-U171.

[12] Wang, C., Yin S., Cen L., Liu Q. H., Liu W., Cao Y. L., and Cui L. *Differentiation of Adipose-Derived Stem Cells into Contractile Smooth Muscle Cells Induced by Transforming Growth Factor-beta 1 and Bone Morphogenetic Protein-4*. Tissue Engineering Part A, 2010. 16: 1201-1213.

[13] Stegemann, J. P., Hong H., and Nerem R. M. *Mechanical, biochemical, and extracellular matrix effects on vascular smooth muscle cell phenotype*. Journal of Applied Physiology, 2005. 98: 2321-2327.

[14] Nikkhah, M., Edalat F., Manoucheri S., and Khademhosseini A. *Engineering microscale topographies to control the cell-substrate interface*. Biomaterials, 2012. 33: 5230-5246.

[15] Cao, Y., Poon Y. F., Feng J., Rayatpisheh S., Chan V., and Chan-Park M. B. *Regulating orientation and phenotype of primary vascular smooth muscle cells by biodegradable films patterned with arrays of microchannels and discontinuous microwalls*. Biomaterials, 2010. 31: 6228-6238.

[16] Birukov, K. G., Shirinsky V. P., Stepanova O. V., Tkachuk V. A., Hahn A. W. A., Resink T. J., and Smirnov V. N. *Stretch Affects Phenotype and Proliferation of Vascular Smooth-Muscle Cells*. Molecular and Cellular Biochemistry, 1995. 144: 131-139.

[17] Chapman, G. B., Durante W., Hellums J. D., and Schafer A. I. *Physiological cyclic stretch causes cell cycle arrest in cultured vascular smooth muscle cells*. American Journal of Physiology-Heart and Circulatory Physiology, 2000. 278: H748-H754.

[18] Hipper, A., and Isenberg G. *Cyclic mechanical strain decreases the DNA synthesis of vascular smooth muscle cells*. Pflugers Archiv-European Journal of Physiology, 2000. 440: 19-27.

[19] Qu, M. J., Liu B., Wang H. Q., Yan Z. Q., Shen B. R., and Jiang Z. L. *Frequency-dependent phenotype modulation of vascular smooth muscle cells under cyclic mechanical strain*. Journal of Vascular Research, 2007. 44: 345-353.

[20] Cappadona, C., Redmond E. M., Theodorakis N. G., McKillop I. H., Hendrickson R., Chhabra A., Sitzmann J. V., and Cahill P. A. *Phenotype dictates the growth response of vascular smooth muscle cells to pulse pressure in vitro*. Experimental Cell Research, 1999. 250: 174-186.

[21] Williams, B. *Mechanical influences on vascular smooth muscle cell function*. Journal of Hypertension, 1998. 16: 1921-1929.

[22] Butt, H. J., and Jaschke M. *Calculation of Thermal Noise in Atomic-Force Microscopy*. Nanotechnology, 1995. 6: 1-7.

[23] Crick, S. L., and Yin F. C. P. *Assessing micromechanical properties of cells with atomic force microscopy: importance of the contact point*. Biomechanics and Modeling in Mechanobiology, 2007. 6: 199-210.

[24] Kuznetsova, T. G., Starodubtseva M. N., Yegorenkov N. I., Chizhik S. A., and Zhdanov R. I. *Atomic force microscopy probing of cell elasticity*. Micron, 2007. 38: 824-833.

[25] Dimitriadis, E. K., Horkay F., Maresca J., Kachar B., and Chadwick R. S. *Determination of elastic moduli of thin layers of soft material using the atomic force microscope*. Biophysical Journal, 2002. 82: 2798-2810.

[26] Rico, F., Roca-Cusachs P., Gavara N., Farre R., Rotger M., and Navajas D. *Probing mechanical properties of living cells by atomic force microscopy with blunted pyramidal cantilever tips*. Physical Review E, 2005. 72.

[27] Radmacher, M. *Measuring the elastic properties of living cells by the atomic force microscope*. Atomic Force Microscopy in Cell Biology, 2002. 68: 67-90.

[28] Mahaffy, R. E., Shih C. K., MacKintosh F. C., and Kas J. *Scanning probe-based frequency-dependent microrheology of polymer gels and biological cells*. Physical Review Letters, 2000. 85: 880-883.

[29] Sarkar, S., Lee G. Y., Wong J. Y., and Desai T. A. *Development and characterization of a porous micro-patterned scaffold for vascular tissue engineering applications*. Biomaterials, 2006. 27: 4775-4782.

[30] Chlupac, J., Filova E., and Bacakova L. *Blood Vessel Replacement: 50 years of Development and Tissue Engineering Paradigms in Vascular Surgery*. Physiological Research, 2009. 58: S119-S139.

[31] Parizek, M., Novotna K., and Bacakova L. *The Role of Smooth Muscle Cells in Vessel Wall Pathophysiology and Reconstruction Using Bioactive Synthetic Polymers*. Physiological Research, 2011. 60: 419-437.

[32] Morrow, D., Sweeney C., Birney Y. A., Cummins P. M., Walls D., Redmond E. M., and Cahill P. A. *Cyclic strain inhibits notch receptor signaling in vascular smooth muscle cells in vitro*. Circulation Research, 2005. 96: 567-575.

[33] Qi, Y. X., Qu M. J., Yan Z. Q., Zhao D., Jiang X. H., Shen B. R., and Jiang Z. L. *Cyclic Strain Modulates Migration and Proliferation of Vascular Smooth Muscle Cells via Rho-GDI alpha, Rac1, and p38 Pathway*. Journal of Cellular Biochemistry, 2010. 109: 906-914.

[34] Colombo, A., Guha S., Mackle J. N., Cahill P. A., and Lally C. *Cyclic strain amplitude dictates the growth response of vascular smooth muscle cells in vitro: role in*

in-stent restenosis and inhibition with a sirolimus drug-eluting stent. Biomechanics and

Modeling in Mechanobiology, 2013. 12: 671-683.

[35] Lee, A. A., Graham D. A., Dela Cruz S., Ratcliffe A., and Karlon W. J. *Fluid shear stress-induced alignment of cultured vascular smooth muscle cells*. Journal of

Biomechanical Engineering-Transactions of the Asme, 2002. 124: 37-43.

[36] Isenberg, B. C., Williams C., and Tranquillo R. T. *Small-diameter artificial arteries engineered in vitro*. Circulation Research, 2006. 98: 25-35.

[37] Sarkar, S., Dadhania M., Rourke P., Desai T. A., and Wong J. Y. *Vascular tissue engineering: microtextured scaffold templates to control organization of vascular smooth muscle cells and extracellular matrix*. Acta Biomaterialia, 2005. 1: 93-100.

[38] Shen, J. Y., Chan-Park M. B., Zhu A. P., Zhu X., Beuerman R. W., Yang E. B., Chen W., and Chan V. *Three-dimensional microchannels in biodegradable polymeric films for control orientation and phenotype of vascular smooth muscle cells*. Tissue Engineering, 2006. 12: 2229-2240.

[39] Chen, S. Y., and Lechleider R. J. *Transforming growth factor-beta-induced differentiation of smooth muscle from a neural crest stem cell line*. Circulation Research, 2004. 94: 1195-1202.

[40] Gong, Z., Calkins G., Cheng E. C., Krause D., and Niklason L. E. *Influence of Culture Medium on Smooth Muscle Cell Differentiation from Human Bone Marrow-Derived Mesenchymal Stem Cells*. Tissue Engineering Part A, 2009. 15: 319-330.

[41] Harris, L. J., Abdollahi H., Zhang P., McIlhenny S., Tulenko T. N., and DiMuzio P. J. *Differentiation of Adult Stem Cells into Smooth Muscle for Vascular Tissue Engineering*. Journal of Surgical Research, 2011. 168: 306-314.

[42] Chang, S., Song S., Lee J., Yoon J., Park J., Choi S., Park J. K., Choi K., and Choi C. *Phenotypic Modulation of Primary Vascular Smooth Muscle Cells by Short-Term Culture on Micropatterned Substrate*. Plos One, 2014. 9.

[43] Numaguchi, K., Eguchi S., Yamakawa T., Motley E. D., and Inagami T. *Mechanotransduction of rat aortic vascular smooth muscle cells requires RhoA and intact actin filaments*. Circulation Research, 1999. 85: 5-11.

[44] Lee, J., Wong M., Smith Q., and Baker A. B. *A novel system for studying mechanical strain waveform-dependent responses in vascular smooth muscle cells*. Lab on a Chip, 2013. 13: 4573-4582.

[45] Hemmer, J. D., Dean D., Vertegel A., Langan E., and LaBerge M. *Effects of serum deprivation on the mechanical properties of adherent vascular smooth muscle cells*. Proceedings of the Institution of Mechanical Engineers Part H-Journal of Engineering in Medicine, 2008. 222: 761-772.

[46] Darling, E. M., Zauscher S., and Guilak F. *Viscoelastic properties of zonal articular chondrocytes measured by atomic force microscopy*. Osteoarthritis and Cartilage, 2006. 14: 571-579.

[47] Darling, E. M., Zauscher S., Block J. A., and Guilak F. *A thin-layer model for viscoelastic, stress-relaxation testing of cells using atomic force microscopy: Do cell properties reflect metastatic potential?* Biophysical Journal, 2007. 92: 1784-1791.

[48] Okajima, T., Tanaka M., Tsukiyama S., Kadowaki T., Yamamoto S., Shimomura M., and Tokumoto H. *Stress relaxation of HepG2 cells measured by atomic force microscopy*. Nanotechnology, 2007. 18.

[49] McDonald, S. J., Dooley P. C., McDonald A. C., Schuijers J. A., Ward A. R., and Grills B. L. *Early Fracture Callus Displays Smooth Muscle-Like Viscoelastic Properties Ex Vivo: Implications for Fracture Healing*. Journal of Orthopaedic Research, 2009. 27: 1508-1513.

[50] Seliktar, D., Black R. A., Vito R. P., and Nerem R. M. *Dynamic mechanical conditioning of collagen-gel blood vessel constructs induces remodeling in vitro*. Annals of Biomedical Engineering, 2000. 28: 351-362.

[51] Na, S., Trache A., Trzeciakowski J., Sun Z., Meininger G. A., and Humphrey J. D. *Time-dependent changes in smooth muscle cell stiffness and focal adhesion area in response to cyclic equibiaxial stretch*. Annals of Biomedical Engineering, 2008. 36: 369-380.

[52] Nikolovski, J., Kim B. S., and Mooney D. J. *Cyclic strain inhibits switching of smooth muscle cells to an osteoblast-like phenotype*. Faseb Journal, 2003. 17: 455-+.

[53] Seliktar, D., Nerem R. M., and Galis Z. S. *Mechanical strain-stimulated remodeling of tissue-engineered blood vessel constructs*. Tissue Engineering, 2003. 9: 657-666.

[54] Solan, A., Mitchell S., Moses M., and Niklason L. *Effect of pulse rate on collagen deposition in the tissue-engineered blood vessel*. Tissue Engineering, 2003. 9: 579-586.

[55] Chizhik, S. A., Huang Z., Gorbunov V. V., Myshkin N. K., and Tsukruk V. V. *Micromechanical properties of elastic polymeric materials as probed by scanning force*

microscopy. Abstracts of Papers of the American Chemical Society, 1998. 216: U141-U141.

[56] Toms, S. R., Dakin G. J., Lemons J. E., and Eberhardt A. W. *Quasi-linear viscoelastic behavior of the human periodontal ligament*. Journal of Biomechanics, 2002. 35: 1411-1415.

[57] Doehring, T. C., Carew E. O., and Vesely I. *The effect of strain rate on the viscoelastic response of aortic valve tissue: A direct-fit approach*. Annals of Biomedical Engineering, 2004. 32: 223-232.

CHAPTER FIVE

EXPERIMENTAL AND COMPUTATIONAL CHARACTERIZATION OF

DIFFERENTIATED VASCULAR SMOOTH MUSCLE CELLS CULTURED IN 3D

CONSTRUCT IN DYNAMIC ENVIRONMENT

5.1 Introduction

Blood vessel wall consist of three distinct layers: adventitia, media and intima. Vascular

smooth muscle cell, as one of the most abundant cells in blood vessel, mainly exist in the

media layer. Under normal physiological condition, VSMC act as the major component

in regulating the constriction and dilation of blood vessel. While under pathological

condition, VSMC can change its phenotype as well as proliferation, migration and matrix

synthesis which can result in unwanted accumulation of plaque and vessel occlusion.

Reconstructing VSMC layer in diseased tissue has not been highly studied for blood

vessel engineering due to the high risk of their excessive proliferation and unexpected

phenotype shifts. However, VSMC play an important role in maintaining physiological

function of vessels and can provide sufficient mechanical strength in dynamic conditions.

Based on this fact, VSMCs should logically be incorporated in the development of tissue-

engineered blood vessels.

Decades of experimental research have provided us the knowledge of how VSMC are

affected by their environment. However, the effect of combing different environmental

factors on regulating VSMC's behavior is not well understood. In addition, the majority

of 2D monolayer studies cannot fully reflect the physiological environment to which VSMC are exposed. The development of more complex and physiologically relevant culture system is therefore needed to better mimic the interaction between VSMC and the surrounding environment. Such culture system is supposed to provide combined biochemical and biophysical stimulation in a 3D environment. At the same time, biomechanical models have the potential to simulate complex physiological condition and can be used to guide the development of engineered blood vessel as well as other engineered tissue. The introduction of computational characterization of cellular behavior in a complex culture condition can not only provide prediction of specific responses of cells to environmental signals but also save the time and effort for repetitive studies and system design. In this study, we first built a simplified 3D culture construct consist of micropatterned PDMS and collagen top layer with cyclic strain to mimic physiological conditions to differentiate ADSCs to VSMC. We then developed a biomechanical model that incorporate the mechanical property of differentiated cell and distinct layers with geometrical information acquired from confocal images to predict cellular behavior. Finite element analysis (FEA) is being applied to determine theoretical strain distribution in cells and culture construct.

5.2 Materials and Method

In this study, many of the methods are similar to the methods used in chapter 4. For previously discussed methods they are briefly outlined here while new concepts are introduced and described in detail.

5.2.1 Sample preparation

Collagen top layer

Type I collagen sourced from rat tail (BD, cat. #354249) was used as the major
component in making collagen gel used in our study. The collagen layer was prepared by
mixing 1:1:8 proportions of HEPES (0.5mM): 10X DMEM: collagen I (4mg/ml) first and
the mixture was placed on ice during the whole procedure to prevent it from gelled.
Before adding collagen layer to the cell culture dish, medium was aspirated and discarded
to leave the plain PDMS substrate with cells seeded on top of it. After that, 500µl
collagen solution was pipetted carefully to the edge of the dish and spread out to form a
thin layer in the dish. The whole dish was incubated at 37°C for 45 minutes until the
collagen layer was gelled and solid. Cell culture media was added back into the dish for
cell growth. (Fig 5.1)
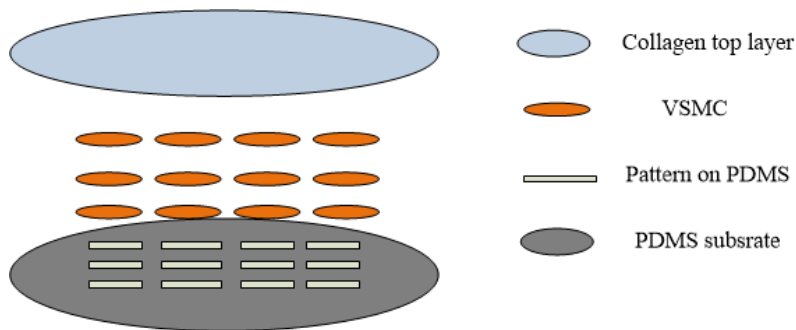
Figure 5.1 Schematic of 3D culture construct

Controls and conditions

ADSCs were seeded on micropatterned PDMS substrate as discussed in section 4.2.1. The negative control group and positive control group were ADSCs cultured with and without differentiating media Tgf-β1 described in 4.24. With the introduction of collagen top layer, three varied conditions were investigated to evaluate the effect of 3D culture on cell behavior. Three different conditions include: (1) 3D culture of cell on PDMS with features parallel to 1 day mechanical stretch (2) 3D culture of cell on PDMS with features perpendicular to 1 day mechanical stretch (3) 3D culture of cells on PDMS without mechanical stretch.

AFM Testing and Data analysis

For cell cultured in 3D construct, collagenase I was used to dissolve the top collagen layer in order to do AFM testing on cells. 1mg/ml collagenase I (Gibco®, 17100-017) in culture media was added to cell culture dish at day 7 followed by 2 hours incubation at 37°C. PDMS substrates with cells on it were then transferred to fluorodish (WPI) with growth media throughout the experiment to undergo AFM indentation. The same AFM indentation experiments and data analysis discussed in section 4.2.5 were performed on all groups in this study. Hertz contact model and QLV model were also used to fit the indentation and stress relaxation data collected in this study.

Proliferation and Alignment study

To evaluate cell growth and migration in 3D culture, same proliferation and alignment study were performed as discussed in section 4.2.8 and 4.2.9. For cells cultured with top collagen layer, CellTiter working solution was added after the collagen layer was

dissolved by collagenase I. Fluorescent images were also taken without collagen layer and analyzed in ImageJ to get the average cell angle between the long axis of the cell nucleus to the long axis of the micropatterned discontinued wall on PDMS.

Immunofluorescence and PCR

In order to corroborate the differentiation from ADSCs to VSMC, immunofluorescence and PCR were carried out to test VSMC specific marker and gene expression. Similar to section 4.2.10 all samples were fixed and stained for nuclei, αSMA, calponin, SM22-α and SM-MHC. In PCR study, specifically for 3D culture samples, the cells on PDMS substrate were transferred to new dish for RNA isolation to prevent protein contamination. Primers used in this study are listed in section 4.2.11.

5.2.2 Build biomechanical model

The geometry of the flexcell system including rigid post and silicone membrane was built in COMSOL. In order to get geometric information of cell seeded on PDMS substrate, confocal images were taken to get the contour of multiple cells. The contour information was then converted to vector graph which can be imported to AutoCAD. The cell contour image was then reconstructed in CAD and exported to COMSOL with a relative repair tolerance of 10^{-5}. Figure below shows the 3D geometry of the model built in this study.
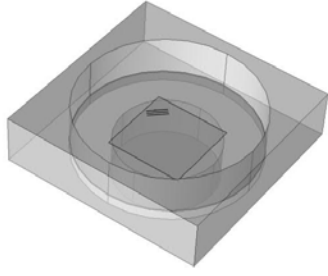
Figure 5.2 3D geometry model built in comsol.

In general, solid mechanics was the major physics applied in Comsol with defined linear elastic, and viscoelastic models as well as fixed constraint and contact pair. In our study, we first assume that the polycarbonate post and the flexcell plate itself are incompressible that can be defined as rigid domains. Secondly, the edge of the silicone membrane was considered as a fixed constraint with zero displacement throughout the entire study. For the boundary load, a 20kPa vacuum pressure was applied at the underside of the silicone membrane with controlled frequency and waveform defined as $\sin(\pi t)$. The cell, PDMS substrate, silicone membrane and rigid post are defined as two contact pairs. Between the silicone membrane and rigid post, a layer of silicone lubricant was applied and modeled with a friction coefficient of 0.03 based on the typical value of silicone lubricants[1]. The contact between silicone membrane and PDMS substrate was fixed since they were stretched to the same degree under vacuum pressure. The adhesion between the cell and PDMS substrate were characterized with a friction coefficient of 0.03 [2]. The collagen top layer was defined to fill up the empty space of a 0.2cm cylinder on top of the cell and pdms surface to form a thin layer. The material properties of these domains are also

141

important for modeling deformation. The silicone membrane of flexcell plate was characterized by generalized Maxwell model of 5 branches with value listed in table 5.1 obtained from the rheology handbook [3].

Table 5.1 Parameters of generalized maxwell model used for silicone membrane

Counting number of the Maxwell elements	Individual relaxation time [s]	Individual relaxation modulus [Pa]
i=1	0.01	200,000
i=2	0.1	100,000
i=3	1.0	10,000
i=4	10	100
i=5	100	10

The material properties of cell, PDMS and collagen top layer were acquired from AFM experiments while the polycarbonate post was defined with a 2.4GPa Young's modulus and a 0.37 Poisson's ratio.

Meshing of the PDMS resulted with 41475 free tetrahedral elements. Meshing of the cell resulted with 3018 free tetrahedral elements. The silicone membrane contains 11175 free tetrahedral elements while rigid post is consisted with 1027 free triangle and 5 layers of rectangles. The collagen top layer consists of 11546 free tetrahedral elements.

5.3 Results

5.3.1 Proliferation

The viability of ADSCs cultured on PDMS in different conditions was evaluated by the MTS assay. The result shows Adding collagen top layer largely reduce the number of viable cells compared to conditions without collagen top layer.
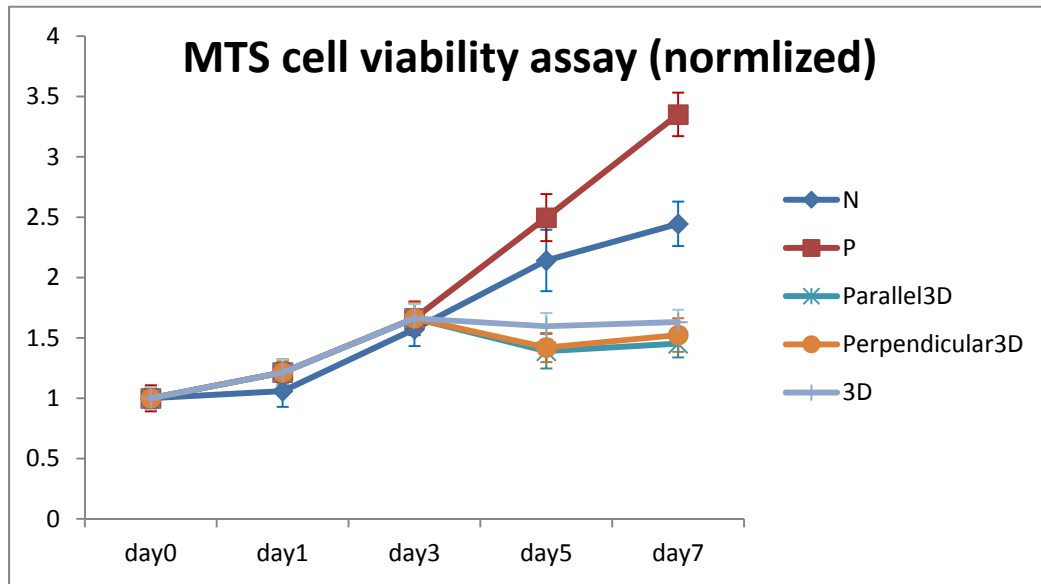
Figure 5.3 The viability of ADSCs cultured in 3D evaluated by MTS assay. Data presented as mean ± standard error.

5.3.2 Cellular alignment in 3D culture

The average cell angle of ADSCs cultured in (1) 3D with features parallel to mechanical stretch and (2) 3D with features perpendicular to mechanical stretch were 29° ±13.4° and 22.14°±16.5° showing that 3D culture inhibited further alignment of cell once collagen top layer was added. The average cell angle of ADSCs cultured on (3) PDMS in 3D

culture without mechanical stretch was 25.19°±11.3° which further confirms the role of

collagen top layer in downregulating cellular alignment.

Cellular alignment
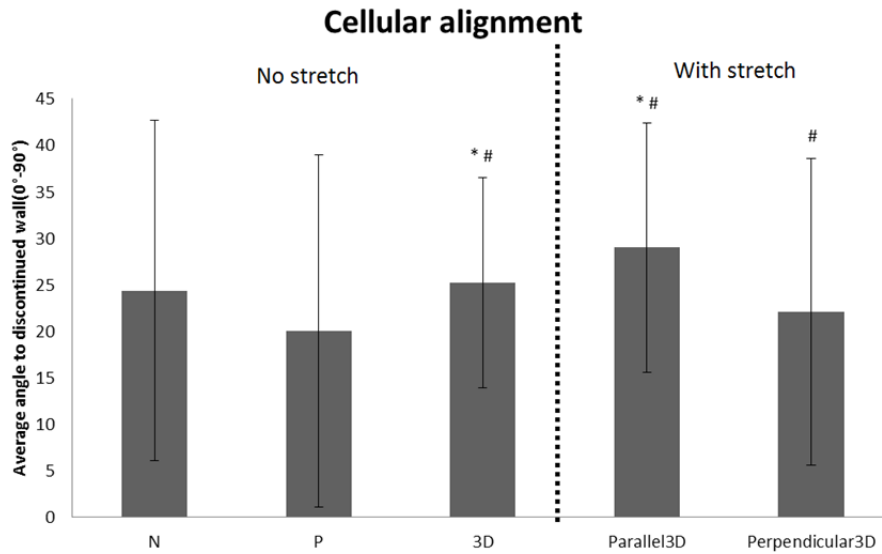
Figure 5.4 Cellular alignment in 3D groups. * p<0.05 compared to negative control, #
p<0.05 compared to positive control. Data presented as mean ± standard error.

5.3.3 Elastic modulus

The elastic modulus of ADSCs cultured in (1) 3D with features on PDMS parallel to 1

day mechanical and (2) 3D with features on PDMS perpendicular to mechanical stretch

followed by 3D culture with collagen top layer were 2.46±0.18KPa and 2.68±0.19KPa

suggesting that cells under 3D culture tend to become softer. The elastic modulus of

ADSCs cultured in (3) 3D without mechanical stretch was 2.33±0.20KPa 20KPa

implying that the collagen layer slightly decrease the stiffness of cells.
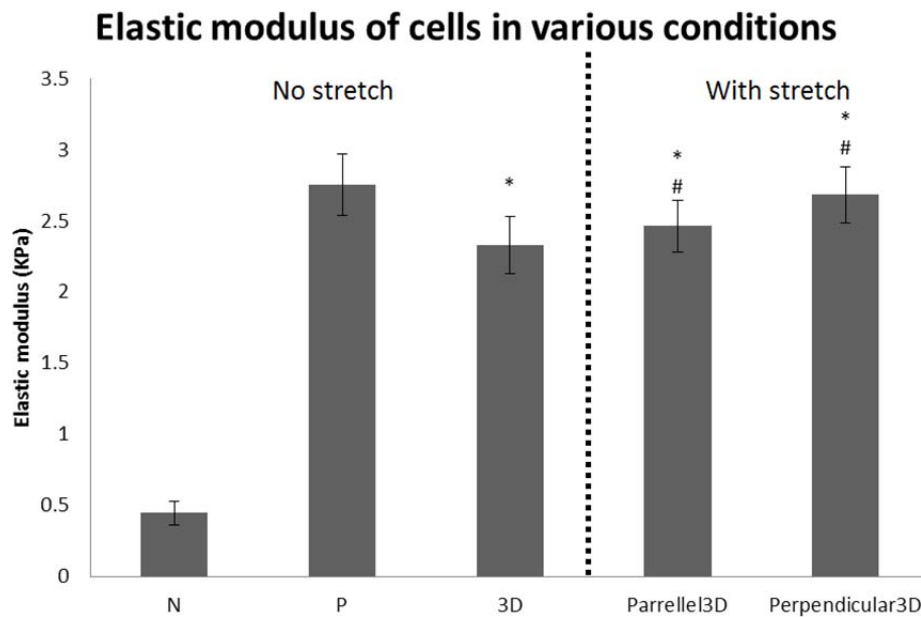
Figure 5.5 Apparent elastic modulus of ADSCs. Data presented as mean ± standard error.

5.3.4 Immunofluorescence and PCR

To verify the differentiation, the expression of SMC specific markers including αSMA, SM22α, calponin and SM-MHC was investigated by fluorescent staining and the gene expression of these markers were further quantified by PCR.

α-SMA   SM22α   calponin   SM-MHC
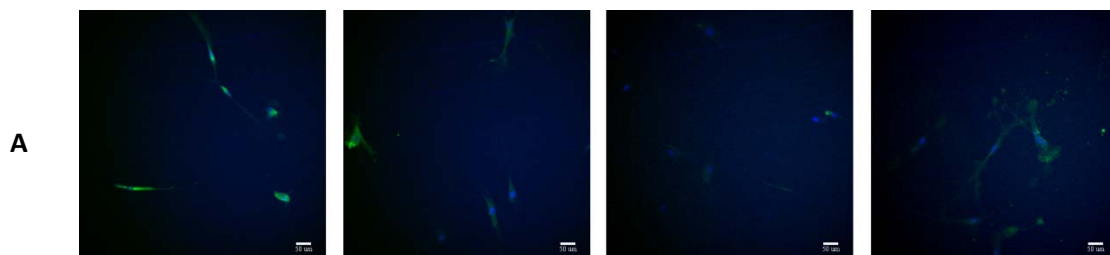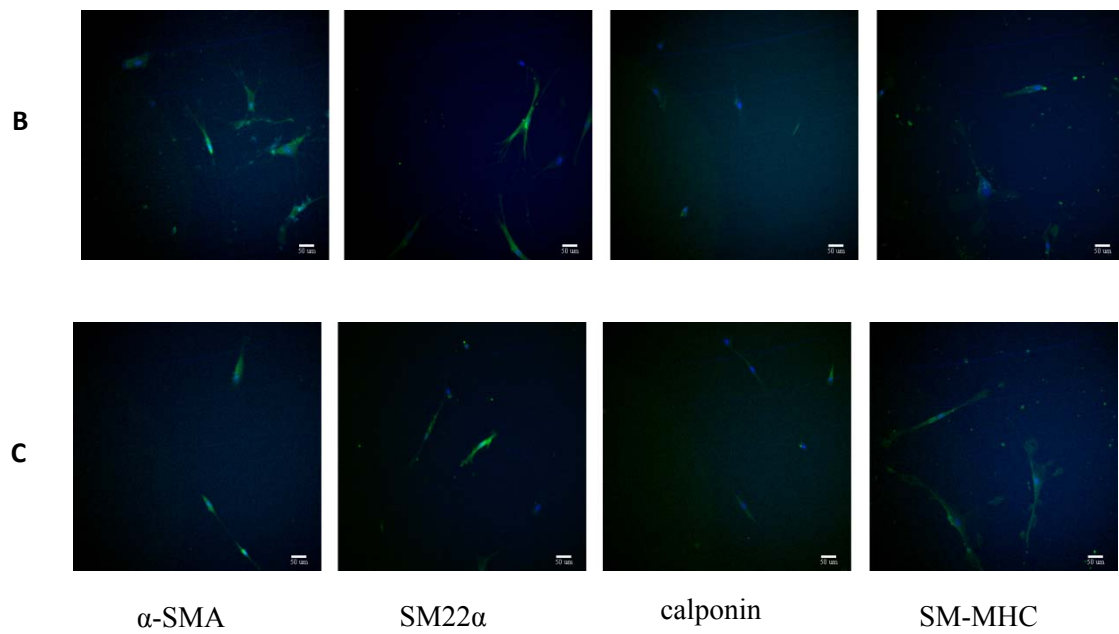
Figure 5.6 Figure 6 Expression of SMC-specific proteins (a-SMA, SM22α, calponin, SM-MHC) in 3D groups
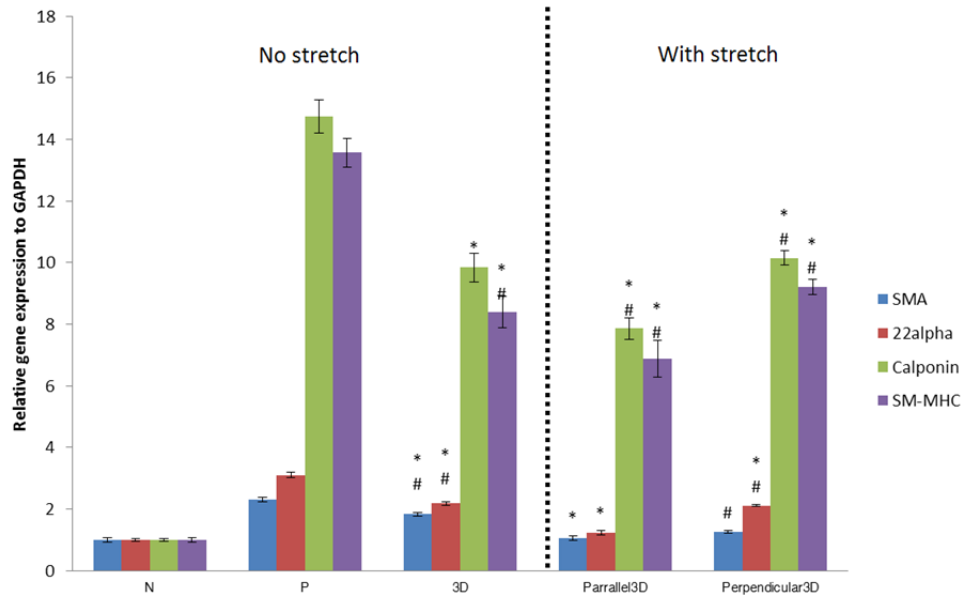
Figure 5.7 RT-PCR was performed to measure the expression of αSMA, SM22α, calponin and SM-MHC of ADSCs cultured for 7 days in 3D groups. Data presented as mean ± standard error.

We found that by adding collagen top layer, the SMC-specific gene expressions were reduced compared to ADSCs cultured in positive no stretch group.

5.3.5 Stationary study in COMSOL

The stress distribution on the surface of flexcell membrane was calculated to be in a range from 5.57×10^5 N/m^2 to 4.01×10^7 N/m^2. For the PDMS substrate, it has a surface stress distribution range from 1.46×10^6 N/m^2 to 1.91×10^7 N/m^2. The displacement of silicone membrane and PDMS show an equal large deformation in the central region of post. At the off-post region of the silicone membrane, the deformation is approximately

zero while the strain field gradually decreases from the center to the edge on the PDMS substrate. This is consistent with a study of complete strain field analysis within the flexcell membrane in which researchers observed similar strain countours from a biaxial post simulations[4].

(a)

(b)

(c)

(d)
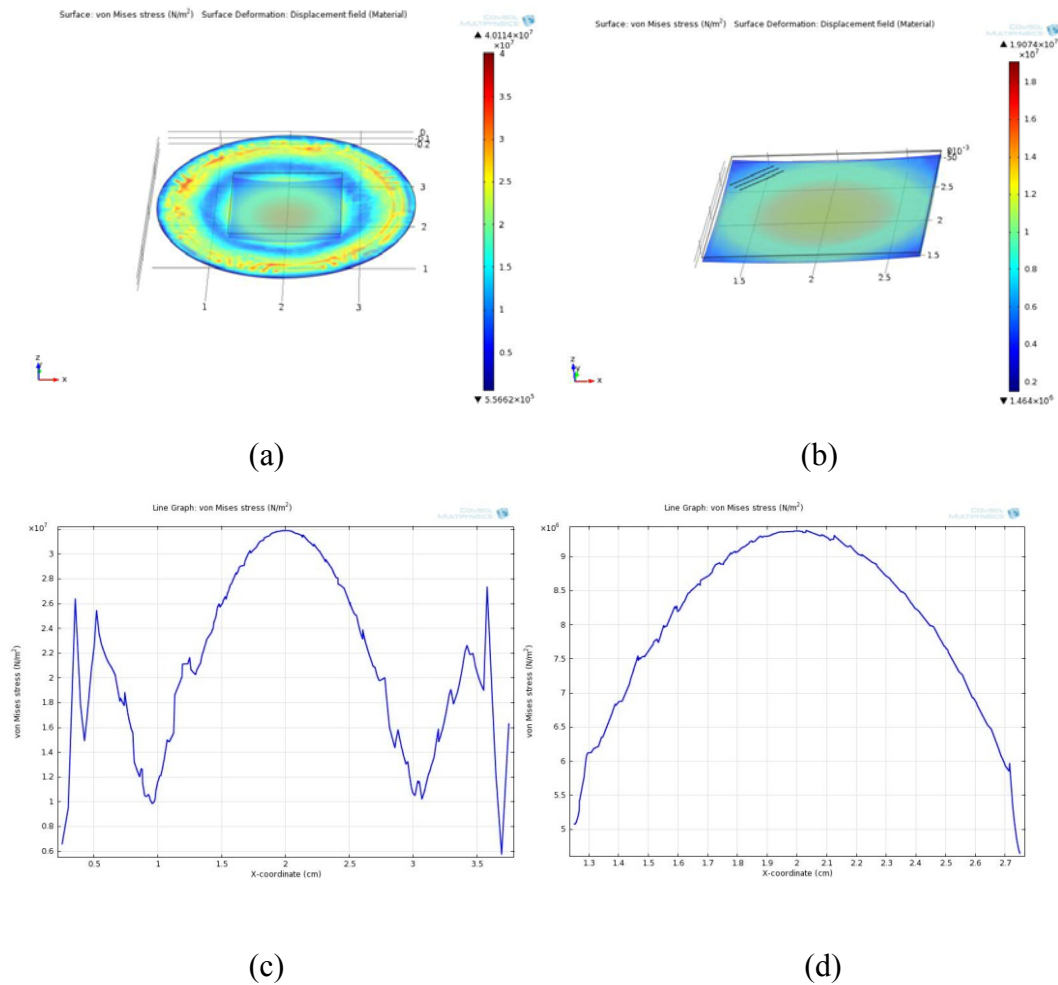
Figure 5.8 Stationary simulation (a) Stress distribution on silicone membrane (b) Stress Distribution on PDMS membrane (c) line graph of stress distribution from silicone membrane (d) line graph of stress distribution from PDMS surface.

For cell seeded on PDMS substrate, the orientation of feature on PDMS was taken into consideration. When the mechanical stretch was applied parallel to the rectangular feature, the cell was modeled perpendicular to the feature and both ends of the cell have higher stress compared to the rest of the cell surface while the cell also has the highest deformation on one end. When the mechanical stretch was applied perpendicular to the rectangular feature, the cell was modeled parallel to the feature and the stress is equally distributed on cell surface while the cell has the highest deformation in the middle. Under both conditions, cell has an approximately 2μm deformation which is about the same distance range we performed in AFM indentation. We believe the different stretch distributed on cell might have an effect on cellular shape and mechanical property.

(a)   (b)

(c)   (d)
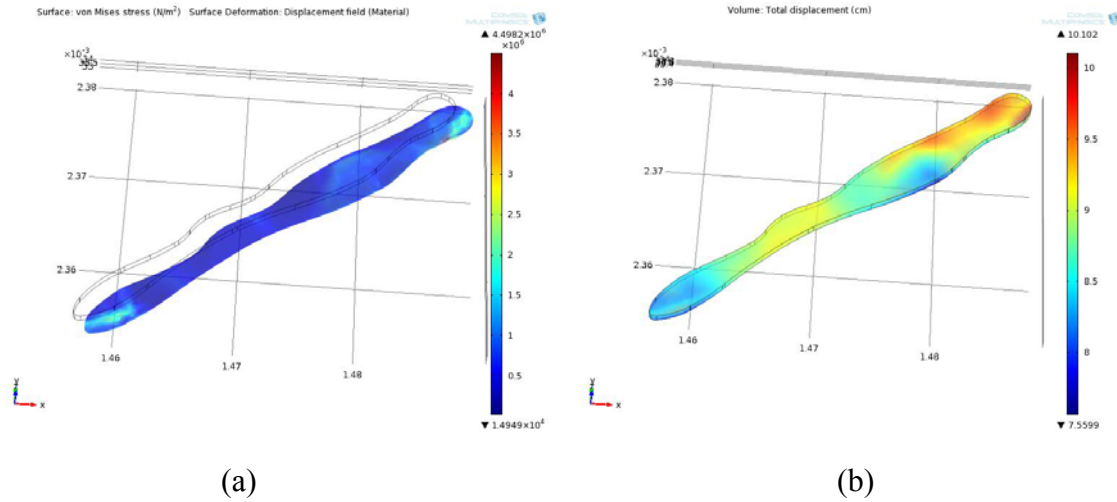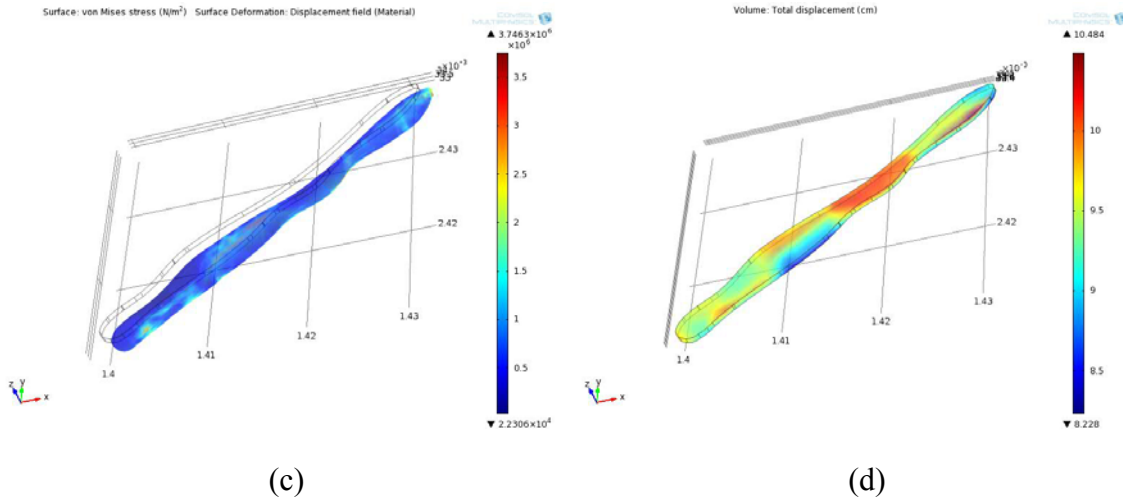
Figure 5.9 (a) stress distribution and (b) deformation of cell cultured on pdms with feature parrallel to mechanical stretch (c) stress distribution and (d) deformation of cell cultured on PDMS with feature perpendicular to mechanical stretch

5.3.6 Time dependent study in COMSOL

To better model the deformation of silicone membrane and PDMS substrate, we performed a time dependent study to simulate the change in cyclic strain as a sinusoidal wave. We defined the boundary load to be $(-20000(\sin\pi t))$Pa and we set the time range from 0 to 1 second to fulfill one circle of the cyclic strain. Each step we take in the time dependent study is 0.1 second with a relative tolerance of 0.01. By modeling the deforming motion of the silicone membrane, we can better characterize the stretch applied to all the components involved in the culture construct.
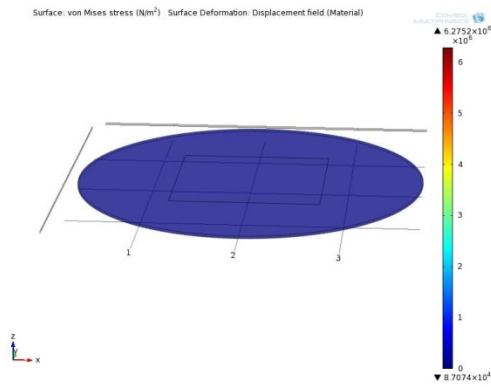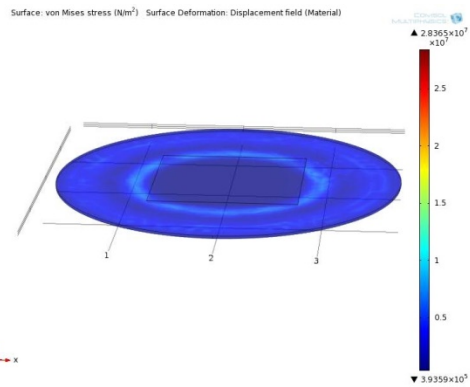
(a) Time=0s   (b) Time=0.25s
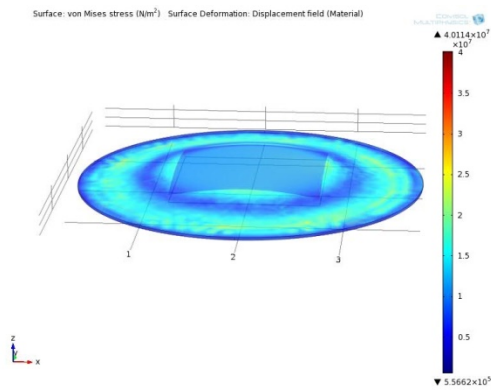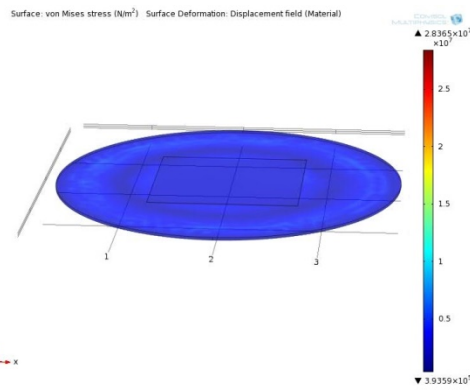
(c) Time=0. 5s   (d) Time=0.75s
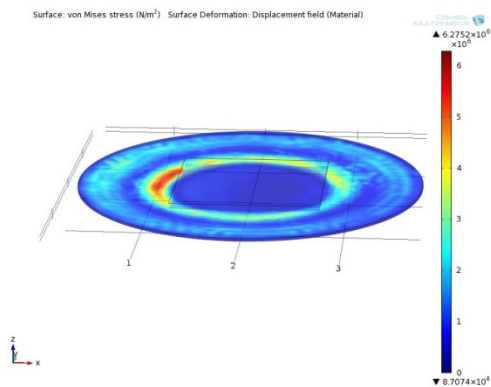
(e) Time=1s

Figure 5.10 Time dependent simulation of stress distribution on silicone membrane over

1 cycle .

5.4 Conclusions

In summary, collagen layer can be used to control the proliferation and mechanical property of differentiated VSMC. For biomechanical model, the stationary study demonstrated similar result in agreement with biaxial post simulations performed by other group [4]and also demonstrated the stretch on cell under 20Kpa vacuum pressure. The average stress on cell surface is around 5×10^5N/m^2 and the maximal difference in deformation is about 2μm. The time dependent study indicated that the silicone membrane on post is pushed upward and then falls back during one cycle of mechanical strain. This finding is consistent with the motion of the membrane on flexcell plate observed in our experiment. The stress distribution and deformation of the PDMS and the cell, on the other hand, change accordingly during one cycle of mechanical strain. These results can be used to determine how much stretch was applied to cell under different biomechanical conditions. Based on cellular behavior, the result of the simulation can in turn guide the optimization of the culture condition for cell.

5.5 Reference

[1] Woolfson, A. D., Malcolm R. K., Gorman S. P., Jones D. S., Brown A. F., and McCullagh S. D. *Self-lubricating silicone elastomer biomaterials*. Journal of Materials Chemistry, 2003. 13: 2465-2470.

[2] Angelini, T. E., Dunn A. C., Uruena J. M., Dickrell D. J., Burris D. L., and Sawyer W. G. *Cell friction*. Faraday Discussions, 2012. 156: 31-39.

[3] Mezger, T. G. (2006). The rheology handbook : for users of rotational and oscillatory rheometers (Hannover: Vincentz).

[4] Geest, J. P. V., Di Martino E. S., and Vorp D. A. *An analysis of the complete strain field within Flexercell(TM) membranes*. Journal of Biomechanics, 2004. 37: 1923-1928.

CHAPTER SIX

CONCLUSIONS AND RECOMMENDATIONS

6.1 Conclusions

This research is motivated by the desire to implement vascular smooth muscle cell in tissue engineered vascular graft. As VSMC play an important role in maintaining physiological function of vessels and can provide sufficient mechanical strength in dynamic conditions, it should be considered as an essential physiological component in the development of tissue-engineered blood vessels. However, the unwanted migration and excessive proliferation can result in restenosis of currently used vascular grafts and might contribute to the development of vascular diseases. In addition, differentiated autologous smooth muscle cells, usually isolated from patient's subcutaneous veins can easily lose their ability to further proliferate and are limited in quantities. As such, attempts have been made to differentiate vascular smooth muscle cells from stem or progenitor cells. In our study, we hypothesized that stem cells can be used as an alternative cell source to differentiate into functional vascular smooth muscle cells in terms of their mechanical strength and marker expression. Also, the proliferation, migration and mechanical property of differentiated cell can be regulated by the combination of different biochemical and biomechanical signals. Furthermore, a biomechanical model was developed to characterize the stress distribution and deformation of cells used in our experiment. The work presented in current study represented the first step of achieving functional VSMCs that can be potentially used in

vascular engineering and the biomechanical model is the first of its kind to characterize cellular behavior using flexcell system. Such model might be used to guide the optimization of the culture condition for cells.

In our first study, we compared the difference in the mechanical property of differentiating bone marrow and adipose-derived stem cells by using atomic force microscopy indentation. Our hypothesis was that BMSCs can be more quickly differentiated to functional SMC-like cells compared to ADSCs with a better mechanical performance during differentiation. The result showed that in vitro 7-day culture of BMSCs induced by TGF-β1 can acquire higher elastic modulus than ADSCs which is closer to the mechanical property of VSMCs cultured in vitro. However, given the fact that ADSCs can take up to 6 weeks to differentiate into VSMC like cell with the same level of differentiation markers as differentiated from BMSCs within 7 days, we believe ADSCs can get stiffer if cultured in a longer period of time. Thus, both of these two candidates were considered a potential candidate in differentiating to functional VSMC in terms of mechanical strength.

With the advantage of easy obtainability, low donor site morbidity and the ability to expand rapidly, ADSCs was used in our second study to evaluate the influence of combining multiple biomechanical and chemical factors to control proliferation, phenotype and mechanical behavior in VSMC differentiation. We investigated the potential of utilizing environmental signals to promote VSMCs differentiation and proliferation while regulate their phenotype to meet the need for vascular engineering.

We found that TGF-β1 promoted the VSMC differentiation of ADSCs with the increase of mechanical strength and SMC specific marker expression of cells. 10% cyclic strain at 1hz for 24hrs slightly inhibit cell proliferation but upregulate SMC marker expression. Collagen top layer significantly reduce the number of viable cells and repress the expression of SMC later markers. Among all the condition, ADSCs cultured on discontinued wall parallel to mechanical strain had the best cellular alignment along with highest elastic modulus and marker expression. Based on our findings, ADCSs as one of the most abundant stem cell in our body can be a competitive candidate in providing functional smooth muscle cell if modulated with proper environmental signals

Finally, a biomechanical model was developed to incorporate the mechanical property of differentiated cell and distinct layers with geometrical information acquired from confocal images to predict cellular behavior. By running the model, it elucidated the stress distribution and deformation of the cell and other components used previously in our experiment which can be used to determine how much stretch was applied to cell under different biomechanical conditions. Based on cellular behavior, the result of the simulation can in turn guide the optimization of the culture condition for cell.

6.2 Recommendations

6.2.1 Investigate the differentiation of VSMC in longer period of time

In our current study, we investigated the differentiation of two stem cells and the behavior of differentiated cell under different conditions for 7 days. This was to ensure cells would not get fully confluent so that Hertz contact model could be used to study

single cell mechanical property. However, 7 days is a relative short period of time to study cellular behavior and differentiation. Although we expect to see similar result in proliferation, alignment with increased stiffness and more percentage of differentiated cell, we suggest that by limiting the initial concentration of cell, a 14 or 21 day study can be performed to evaluate cellular behavior in a longer period of time. Compare the result with the current 7 day data will reveal if time can be a significant factor in determining the cellular behavior of VSMCs differentiated in vitro.

6.2.2 Obtain better mechanical property measurement

One of our research goals is to determine if stem cell can differentiate into functional VSMC in terms of their mechanical strength. Currently, the mechanical property of cell is evaluated by using Hertz contact model to fit the indentation data acquired by AFM indentation. However, Hertz contact model makes several simplifying assumptions including linear elasticity and homogeneity which is apparently not the case for cell. While Hertz contact model still remain accurate in the calculation of elastic modulus for cells within the first several hundred nanometer indentation, we suggest that a more complex model can be used to better fit the AFM indentation data. Recently, researcher from other group suggest a "brush model" that assume the majority of cells have a surface covered with various membrane protrusions and corrugations. They verified that independence of the elastic modulus of the indentation depth could only be observed when processing the data with the brush model [1]. While the accuracy of the model for VSMC still need to be tested, such a model can be used to achieve a potential improvement in evaluating the overall elastic modulus of cell if used appropriately.

6.2.3 Replicate experiments in more conditions

In this work, we compared the combination of different biochemical and biomechanical signals in determining cell proliferation, migration and differentiation. With the use of soft lithography, we managed to fabricate feature in different orientation on PDMS. While currently the size of discontinued wall on PDMS is 30μm×300μm with 300μm space between walls, we suggest that by changing the size of the rectangular wall and the space between two walls, cells might be constrained differently that could result in altered shape and migration. It has also been suggested that the magnitude and duration of the strain might contribute to the outcome of phenotype response of VSMC[2]. In our study, a 10% cyclic strain at 1hz were applied to cells for 24 hours. While the frequency of strain was set to simulate the cardiac cycle, the magnitude and duration of strain could be changed to study different cellular response. These strategies could provide more insight into the effect of environmental factors on cellular behavior.

6.2.4 Seeding vascular smooth muscle cell on tubular scaffold

In this work, we created a 3D sandwich construct to mimic the distinct layers of vessel wall and provided some insights into cellular behavior under physiologically relevant environment. At this point, it is important to take the next step to incorporate VSMC onto a tubular structure that better represent the physiological condition of blood vessel. While seeding VSMC onto tubular scaffold is the first and important step for vascular tissue engineering, the delivery efficiency of cells has been the key issue for the subsequent patency and functionality of the scaffold. According to that, numerous cell seeding techniques have been investigated. Common SMC-seeding techniques include rotated

bioreactor, static-seeding and cell sheet wrapping. More recently, a method based on magnetite nanoparticles and magnetic force has also been introduced[3]. These technologies could be used to study VSMC behavior when cultured in a tubular culture system. Cells could be colonized in the luminal surface of the construct and applied with dynamic loading. When necessary, part of the construct could be cut off to study the mechanical property of the cell on its surface. This could give us a better understanding of the celluar behavior when used in a tissue engineered vascular graft.

6.2.5 Build more complex model to represent viscoelasticity of cell

In the current biomechanical model we built to predict cellular behavior, we assumed cell to be homogenous and linear elastic. By doing this, we can simply assign the young's modulus calculated from experimental data to the material property of the single cell for the whole geometry. However, this neglects the fact that cell is heterogenous and viscoelastic. A more complex model which can successfully incorporate the heterogeneity and viscoelasticity of cell are expected to be more accurate than the model presented in chapter 5. Furthermore, the ultimate goal is to incorporate VSMC in bioartificial vascular graft. Some modification of the model is needed if cell is cultured on luminar surface of a tubular structure. While some layer specific model is introduced to study the stress-strain relation in the vessel wall [4], these concepts could be used in developing our model for the purpose of future study.

6.3 Reference

[1] Guz, N., Dokukin M., Kalaparthi V., and Sokolov I. *If Cell Mechanics Can Be Described by Elastic Modulus: Study of Different Models and Probes Used in Indentation Experiments*. Biophysical Journal, 2014. 107: 564-575.

[2] Cappadona, C., Redmond E. M., Theodorakis N. G., McKillop I. H., Hendrickson R., Chhabra A., Sitzmann J. V., and Cahill P. A. *Phenotype dictates the growth response of vascular smooth muscle cells to pulse pressure in vitro*. Experimental Cell Research, 1999. 250: 174-186.

[3] Shimizu, K., Ito A., Arinobe M., Murase Y., Iwata Y., Narita Y., Kagami H., Ueda M., and Honda H. *Effective cell-seeding technique using magnetite nanoparticles and magnetic force onto decellularized blood vessels for vascular tissue engineering*. Journal of Bioscience and Bioengineering, 2007. 103: 472-478.

[4] Wang, C., Garcia M., Lu X., Lanir Y., and Kassab G. S. *Three-dimensional mechanical properties of porcine coronary arteries: a validated two-layer model*. American Journal of Physiology-Heart and Circulatory Physiology, 2006. 291: H1200-H1209.

APPENDICES

Additional PDMS fabrication

A.1 Background

The effect of biophysical signals on cellular function, orientation and movement has long been recognized. Vascular smooth muscle cells (VSMCs) exist in a quiescent, differentiated state in the tunica media layer of blood vessel and are primarily subjected to cyclic stretch resulting from pulsatile changes in blood pressure. Prior studies have shown that VSMCs cultured in vitro can respond to dynamic mechanical loading by changing its phenotype and alignment [1,2]. Controlling cell shape by micropatterning has also been shown to affect VSMC phenotypic shift. However, it is not yet clear how shape and alignment of VSMCs can be modulated by seeding them inside different micropatterned features. Comparison of cell behavior in different features could help us understand the effect of constraining VSMCs in grooves with different shapes on the stiffness and phenotype change of VSMCs. Atomic Force Microscopy (AFM) and Confocal Microscopy were used in conjunction with each other to locate cells in features and perform nanoindentation to evaluate the mechanical property of VSMC.
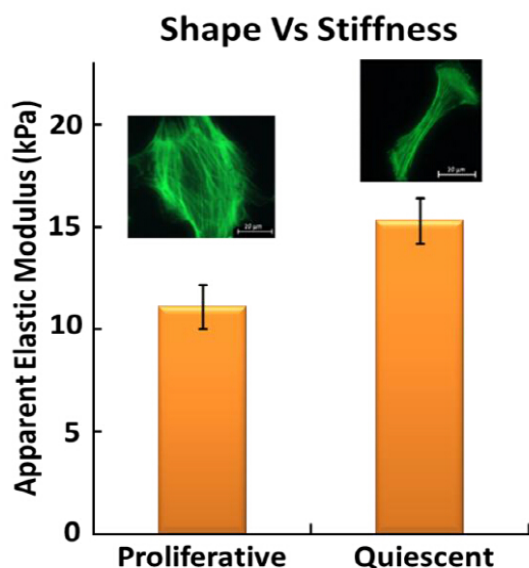
Figure A.1 Relation between shape and stiffness of rat arotic VSMCs, AlexaFluor 488 phallodin was used for staining f-actin [3].

A.2 Methods

A.2.1 Substrate preparation

Microscale patterned substrate was be fabricated by using soft lithography. Silicon wafer, photomask, Sylgard 184 polydimethylsiloxane (PDMS) elastomer kit and SU-8 photoresist were used for substrate fabrication. SU8 photoresist was spinned at 1000rpm for 60 seconds in a spinner to get 8-10μm features. In order to do that, the wafer was carefully centered on the spinner chuck and then a small amount of photoresist was poured on the silicon wafer. A pre-bake step was used to harden the SU-8 resist before exposure. For this, the wafer was moved from the spinner, using vacuum tweezers to transfer it to the hotplates. Silicon wafer was soft baked at 65°C for 5mins and then at 95°C for 5mins after photoresist was spread uniformly on it. The patterning of the

photoresist was performed using ultraviolet light and a patterned mask. While the wafer was brought into contact with a mask, the pattern from the mask was replicated into the photoresist by ultraviolet illumination. The SU-8 patterned wafer was then ready to be used as a mold for PDMS. The patterned PDMS was be rinsed with 100% ethanol and 70% ethanol for 2 hours followed with overnight UV light sterilization before it was used for cell culture.

15μm rectangle

60μm rectangle

30μm rectangle

Circle in 200μm diamerter
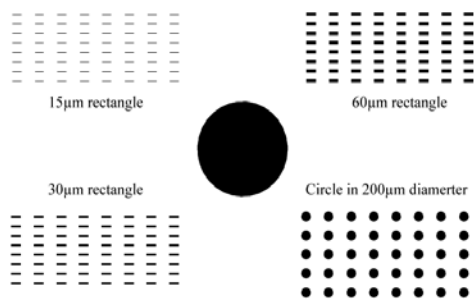
Figure A.2 Photomask designed for PDMS substrate, features include rectangles of 15μm, 30μm and 60μm width, circle of 200μm diameter

A.2.2 VSMC isolation and culture

In the cell culture study, we compared cellular behavior of VSMC harvested from week 12 Sprague-Dawley in different features. To get isolate VSMCs, the aorta was clipped at the pelvic bifurcation and dissected away from the dorsal abdominal wall to the aortic arch. Arterioles were trimmed and the endothelial layer was scraped away. Arterial segment left was digested to get VSMC. VSMC was then cultured in each T75 flask to reach 80% confluency. They were passaged using standard techniques to Φ 50-mm fluorodishes at 1×104 cells/cm^2 concentration. Dulbecco's modified high glucose Eagle

medium (HG-DMEM, Gibco) supplemented with 10% FBS (Atlanta Biologicals, Lawrenceville, GA, USA) and 1% 100X penicillin-streptomycin (Fisher Scientific, Pittsburgh, PA, USA) was used as VSMC culture media. VSMCs were subjected to 10% cyclic strain at the frequency of 1Hz for 24hr at day 3 by using the Flexcell system. The cells were allowed to continue to grow until day 7.

A.2.3 PDMS on flexcell membrane

To verify that the vacuum pressure applied on the bottom of flexcell plate can provide equibiaxial strain to the silicone membrane. A calibration paper was adhered on top of the rigid post while the silicone membrane was marked with dot. By tracking the movement of dot on the calibration paper, the strain filed of silicone membrane can be verified. To ensure that the PDMS is tightly adhered and stretched to the same extent as silicone membrane, dots were marked on both the bottom of the plate and the PDMS. The dots marked on both sides matched up with each other when deformation was applied on silicon membrane indicating same strain field was experienced on PDMS and the bottom of Bioflex plate.
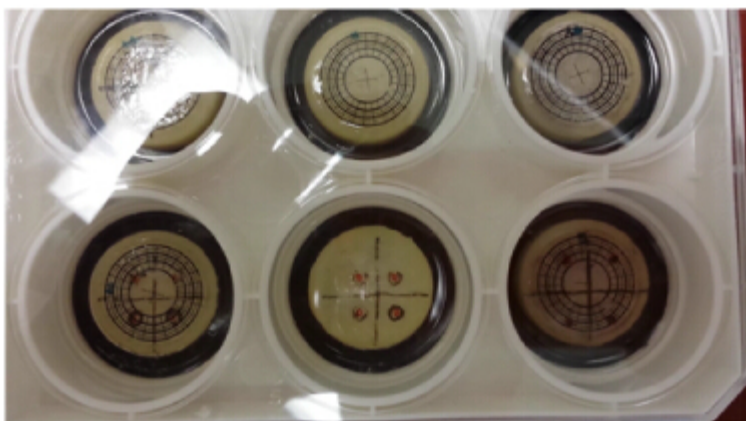
Figure A.3 Flexcell plate with calibration paper.

A.2.4 AFM mechanical testing

Day 7 VSMCs were mechanically probed using an Asylum Research MFP-3D AFM operating in contact mode with a fluid cell. Cells were kept in 50-mm culture dishes with growth media throughout the experiment. A 5 µm diameter borosilicate spherical-tipped AFM probe on a silicon-nitride cantilever (Nanoandmore, spring constant ~0.2 N/m) was used to mechanically probe individual cell which was grown inside features on PDMS substrate as shown in Fig A.3. Each cell with be indented five times to for around 1µm indentation.
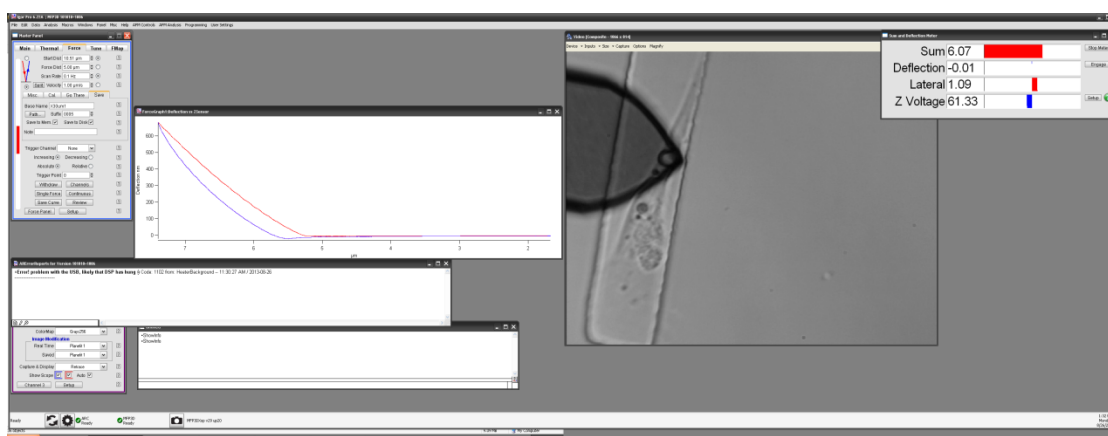
Figure A.4 AFM mechanical testing on VSMC cultured in patterned PDMS substrate.

A.3 Results

Results are shown in Figure A.4 and A.5.
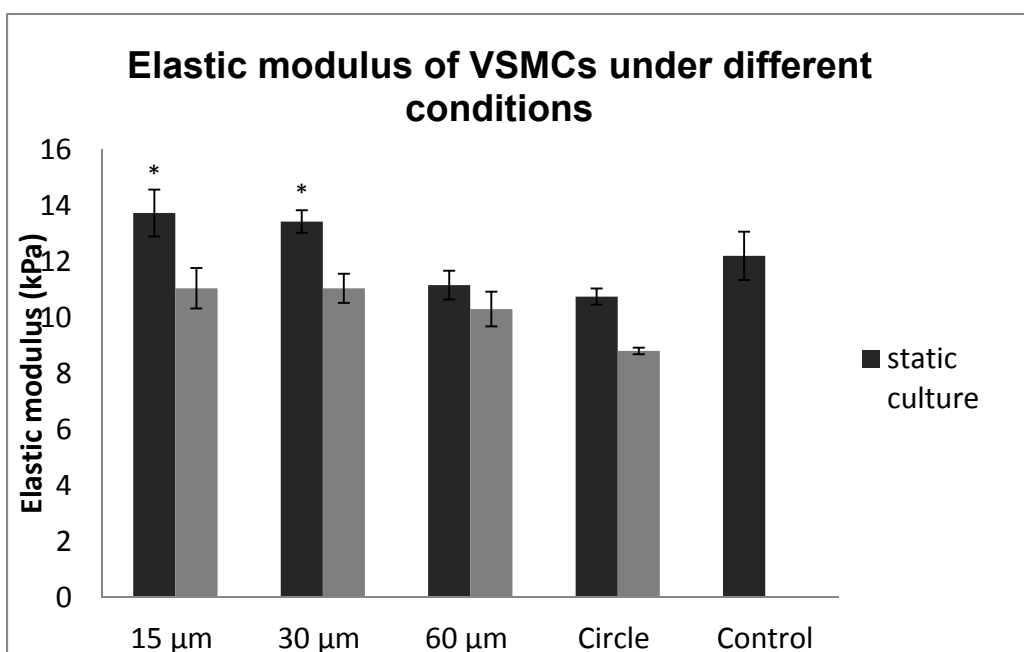
Figure A.5 Elastic modulus of VSMCs seeded inside different features. Data are

presented as mean ± standard error.
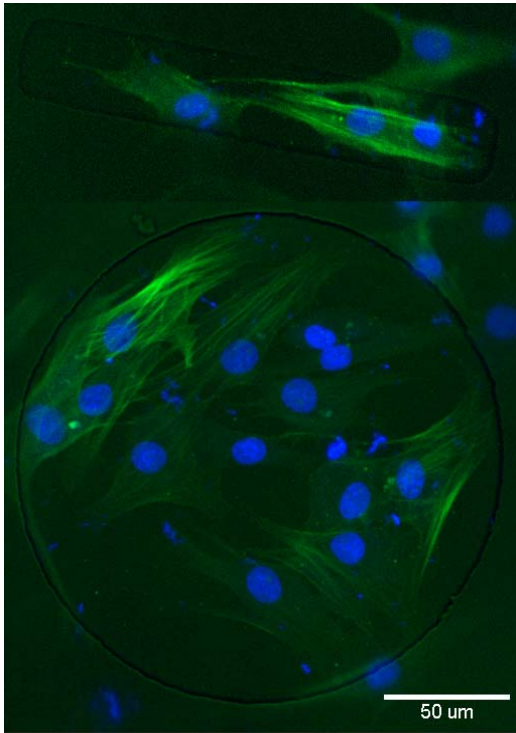
Figure A.6 Immunofluorescence imaging of αSMA and nuclei for VSMCs cultured in 30μm rectangle and 200μm circle.

A.4 Conclusion

The results show that VSMCs seeded inside rectangular features can be constrained to spindle like shape. The elastic modulus of VSMCs is dependent on the size of the features. VSMCs were found to be stiffer when cultured in smaller rectangle compared to larger rectangle. This can be explained by the relation between cell shape and stiffness. According to previous study, contractile VSMCs with spindle like shape have better mechanical strength than synthetic VSMCs with round shape [3]. For cells underwent 10% cyclic strain, an overall decrease in elastic modulus was observed. Further research is required to investigate if the phenotype shift of VSMCs can be controlled by

environmental change including surface topography and mechanical loading. Optimization of such culture conditions can have potential use in clinical application in future.

A.5 Reference

[1] Nikolovski, J., Kim B. S., and Mooney D. J. *Cyclic strain inhibits switching of smooth muscle cells to an osteoblast-like phenotype*. Faseb Journal, 2003. 17: 455-+.

[2] Standley, P. R., Camaratta A., Nolan B. P., Purgason C. T., and Stanley M. A. *Cyclic stretch induces vascular smooth muscle cell alignment via NO signaling*. American Journal of Physiology-Heart and Circulatory Physiology, 2002. 283: H1907-H1914.

[3] Hemmer, J. D., Dean D., Vertegel A., Langan E., and LaBerge M. *Effects of serum deprivation on the mechanical properties of adherent vascular smooth muscle cells*. Proceedings of the Institution of Mechanical Engineers Part H-Journal of Engineering in Medicine, 2008. 222: 761-772.

Appendix B

Matlab code

B.1 Elastic modulus script

B.1.1 Script to load raw data: massexcompile

```matlab
function [elasticity Curves] = massexcompile(folderin)
% folderin should be the folder your data is in. something like "C:\Documents and
Setting\My Documents\MyData"
mainfolder = cd
format long
fnames = dir(folderin);
numfids = length(fnames);
cd(folderin);
%filtering out irrelevent "files" such as '.' and '..'
cellnames = {};
for s = 1:numfids;
    if 'B' == fnames(s).name(1) % 'd' represents the letter that the relevent file names begin
with
        cellnames{end+1} = fnames(s).name;
    end
end
%combine every 3 files and write
```

```matlab
counter = 1;

numcell = length(cellnames);

numfile = 1;

elasticity = [];


% OMIT THIS WHILE LOOP IF YOU WANT TO LOAD CELLS INDIVIDUALLY

Curves(numcell, 1) = struct('extension', [], 'retraction', []);

CurrentCell =1;

while counter <= numcell

    a = load(cellnames{counter});

    c = load(cellnames{counter+2});


    cd(mainfolder);

    [elasticity(end+1,1) xe ye xr yr] = elast_analysis(c,a,mainfolder,counter);

    Curves(CurrentCell).extension = [xe ye];

    Curves(CurrentCell).retraction = [xr yr];

%    figure('Name',sprintf('Cell %d', ((counter-1)/3)+1),'NumberTitle','off')  %comment

out in order to turn plotting off

%    plot(c,a)              %comment out in order to turn plotting off


    counter = counter+3;

    CurrentCell = CurrentCell+1;
```

```matlab
    cd(folderin);
%    numfile = numfile+1
end

cd(mainfolder)
```

B.1.2 Script to find contact point: xycorrect.m

```matlab
function [xc,yc] = xycorrect(x,y)

s = 0.01; %slope sensitivity



%correction for y
format long

region = [1:length(x)/4];

slope = polyfit(x(region),y(region),1);

yci = y-(polyval(slope, x));



%correction for x
numslope = diff(yci)./diff(x);

index = 1;

condition = 0;

contactx = 0
```

```
while condition == 0 && index ~= length(numslope)

    if numslope(index) > s && mean(numslope(index:5:index+200)) > s;

        condition = 1;

        contactx = index;

    end

    index = index+1;

end


xc = x-x(contactx)-yci;


% correct again for y

yc = yci-yci(contactx);
```

B.1.3 Script to calculate elastic modulus: elast_analysis.m

```
function [e xe ye xr yr] = elast_analysis(c,a,mainfolder,counter)

cd(mainfolder)

format long

k = 0.208; %spring constant value N/m

v = 0.5; %poisson's ratio

R = 2.5*10^-6;  % tip radius in meters

L = 30*10^-9 ;    %lower bound for elasticity (in m from contact point)
```

U = 330*10^-9 ;   %upper bound for elasticity (in m from contact point)

%adjust deflection

ak = a;

%filter deflection values

d = AFM_butter(ak);

%Separation of extension and retraction

l = floor(length(c)/2);

xe = c(200:l);% add 200 in order to omit first several data points (irratic behavior due to

filtering

ye = d(200:l);

if rem(length(c),2)==0;

   xr = c(end-200:-1:l+1); % subtract 200 in order to omit first several data points

   yr = d(end-200:-1:l+1);

   else

   xr = c(end-200:-1:l+2);

   yr = d(end-200:-1:l+2);

end

%correct x,y offsets

```
[xe,ye] = xycorrect(xe,ye);

[xr,yr] = xycorrect(xr,yr);


ye = k * ye;

yr = k * yr;


format long;

erange = [];

for i = [1:1:length(xe)];

   if xe(i)>=L && xe(i)<=U;

     erange(end+1) = i;

   end;

end;

rrange = [];

for i = [1:1:length(xr)];

   if xr(i)>=L && xr(i)<=U;

     rrange(end+1) = i;

   end;

end;


emodulus = mean((3.*ye(erange).*(1-v^2))./(4.*xe(erange).^(3/2).*R.^(1/2)));
```

```matlab
rmodulus = mean((3.*yr(rrange).*(1-v^2))./(4.*xr(rrange).^(3/2).*R.^(1/2)));

figure('Name',sprintf('Sample %d', ((counter-1)/3)+1),'NumberTitle','off')

plot(xe,ye)

hold on

plot(xe(erange),ye(erange),'r')


e = [emodulus];
```

B.2 Stress relaxation Scripts

B.2.1 Script to load and normalize raw data: stressrelax.m

```matlab
% function [data_final, depth, delta_strain] = stressrelax(data, defsens, ramp)

function [data_final change_strain] = stressrelax(data, defsens, k)

%lintime = linspace(0.01,120,12000)';

HoldTime = 60;

HoldSamples = HoldTime/0.2;

lintime = data(:,1); %Time (s)

deflection = data(:,2); %Deflection (V)

deflection = deflection*defsens; %Deflection (nm)

Zsens = data(:,3); %Zsens (V)

% Zsens = Zsens*defsens; %Zsens (nm)

subplot(3,4,1)

plot(lintime,deflection)

title('deflection')
```

```matlab
baseline_shift = mean(deflection(1:100)); %(nm)

data_shift = (deflection-baseline_shift); %(nm)

subplot(3,4,2)

plot(lintime,data_shift)

title('data shift')

data_small = data_shift(1:25100); %(nm)

[y n] = max(data_small); %(nm)

data_norm = (data_shift(n+1)).\(data_shift(n+1:n+HoldSamples));

data_cut = data_shift(n+1:n+HoldSamples);  %(nm)

%sum(data_norm);

for i = 1:length(data_cut),

    if data_cut(i) < 0

        data_cut(i) = 0.01;

    end

end

subplot(3,4,3)

cutlinetime = lintime(n+1:n+HoldSamples)-lintime(n+1)

plot(cutlinetime,data_cut)

title('data cut')

%Zbase_shift = mean(Zsens(1:100));

Zcut = Zsens(n+1:n+HoldSamples); %(nm)

subplot(3,4,4)
```

```matlab
plot(lintime(1:HoldSamples),Zcut)

title('Zcut')

Zshift = 1000-abs(Zcut(1));

Zshift = Zcut-Zshift;

subplot(3,4,5)

plot(lintime(1:HoldSamples),Zshift)

title('Z shift')

data_depth = abs(Zshift - data_cut); %(nm)

subplot(3,4,6)

plot(lintime(1:HoldSamples),data_depth)

title('data depth')

data_force = data_depth.*k/1e9; %(N/m)(nm)(m/nm) = (N)

subplot(3,4,7)

plot(lintime(1:HoldSamples),data_force)

title('data force')

nu_tip = 0.22;

nu_cell = 0.49;

E_tip = 6.2e10; %(Pa)

E_cell = 5628.1; %(Pa)

K = 1/((1-nu_tip^2)/E_tip+(1-nu_cell^2)/E_cell); %(Pa)

R_tip = 2.5e-6; %(m)

R_cell = 5e-6; %(m)
```

```matlab
R = 1/(1/R_tip+1/R_cell); %(m)

cube_radius = ((3*R)/(4*K).*data_force); %(N)(m)/(N/m^2) = (m^3)^1/3 = (m)

contact_radius = cube_radius.^(1/3);

subplot(3,4,8)

plot(lintime(1:HoldSamples),contact_radius)

title('contact radius')

contact_area = pi.*contact_radius.^2; %(m^2)

subplot(3,4,9)

plot(lintime(1:HoldSamples),contact_area)

title('contact area')

data_stress = data_force./contact_area./1000; %(N)/(m^2) = (Pa)*(kPa/Pa) = (kPa)

subplot(3,4,10)

plot(lintime(1:HoldSamples),data_stress)

title('data stress')

data_strain = data_depth./2000; %(nm)/(nm)

data_strain = data_strain(1);

subplot(3,4,11)

plot(lintime(1:HoldSamples),data_strain)

title('data strain')

data_modulus = data_stress./data_strain; %(kPa)

subplot(3,4,12)

plot(lintime(1:HoldSamples),data_modulus)
```

```matlab
title('data modulus')

data_final = [data_norm cutlinetime]; %[(kPa) (s)]

% lintime2 = linspace(0,120,12000)';

% depth = [data_norm lintime2];

% delta_strain = (((defsens*y)-(defsens*data_norm(12000)))/depth)*100;

change_strain = (((data_shift(n)-data_shift(HoldSamples))*defsens)/1000)*100

% G120=data_final(100)

maxforce = data_shift(n)*k

minforce = data_shift(HoldSamples)*k

% delta_strain = (((maxforce-minforce)/k)/1000)*100

% data_shift(n)


end
```

B.2.2 Script to calculate reduced relaxation G: The G function.m

```matlab
function G = TheGFunction(a, t)

G = 0*t;

C = a(1);

tau1 = a(2);

tau2 = a(3);

dtau = (tau2-tau1)/800;
```

```matlab
taus = linspace(tau1, tau2,800)';

for i = 1:length(t),

%    fun1 = @(tau) (exp(t(i)/tau)/tau);

%    fun2 = @(tau) (1/tau);

%    int1 = quad(fun1, tau1, tau2);

%    int2 = quad(fun2, tau1, tau2);

   int1 = sum(exp(-t(i)./taus)./taus)*dtau;

   int2 = sum(1./taus)*dtau;

   G(i) = (1 + C.*int1)./(1+ C.*int2);

end
```

B.2.3 Script to fit data to QLV model: QLVfit.m

```matlab
function [R2, fit, coefEsts] = QLVFit(data);


% QLVfun2 = @ (a,t) [1+a(1).*quad((exp(-t./a(2))./a(2)),a(3),a(4))] ./
[1+a(1).*quad((1./a(2)),a(3),a(4))];


%
lintime = linspace(0.2,60,300)';

logtime = log10(lintime);
```

```matlab
% t=logspace(-2,2.079,100)';

StartingVals = [1 0.05 100];

coefEsts = nlinfit(data(:,2), data(:,1), @TheGFunction, StartingVals)

% xgrid = logspace(-2,2.079,100);

xgrid = data(:,2);

plot(xgrid, data(:,1), '.')

plot(xgrid, TheGFunction(coefEsts, xgrid), 'r');

hold on

fit = TheGFunction(coefEsts, xgrid);

R = corr2(fit, data(:,1));


R2 = R^2
```

Comsol Protocol

C.1 Building geometry

C.1.1 Plastic plate

▲ 🧭 Work Plane 1 *(wp1)*
   ▲ 𝒜 Geometry
      ◻ Square 1 *(sq1)*
      ◯ Circle 1 *(c1)*
      ▣ Difference 1 *(dif1)*
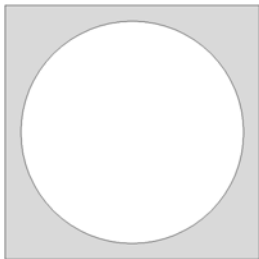
C.1.2 Rigid post

▲ 🧭 Work Plane 2 *(wp2)*
   ▲ 𝒜 Geometry
      ◻ Circle 1 *(c1)*
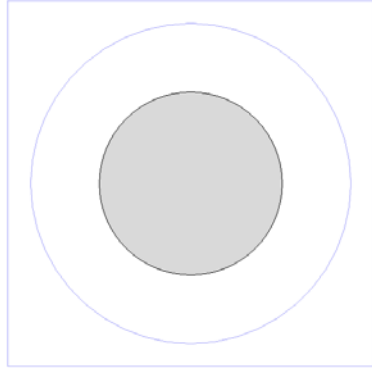
C.1.3 Silicon Membrane
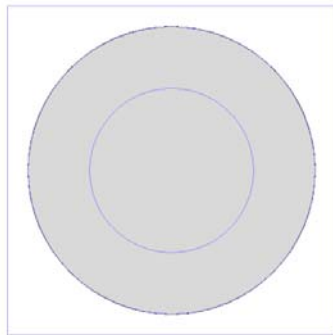
C.1.4 PDMS
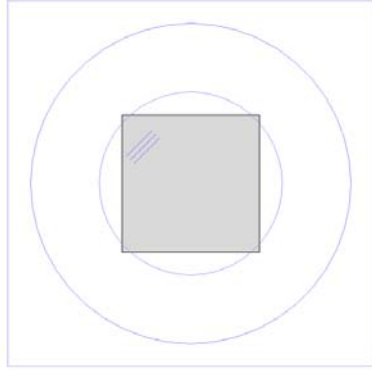
C.1.5 Cell geometry

Cell geometry conversion from Confocal image
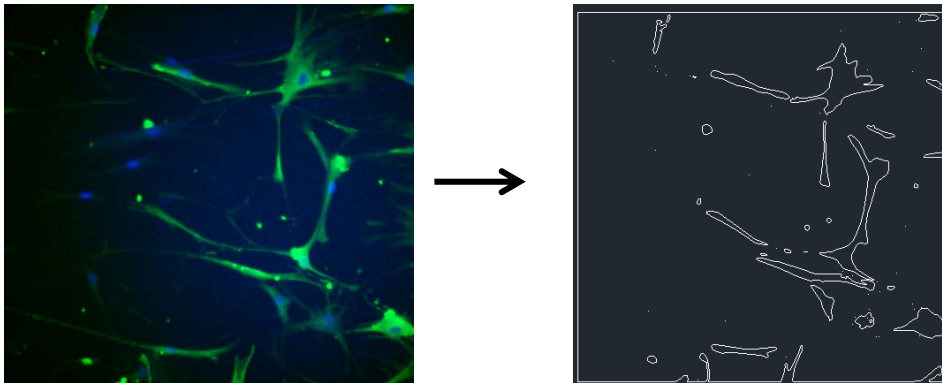
After vector information is coverted to CAD, we can export the cell geometry to

COMSOL
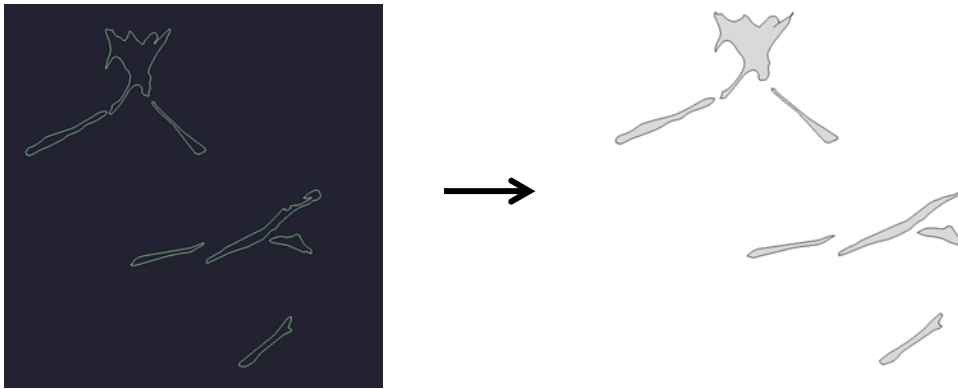
C.2 Material property definition

C.2.1 Rigid post

	Property	Name	Value	Unit	Property group
✓	Young's modulus	E	2e9	Pa	Basic
✓	Poisson's ratio	nu	0.37	1	Basic
✓	Density	rho	120	kg/m^3	Basic

C.2.2 Silicon membrane

	Property	Name	Value	Unit	Property group
✓	Density	rho	110	kg/m^3	Basic
✓	Bulk modulus	K	1.5e9	Pa	Bulk modulus and shear modulus
✓	Shear modulus	G	3e5	Pa	Bulk modulus and shear modulus

C.2.3 Plate

	Property	Name	Value	Unit	Property group
✓	Density	rho	1160[kg/m^3]	kg/m^3	Basic
✓	Young's modulus	E	3.2e9	Pa	Basic
✓	Poisson's ratio	nu	0.49	1	Basic

C.2.4 PDMS

	Property	Name	Value	Unit	Property group
✓	Young's modulus	E	3.6e6	Pa	Basic
✓	Density	rho	965	kg/m^3	Basic
✓	Poisson's ratio	nu	0.49	1	Basic

C.2.5 Cell

	Property	Name	Value	Unit	Property group
✓	Young's modulus	E	2000	Pa	Basic
✓	Poisson's ratio	nu	0.49	1	Basic
✓	Density	rho	106	kg/m^3	Basic

C.3 Solid mechanics

C.3.1 Global defination

- ▲ 🗋 Solid Mechanics *(solid)*
    - �— Linear Elastic Material Model 1
    - 🔲 Free 1
    - 🔗 Initial Values 1
    - 🔲 Fixed Constraint 1
    - ▷ 🔲 Rigid Connector 1
    - ▷ 🔲 Contact 1
    - ▷ 🔲 Contact 2
    - 🔗 Viscoelastic Material Model 1
    - 🔲 Boundary Load 1
    - ▷ 🔲 Contact 3
    - 🔲 Fixed Constraint 2

The edge of silicone membrane is fixed and contact pair is defined between rigid post and silicon membrane with free displacement. Contact pairs between silicone membrane, PDMS and cell are fixed. The plate and post are considered rigid body with zero displacement.
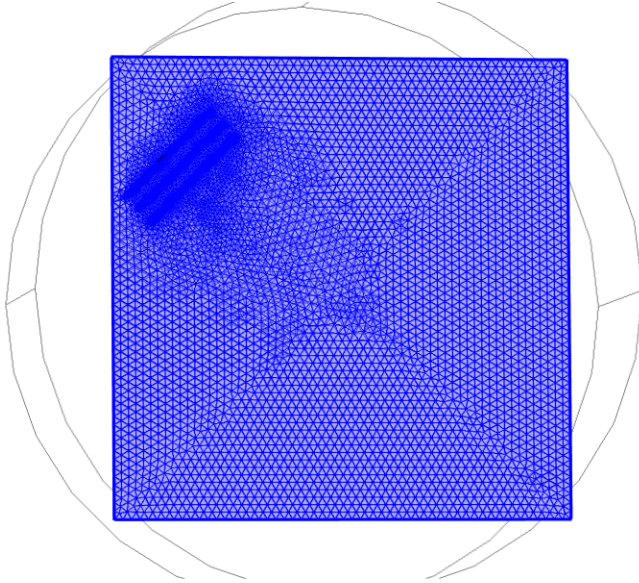
C.3.2 Viscoelastic model

▾ Generalized Maxwell Model

Branch	Shear modulus (Pa)	Relaxation time (s)
1	200000	0.01
2	100000	0.1
3	10000	1
4	100	10
5	10	100

Generalized Maxwell model is used to fit stress-strain relation of silicon membrane
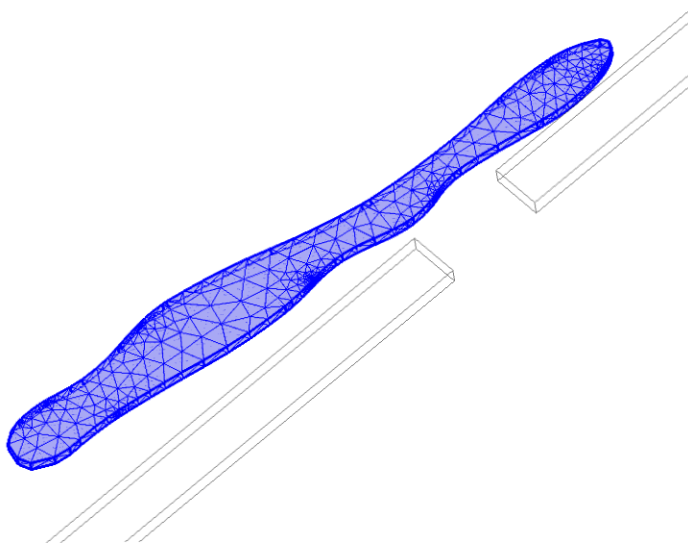
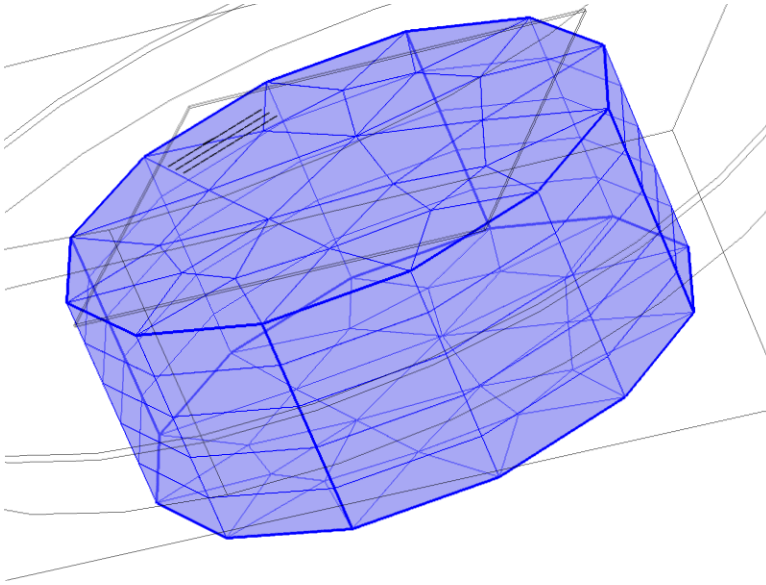## C.4 Mesh

C.4.1 PDMS

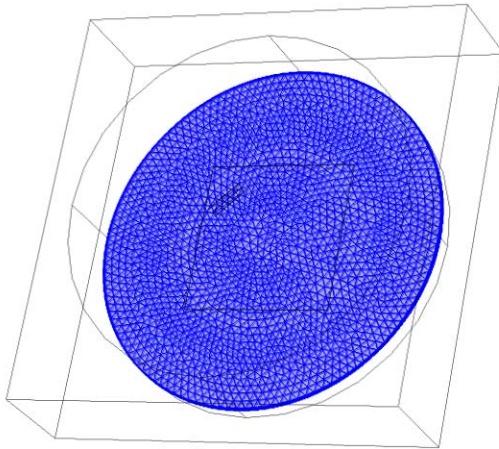PDMS is meshed with 41475 free tetrahedral elements

C.4.2 Cell

Cell is meshed with 3018 free tetrahedral elements
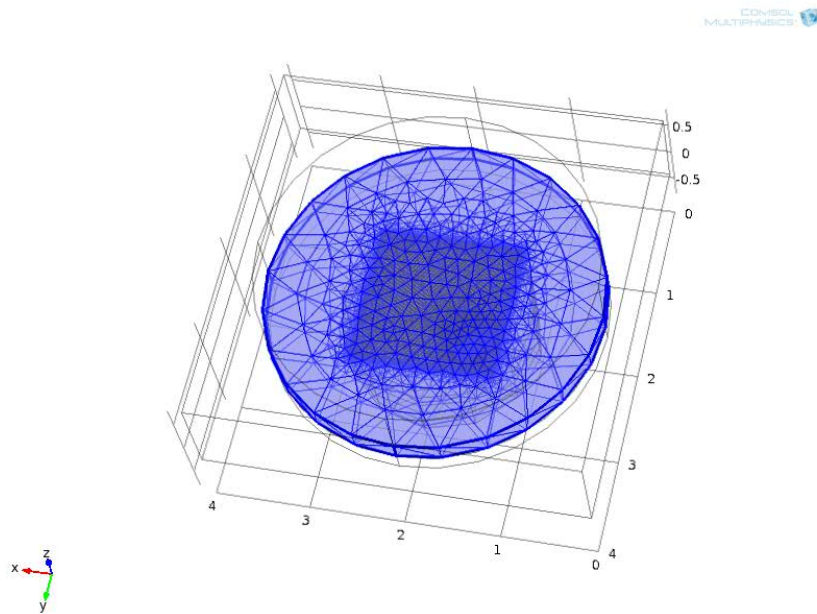
C.4.3 Post

Rigid post is meshed with free triangle and rectangle

C.4.4 Mesh of silicon membrane

Silicon membrane is meshed with 11175 free tetrahedral elements

C.4.5 Mesh of collagen layer

Collagen layer is meshed with 11546 free tetrahedral elements

C.4.6 Mesh of the whole geometry